University of Alberta

The role of YVH1, a dual specificity phosphatase, in the production of alternative oxidase in the filamentous fungus *Neurospora crassa*

by

Adrien Beau Desaulniers

A thesis submitted to the Faculty of Graduate Studies and Research
in partial fulfillment of the requirements for the degree of

Master of Science
in
Molecular Biology and Genetics

Department of Biological Sciences

Fall 2013
Edmonton, Alberta

ABSTRACT

Alternative oxidase (AOX) is a single protein enzyme that carries electrons from ubiquinol to molecular oxygen. AOX is induced in many organisms, including *Neurospora crassa*, when the standard electron transport chain is blocked through various inhibitors or mutations. A knockout (KO) for a dual specificity phosphatase, termed YVH1, cannot properly induce AOX and has a slow growth phenotype. YVH1 contains a HCX_5R phosphatase domain and a zinc-binding domain. YVH1 localizes to the nucleus and cytosol equally under all conditions studied. The phenotype of the KO is rescued with constructs that contain only a functional zinc-binding domain. The phosphatase domain appears to be non-essential. The protein has been shown to play a role in ribosome biogenesis in yeast. Preliminary RNA-seq experiments revealed that expression of 17% of the 10,000 protein coding genes of *N. crassa* is altered at least 2 fold by loss of *yvh1* when grown in inducing conditions.

TABLE OF CONTENTS

1 INTRODUCTION 1

1.1 Mitochondrial morphology and dynamics 1

1.2 Mitochondrial function 4

1.2.1 Oxidative phosphorylation 4

1.3 Mitochondrial evolution 7

1.4 Mitochondrial DNA 9

1.5 Import complexes of the mitochondria 10

1.6 Introduction to retrograde regulation 11

1.7 Introduction to alternative oxidase 14

1.7.1 Alternative oxidase is present in numerous species 15

1.7.2 Alternative oxidase protein structure 16

1.7.3 Multiple gene families of AOX 18

1.7.4 Regulation of alternative oxidase 19

1.7.5 AOX activation 20

1.7.6 Functions of AOX 22

1.8 Alternative oxidase in *Neurospora crassa* 23

1.8.1 Knockout screen for AOX mutants 27

1.9 Assembly of the ribosome 28

1.9.1 60S formation from the nucleolus to the cytoplasm 28

1.10 The YVH1 DUSP 31

1.11 Human YVH1 (hYVH1 or DUSP12) 35

1.11.1 A role of hYVH1 in human diseases 36

1.12 YVH1 in other organisms 36

1.13 Objective of this Study 37

2 MATERIALS AND METHODS 38

2.1 Handling of *N. crassa* strains 38

2.2 Measurement of growth rates 38

2.3 Transformation of *N. crassa* and isolation of working strains 39

2.4 Creation of N- and C- YVH1 3xHA tagged wild type and mutant plasmids 40

2.5 Isolation of mitochondria, cytosolic, and post-mitochondrial pellet fractions 41
2.6 Extraction and purification of nuclei 43
2.7 Whole cell extracts 44
2.8 Quantitative real time polymerase chain reaction (qPCR) 44
2.9 Cytosolic ribosome isolation 45
2.10 Spectral analysis 46
2.11 RNA-seq 46
2.12 General procedures and other techniques 47
2.13 Oligonucleotides and plasmids 47

3 RESULTS 53

3.1 A dual specificity phosphatase protein has a role in AOX production in *N. crassa* 53
3.2 *aod-1* transcript levels in the *Δyvh1* strain 53
3.3 Analysis of cytochrome spectra for efficiency of Cm inhibition 59
3.4 A construct expressing an HA-tagged version of YVH1 restores expression of AOX in *Δyvh1* 61
3.5 The HA tagged YVH1 protein localizes to the nuclear and PMP fractions of the cell 64
3.6 AOX expression requires a functional zinc binding domain but not the phosphatase domain of YVH1 69
3.7 Localization of mutant YVH1 protein 71
3.8 RNA-Seq analysis of *Δyvh1* and the control grown in the presence of Cm for 12 hr 74

4 DISCUSSION 80

4.1 Growth and AOX protein levels in *Δyvh1* 80
4.2 YVH1 localization 83
4.3 Functional domain of YVH1 85
4.4 RNA-seq 87
4.5 Significance and future directions 89

5 REFERENCES **92**

LIST OF FIGURES

Figure 1. Organization of mitochondrial compartments. 2

Figure 2. Standard electron transport chain (sETC) of the inner membrane of mitochondria. 5

Figure 3. The pathway of retrograde regulation that occurs between the mitochondrion and the nucleus. 13

Figure 4. Structural models of AOX. 17

Figure 5. The ribosomal stalk of the 60S subunit. 30

Figure 6. Model for the role of YVH1 in assembling the ribosome stalk base during ribosome biogenesis. 34

Figure 7. Structure of the *yvh1* gene and protein. 54

Figure 8. Induction of AOX and growth of *Δyvh1*. 55

Figure 9. AOX protein and transcript levels in the control and the *Δyvh1* strain. 58

Figure 10. Qualitative cytochrome spectra of the NCN251 control strain (A) and *Δyvh1* (B). 60

Figure 11. Western blot analysis of N- and C-terminal HA tagged YVH1 containing strains. 62

Figure 12. Growth rate of N-HA-2 and C-HA-1 YVH1 transformants. 63

Figure 13. Subcellular localization of YVH1. 66

Figure 14. Western blot analysis of N- and C- terminal HA tagged YVH1 strains derived by transformation of *Δyvh1*. 68

Figure 15. Analysis of phosphatase domain and zinc binding domain mutants. 70

Figure 16. Subcellular fractionation of N-HA tagged P- and Z-mutant YVH1 strains. 73

Figure 17. Data from RNA-seq. 77

Figure 18. Possible models for effects on AOX production caused by loss of YVH1. 91

LIST OF TABLES

Table 1. Strains used in this study. 48

Table 2. Oligonucleotides. 49

Table 3. Plasmids used in this study. 51

Table 4. Top 20 down-regulated genes as determined from RNA-seq. 78

Table 5. Top 20 up-regulated genes as determined from RNA-seq. 79

LIST OF ABBREVIATIONS

3D	three dimensional
$\Delta\Psi_m$	mitochondrial membrane potential
A	adenine or alanine
AMP	adenosine monophosphate
AN	Andersson and Nordlund
AOX	alternative oxidase
ATP	adenosine triphosphate
BLAST	basic local alignment search tool
bp	base pair
°C	degrees Celsius
C	cytosine
CS	clarifying spin
Cm	chloramphenicol
cDNA	complimentary DNA
Cys or C	cysteine
Δ	deletion
D	aspartic acid
Da	Dalton
DNA	deoxyribonucleic acid
DUSP	dual specificity phosphatase
E	glutamic acid
EDTA	ethylenediaminetetraacetic acid
EMS	Ethyl methane sulfonate
EMSA	electrophoretic mobility shift assay
ER	endoplasmic reticulum
ERMIONE	ER-mitochondria organizing network
FADH2	flavin adenine dinucleotide
FGSC	fungal genetics stock center
G	guanine
g	gravity or gram
GFP	green fluorescent protein
GTP	guanine triphosphate
H	histidine
HA	hemaglutinin
hr	hour
Hsp	heat shock protein
IBM	inner boundary membrane
IMS	intermembrane space
kbp	kilobasepair
kDA	kilodalton
l	litre

KO	knockout
kV	kilovolts
µF	microfarad
µg	microgram
µl	microlitre
M	molar
MBSU	molecular biology service unit
mg	miligrams
MICOS	mitochondrial contact site
MIM	mitochondrial inner membrane
ml	milliliter
mM	millimolar
min	minute
MINOS	mitochondrial inner membrane organizing system
MitOS	mitochondrial organizing structure
MOM	mitochondrial outer membrane
MOPS	4-morpholinepropanesulfonic acid
mRNA	messenger RNA
mtDNA	mitochondrial DNA
NADH	nicotinamide adenine dinucleotide reduced form
Ω	ohm
OM	outer membrane
OXPHOS	oxidative phosphorylation
P	proline
PAGE	polyacrylamide gel electrophoresis
PCR	polymerase chain reaction
PMFS	phenylmethylsulfonyl fluoride
PMP	post-mitochondrial pellet
P-mutant	phosphatase domain mutant
Q	glutamine
qPCR	quantitative real time PCR
R	arginine
RNA	ribonucleic acid
RNAi	RNA interference
RNA-seq	RNA sequencing
rRNA	ribosomal RNA
ROS	reactive oxygen species
rpm	revolutions per minute
r-protein	ribosomal protein
S or Ser	serine
SAM	sorting and assembly machinery
SDS	sodium dodecyl sulfate
SDS-PAGE	Sodium dodecyl sulfate polyacrylamide gel electrophoresis

SEMP	sucrose EDTA MOPS PMFS buffer
sETC	standard electron transport chain
SHAM	salicylhydroxamic acid
TIM	translocase of the inner membrane
TOB	topogenesis of outer membrane β-barrels
TOM	translocase of the outer mitochondrial membrane
Tris	tris (hydroxymethyl) aminomethane
tRNA	transfer RNA
UTR	untranslated region
V	valine
VSoTB	Vogel's salts with sorbose, trance elements and biotin
VSuTB	Vogel's salts with sucrose, trance elements and biotin
X	any amino acid
Y	tyrosine
Z-mutant	zinc binding domain mutant

1 INTRODUCTION

1.1 Mitochondrial morphology and dynamics

Mitochondria are dynamic organelles found in the majority of eukaryotic cells. The double membrane of mitochondria results in four distinct compartments within the organelle: the mitochondrial outer membrane (MOM), the intermembrane space (IMS), the matrix, and the mitochondrial inner membrane (MIM) (Figure 1). The MIM can be further subdivided into the inner boundary membrane (IBM) and the cristae membrane (LOGAN 2006). The MOM is a relatively simple phospholipid bilayer that contains pores and transport complexes that allow for the movement of molecules across the membrane (GEBERT *et al.* 2011; VOGEL *et al.* 2006). The MIM is a protein rich lipid bilayer that encloses the matrix space and only allows the passage of solutes through the use of carrier proteins (CHACINSKA *et al.* 2009; VOGEL *et al.* 2006). The cristae are structures that increase the surface area of the MIM. The original model of the cristae folding was the baffle model, which depicted the cristae as random invaginations and in-folds of the MIM (PALADE 1952). However, using high-resolution scanning electron microscopy, researchers have determined that this model is not entirely correct (LEA *et al.* 1994; MANNELLA 2006; MANNELLA *et al.* 1994). Instead, the cristae junction model suggests that tubular cristae, instead of lamellar, are the most prominent and are structurally distinct from the rest of the MIM. Cristae junctions, which are connections to the IBM through membranous tubules and not just simple invaginations of the MIM, were also discovered and reinforced the cristae junction model (LOGAN 2006). The IBM forms tight attachments with the MOM and these two structures interact to import proteins, export ATP, and coordinate fusion and fission of the mitochondria (HARNER *et al.* 2011; REICHERT and NEUPERT 2002).

Three different research groups simultaneously discovered a scaffolding-organizing complex of the MIM. The MINOS (mitochondrial inner membrane organizing system) (VON DER MALSBURG *et al.* 2011), MICOS (mitochondrial contact site) (HARNER *et al.* 2011), or MitOS (mitochondrial organizing structure)

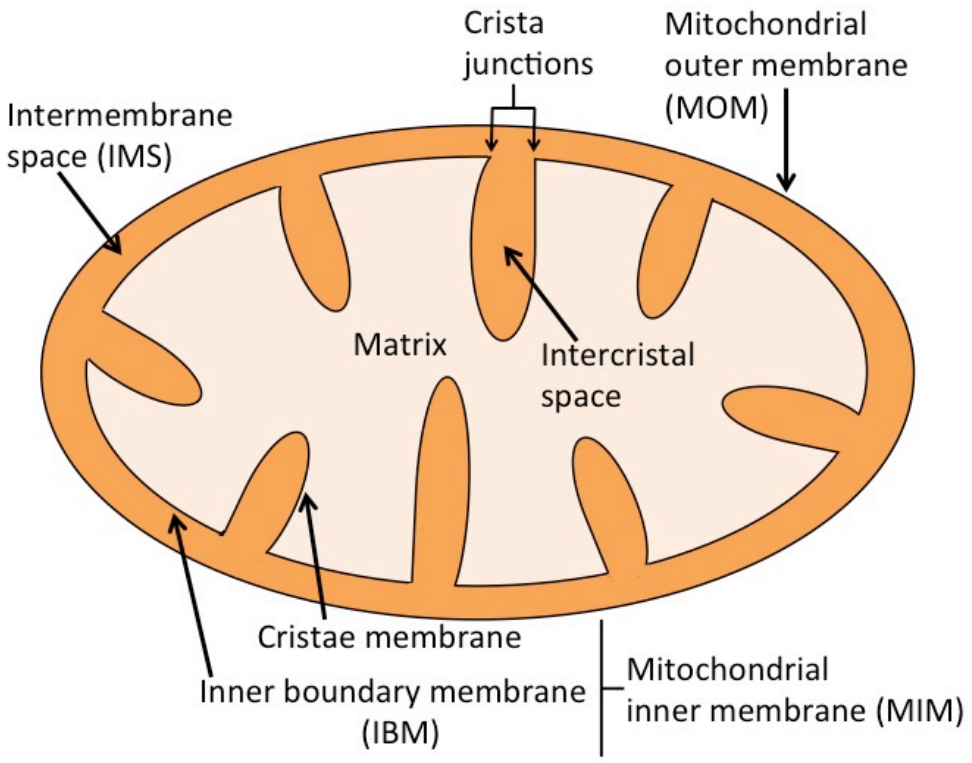

Figure 1. Organization of mitochondrial compartments. Four distinct compartments of the mitochondria arise due to the double membrane structure of the organelle: the mitochondrial outer membrane (MOM), the intermembrane space (IMS), the mitochondrial inner membrane (MIM), and the matrix. The MIM can be divided into the cristae membrane and the inner boundary membrane (IBM). Cristae junctions are narrow tubular openings that connect to the IBM. Diagram based on the cristae-junction model of mitochondrial structure (Logan 2006).

(HOPPINS *et al.* 2011) complex consists of multiple proteins that are enriched at contact sites of the MOM-MIM. The MINOS complex interacts with proteins of the MOM and it has been suggested that MIM cristae junction formation requires MINOS. Therefore, MINOS may be responsible for the organization of the MIM structure in regards to the MOM (HARNER *et al.* 2011; KORNER *et al.* 2012; VAN DER LAAN *et al.* 2012). It has been proposed that there is an extensive network consisting of many organelles that create a multi-membrane spanning organization of the structures, termed ERMIONE (ER-mitochondria organizing network) (van der Laan *et al.*, 2012). This suggests that within the cell there is tight coordination between membranes and complexes of different organelles.

Mitochondria are highly dynamic organelles in that they are constantly moving inside the cell and are frequently fusing and dividing independently of host cell division (KIEFEL *et al.* 2004; SHUTT and MCBRIDE 2013). There is a delicate balance of fusion and fission events that occur within the cell to maintain mitochondrial shape, size and number (OKAMOTO and SHAW 2005; PALMER *et al.* 2011; WESTERMANN 2010). Fusion events bring together the mitochondrial compartment and create an extended interconnected mitochondrial network. Fission on the other hand produces morphologically distinct organelles (WESTERMANN 2008). The events of fusion and fission are tightly regulated to ensure the integrity of the membranes is maintained throughout the processes. Dynamin related GTPases are the main proteins involved in both pathways (HOPPINS *et al.* 2007a). If cells are lacking genes involved in fusion events, mitochondria become fragmented. On the other hand, if they are lacking genes involved in fission, mitochondria become hyper-connected or condensed. The endoplasmic reticulum (ER) has also been shown to be involved in mitochondrial fission. Sites where the ER contacts mitochondria have been shown to constrict the organelle and mark the sites of division (FRIEDMAN *et al.* 2011). Fusion and fission are tightly regulated due to the fact that many processes are affected by mitochondrial dynamics including, apoptosis, mitophagy, metabolic efficiency and mitochondrial DNA (mtDNA) quality (NUNNARI and SUOMALAINEN 2012).

1.2 Mitochondrial function

There are many functions of the mitochondria within the eukaryotic cell. One such function includes a role in cellular iron regulation and the biogenesis and assembly of iron sulfur clusters required as cofactors for specific proteins (LILL *et al.* 2012). Mitochondria also have a role in programmed cell death to control cell number and remove unwanted and potentially dangerous cells (ESTAQUIER *et al.* 2012). In calcium signaling, there is interplay between the cytosolic and mitochondrial calcium molecules in regulating metabolic homeostasis (GLANCY and BALABAN 2012). In yeast it has been demonstrated that mitochondria synthesize their own fatty acids in a process similar to bacteria, revealing another role of the mitochondria (HILTUNEN *et al.* 2010). However, the main function that mitochondria are known for is the production of adenosine triphosphate (ATP) through oxidative phosphorylation (OXPHOS). This is the reason why mitochondria are also known as the "power house" of the cell.

1.2.1 Oxidative phosphorylation

OXPHOS is the process by which cells produce ATP through the energy released by the oxidation of nutrients. The standard electron transport chain (sETC) is the site of OXPHOS. The sETC is located in the MIM and is an arrangement of four complexes and two mobile components [reviewed in (LENAZ and GENOVA 2010)] (Figure 2). In its simplest form, electrons enter the sETC from two different carriers. The electron carrier NADH + H^+, which is produced in glycolysis and the Krebs cycle, donates two electrons to Complex I (NADH dehydrogenase). $FADH_2$, produced from the Krebs cycle, donates 2 electrons to the sETC through complex II (succinate dehydrogenase). The electrons from both complex I and II then flow to the mobile element ubiquinone (coenzyme Q) and then to complex III (cytochrome c reductase). Electrons then pass to the mobile element cytochrome c, then to complex IV (cytochrome c oxidase) and then are donated to the terminal electron receptor, oxygen. Protons are pumped from the matrix into the IMS at complexes I, III and IV as electrons flow through the

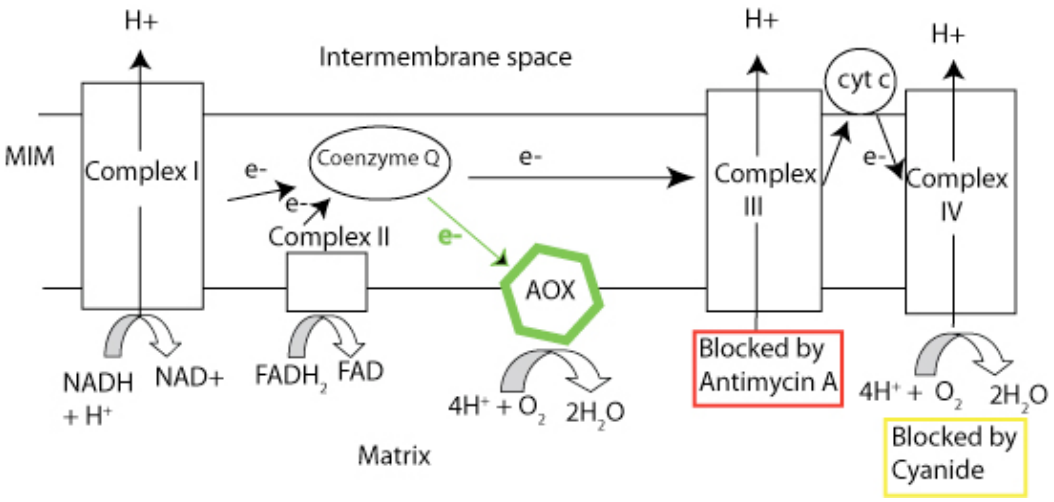

Figure 2. Standard electron transport chain (sETC) of the inner membrane of mitochondria. Electrons derived from $NADH_2$ or $FADH_2$ are passed along the cytochrome-mediated pathway under normal growth conditions to oxygen (black arrows). H^+ ions are pumped across the inner membrane to the intermembrane space at complex I, III, and IV. This leads to a proton gradient, which is harnessed by ATP synthase to produce ATP (not shown). Conditions that block the sETC (antimycin A (red), or cyanide (yellow)) leads to the induction of alternative oxidase (AOX). AOX passes electrons from the coenzyme Q pool directly to oxygen (green). ATP is produced at a lower rate because only complex I contributes to the proton gradient. MIM, mitochondrial inner membrane; AOX, alternative oxidase; cyt c, cytochrome c; e-, electrons.

structures. The proton gradient created by proton pumping is then harnessed by Complex V (F_1F_0 ATP synthase) to produce ATP. Complex V allows protons to diffuse back into the matrix through chemiosmosis and the vast majority of ATP is produced this way in most eukaryotic cells.

The respirasome model describes a supramolecular association of components of the respiratory chain to facilitate electron transfer [reviewed in (LENAZ and GENOVA 2012)]. Blue-native polyacrylamide gel electrophoresis experiments of mitochondria solubilized with digitonin showed that the complexes of the sETC are not distributed in the membrane in a random fashion (SCHAGGER and PFEIFFER 2000). Instead the complexes associate with each other to form supramolecular structures, which consist of complex I, III, and IV arranged in a specific manner (BOEKEMA and BRAUN 2007; SCHAGGER and PFEIFFER 2000). The arrangement of the OXPHOS complexes into supramolecular structures has been detected in numerous organisms including bacteria (STROH *et al.* 2004), fungi (MARQUES *et al.* 2007), plants (EUBEL *et al.* 2004) and mammals (SCHAGGER and PFEIFFER 2000). It is believed the benefit of this supramolecular organization of the electron transport chain occurs because it allows for substrate channeling of electrons between enzymes, and the organization also increases the stability of the complexes (LENAZ and GENOVA 2012).

In *N. crassa* supercomplexes were discovered in an I-III-IV and III-IV arrangement. This organization matches what is observed in the respiratory chain of mammals (MARQUES *et al.* 2007). Putative complex I dimers were also identified in the mitochondria of *N. crassa* although complex I is usually observed as a monomer in other organisms (LENAZ and GENOVA 2012; MARQUES *et al.* 2007). Complex I was also observed to not be essential for the formation of supercomplexes because complex III-IV were formed in the absence of complex I (MARQUES *et al.* 2007). In the absence of complex III, complex I and IV can still form but mitochondria are lacking supercomplexes containing III. The major complexes formed in the absence of complex III are complex I dimers and I_1IV_1. In this scenario the alternative oxidase (AOX) pathway, the major topic of this

thesis, is induced (discussed in section 1.7), which is a respiratory pathway that allows electron flow to continue in the absence of complex III (DUARTE and VIDEIRA 2009).

1.3 Mitochondrial evolution

One of the earliest theories for the origin of mitochondria inside the cell stated that the organelle originally evolved from free-living bacteria that had been trapped and enslaved as an endosymbiont in an ancestral anaerobic eukaryotic cell (O'MALLEY 2010; SAGAN 1967). As time passed, a mutualism developed that favoured both cells and the trapped cell remained intact and was able to transfer genes over from it's own genome to the nuclear genome of the host cell (GRAY 2012; GRAY *et al.* 2001; LANG *et al.* 1999). Originally proposed by Constantin Mereschkowsky in the early 1900s, the idea was not accepted by the scientific community – due to lack of evidence – until Lynn Margulis reintroduced the idea in 1967 (O'MALLEY 2010; SAGAN 1967).

There is a considerable amount of molecular data that supports the endosymbiont theory. Such evidence included that mitochondria contain their own circular DNA and sequence analysis of many mtDNAs has led to the conclusion that the evolutionary origins of mitochondria stem from α-proteobacteria (ANDERSSON *et al.* 2003; CAVALIER-SMITH 2006). Also, the Rickettsia, one of the closest known eubacterial relatives of mitochondria, is a group of obligate intracellular parasites that live within host cells, much like mitochondria live within a host cell (EMELYANOV 2001; YANG *et al.* 1985). Finally, comparison of mitochondrial rRNA sequences from eukaryotes, bacteria, and archaea, showed that the original endosymbiont was likely a α-proteobacterium from which all mitochondria originated (GRAY 2012; YANG *et al.* 1985). These examples give evidence that there was a single endosymbiont event and that all current mitochondria have evolved from a single ancient primitive mitochondria (VAN DER GIEZEN *et al.* 2005).

Although it is now accepted that the origin of mitochondria was through an endosymbiont event involving an ancient α-proteobacterium, it is not clear if

the host cell became eukaryotic before or after engulfment of the symbiont (MARTIN 2011; VESTEG and KRAJCOVIC 2011). Two opposing hypothesis have been suggested for what type of host cell was present when endosymbiosis occurred [reviewed in (O'MALLEY 2010)]. The first, termed the phagotrophy model, predicts that the engulfing host was already a protoeukaryote before trapping the symbiont. This means that the host already had some organelles, like the nucleus, that distinguished it as an early eukaryote, but lacked others like the mitochondria. The protoeukaryote had the ability to phagocytose the endosymbiont, which somehow escaped digestion and benefited the host. Up until the early 1990s, it was thought that amitochondrial species of eukaryotes existed. The existence of such organisms supported this theory. These species were believed to be descendants of ancient eukaryotes from a time before the engulfment of the mitochondria by the eukaryotic cell (CAVALIER-SMITH 1987). However, in 1995 it was discovered that these species had at one time possessed mitochondria, but they have evolved into less complex organelles termed mitosomes or hydrogenosomes (CLARK and ROGER 1995; VAN DER GIEZEN 2009). It was shown that some of the genes from the original endosymbiont had in fact migrated to the nuclear genome in the species containing the simple organelles (VAN DER GIEZEN 2009). Therefore, it now appears that there might never have been a protoeukaryotic species before engulfment of the mitochondria and new models were hypothesized pertaining to the origin of eukaryotes.

The syntrophy model emerged as the favoured model from the main competitors of the phagotrophy model [reviewed in (EMBLEY and MARTIN 2006; O'MALLEY 2010)]. In the syntrophy model, an archaebacterium host integrates a proteobacterium endosymbiont as the two exchange metabolites in a symbiotic relationship. The host cell does not become eukaryotic until after the endosymbiont transfers its genes and becomes the mitochondria. Eukaryotic organelles would form after endosymbiosis. The best example of the syntrophy model is the hydrogen hypothesis. In this hypothesis, the original symbiont would metabolize an organic substrate like methane to produce hydrogen and carbon dioxide (MARTIN and MULLER 1998). The archaebacterial host would use these

substrates as a source of energy and carbon and produce methane as a waste product. The eukaryote nucleus is thought to have evolved after acquisition of the symbiont since all extant eukaryotes contain mitochondria or their relatives. Thus, obtaining the endosymbiont was the key moment in the evolution to the eukaryote according to the syntrophy model.

1.4 Mitochondrial DNA

Mitochondria contain their own genome termed mtDNA. In the majority of eukaryotes, mtDNA encodes ribosomal RNA (rRNA) genes, transfer RNA (tRNA) genes, and a small number of protein coding genes. Genes for the mitochondrial rRNAs of the small and large ribosomal subunits are present in all mitochondrial genomes that have been characterized to date (GRAY 2012). Mitochondrial tRNA genes can be present or absent from mtDNA, and if absent, tRNA proteins are assumed to be imported from the cytoplasm (GRAY *et al.* 1998; SCHNEIDER 2011). Different organisms show considerable variability in the number of protein coding genes contained within mtDNA, ranging from 3 to 67 proteins throughout eukaryotes (GRAY 2012; TIMMIS *et al.* 2004). The genomes of two of mitochondria's closest relatives, the α-proteobacteria *Rickettsia prowazekii* and *R. conori*, encode 834 proteins and 1300 annotated genes, respectively (ANDERSSON *et al.* 2003). Gene reduction and loss of mtDNA from the original endosymbiont genome seems to have occurred over the course of evolution with genes either being transferred to the host nucleus or completely lost (ANDERSSON *et al.* 1998; GRAY *et al.* 1999). However, mtDNA always contains at least some genes encoding proteins of the respiratory complexes. In *N. crassa*, the mtDNA contains 26 open reading frames, 2 mitochondrial rRNAs, and 27 tRNAs. Of the 26 open reading frames, 14 encode protein subunits for the complexes of the sETC of the inner membrane (NARGANG and RAPAPORT 2007), 1 encodes a ribosomal protein, and the other 11 encode unknown products.

The mitochondrion was able to withstand the loss of functional genes from the genome for a few reasons [reviewed in (ADAMS and PALMER 2003)]. First, once engulfed by the host, the eubacteria endosymbiont no longer needed genes

for certain functions and these could be lost over time. This was probably a major factor in the beginning of endosymbiosis when the protomitochondria lost the need for genes required for survival as a bacterium living outside the host cell. Secondly, the function of other genes might have been substituted or replaced by a preexisting gene in the nuclear genome that had the same role in the mitochondria. Finally, other genes were lost from the mitochondria through transfer to the nucleus. This allows the nuclear genome to control the expression of mitochondrial genes, which leads to coordinate expression of overlapping processes between organelles.

There are a few hypotheses that attempt to explain why certain genes remained in the mitochondrial genome and did not transfer over to the nuclear genome. One hypothesis, known as the hydrophobicity hypothesis, states that hydrophobic mitochondrial proteins, if encoded in the nucleus, would be difficult to import across the mitochondrial membranes because mitochondrial targeting signals would be disrupted. Very hydrophobic proteins may also be mis-targeted to a different organelle like the ER (CLAROS *et al.* 1995; DALEY and WHELAN 2005; DE GREY 2005; POPOT and DE VITRY 1990). In soybean, a decrease in hydrophobicity is observed in the nuclear encoded cytochrome c oxidase subunit 2 compared to the mitochondrial-encoded counterpart, giving support to the hydrophobicity hypothesis (DALEY *et al.* 2002). The other hypothesis, known as the co-localization for redox regulation (CORR) hypothesis, suggests that the genes that remained in the mitochondria are required for responding to redox poise within the organelle (ALLEN 2003; PUTHIYAVEETIL *et al.* 2010). The mitochondria can therefore respond quicker to changes in redox state by having the genes involved in redox regulation in the mtDNA. The mitochondrion would be unable to respond as quickly if these genes were exclusively present in the nuclear genome.

1.5 Import complexes of the mitochondria

The mitochondrial genome only encodes roughly 1% of the proteins required for proper mitochondrial function. Thus 99% of the proteins are encoded

by nuclear genes, transcribed in the nucleus, translated on cytosolic ribosomes, and imported into the mitochondria where they are properly targeted and inserted at their final destination. Proteins destined for the mitochondria contain one of two types of signal that targets them to a specific location in the mitochondria. The first is a signal at the amino terminal end of the protein that is cleaved upon import into the mitochondria. The second is an internal signal within the protein that is not cleaved (MOSSMANN *et al.* 2012).

To import proteins into the mitochondria, a series of complexes exists in the inner and outer membranes that direct proteins to a functional destination [reviewed in (DUKANOVIC and RAPAPORT 2011; ENDO *et al.* 2011; GEBERT *et al.* 2011; SCHMIDT *et al.* 2010)]. The majority of preproteins targeted to the mitochondria are recognized and imported by the translocase of the outer membrane or TOM complex. Once through the TOM complex, preproteins follow different pathways to reach a specific subcompartment depending on the targeting signal present on the peptide. Proteins with a cleavable signal destined for either the MIM or matrix are passed to the translocase of the inner membrane (TIM) TIM23 complex. Proteins that contain numerous transmembrane segments that are targeted for the MIM interact with the TIM22 protein complex. The TIM22 complex then laterally releases the protein into the MIM. Proteins targeted to the outer membrane interact with the TOM complex and also the topogenesis of β-barrel proteins (TOB)/ sorting and assembly machinery (SAM) complex. This complex facilitates the insertion of β-barrel proteins into the outer membrane from the intermembrane space. Many α-helical outer membrane proteins are not transported through the TOM complex. Instead these proteins are inserted into the outer membrane by interacting with mitochondrial import protein 1 (STEFAN DIMMER and RAPAPORT 2010).

1.6 Introduction to retrograde regulation

For proper function the mitochondrion is constantly communicating its functional state to the nucleus. This is because the nuclear genome stores the majority of genetic information required for proper mitochondrial activity. This

pathway of signals that originate in the mitochondria but affect the expression of nuclear genes is termed retrograde regulation or the retrograde response (Figure 3). This is different than anterograde regulation, where the transfer of information occurs from the nucleus and cytoplasm to the mitochondria (BUTOW and AVADHANI 2004).

The retrograde response of *Saccharomyces cerevisiae* is a well-characterized pathway of mitochondria to nucleus communication [reviewed in (JAZWINSKI and KRIETE 2012; LIU and BUTOW 2006; WOODSON and CHORY 2008)]. This pathway of intracellular signaling in response to the functional state of the mitochondria involves many positive and negative regulators. A nuclear gene, *CIT2*, is highly upregulated in cells lacking mtDNA (LIAO *et al.* 1991). The promoter region of *CIT2* contains an upstream activation site required to initiate the retrograde response and this region was used to uncover regulatory factors of the pathway (LIAO and BUTOW 1993). This included two basic helix leucine zipper transcription factors, RTG1 and RTG3, which bind to the promoter region of target genes as a heterodimer. Under normal conditions RTG3 of the RTG1/3 heterodimer is phosphorylated and the complex remains in the cytoplasm until activation of the retrograde pathway (LIU *et al.* 2003; SEKITO *et al.* 2000). Dephosphorylation of RTG3 requires RTG2, a cytoplasmic protein that contains an N-terminal ATP binding domain (LIU *et al.* 2003). Once RTG3 is partially dephosphorylated, the RTG1/3p heterodimer enters the nucleus and binds to specific sequences upstream of their target genes, and activate their transcription. There are other positive and negative regulators of this pathway, all of which interact to maintain a balance to the pathway (BUTOW and AVADHANI 2004). The signal that leads to the activation of the retrograde pathway may be a drop in mitochondrial membrane potential ($\Delta\Psi_m$). However how this signal is read by RTG2 still remains to be determined (MICELI *et al.* 2011).

The retrograde response pathway is also thought to be present in other organisms although it is not as well characterized as in yeast (JAZWINSKI and KRIETE 2012). In *C. elegans*, RNA interference (RNAi) of genes involved in

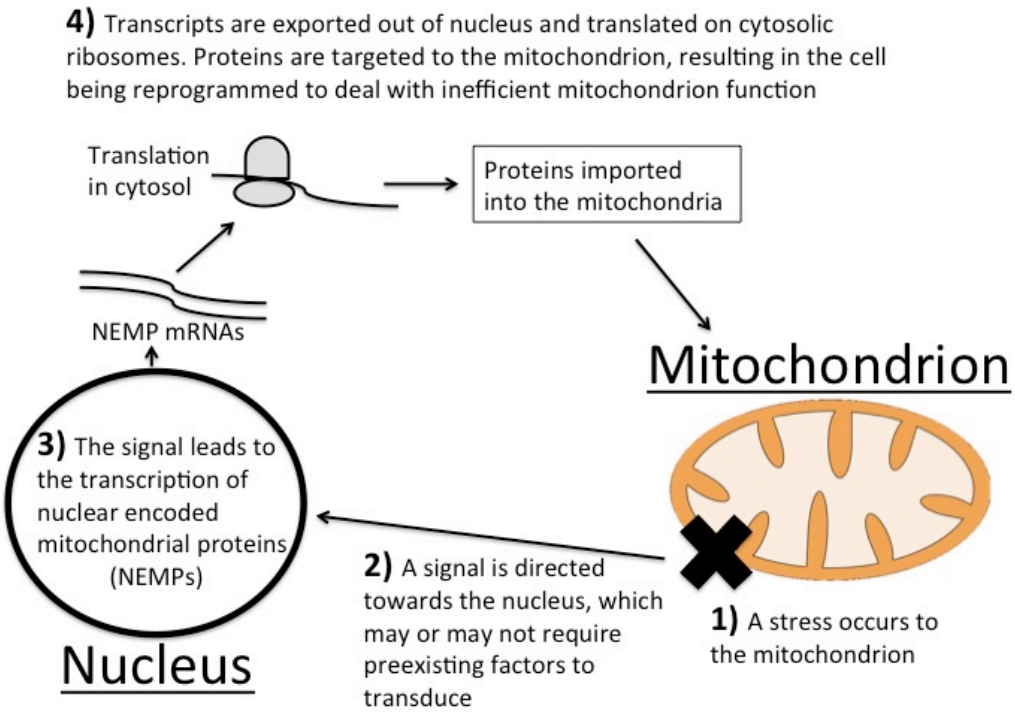

Figure 3. The pathway of retrograde regulation that occurs between the mitochondrion and the nucleus. A stress on the mitochondrion leads to the expression of nuclear encoded mitochondrial proteins (NEMPs) in an attempt to deal with the stress on the organelle. The flow of information follows steps 1 to 4.

respiration has suggested the presence of a retrograde response pathway. It appears that the signal that mediates this response is reactive oxygen species (ROS) but whether this occurs after a change in $\Delta\Psi_m$ is still unclear (CRISTINA *et al.* 2009; LEE *et al.* 2010). In *D. melanogaster*, RNAi screens of respiratory complex genes also showed the presence of retrograde regulation. However, the retrograde response-signaling pathway has not been characterized (COPELAND *et al.* 2009; FREIJE *et al.* 2012). Mammalian cells also show signs of a retrograde response when the mitochondrial respiratory complexes are disrupted (GUHA *et al.* 2009; LAPOINTE and HEKIMI 2008). Both calcium signaling and the nuclear master regulator NFκB, which responds to ROS amongst other stresses, are two potential signaling pathways connected to the retrograde response in mammalian cells. (BUTOW and AVADHANI 2004; SRINIVASAN *et al.* 2010). Plant mitochondria can function as a general sensor to cellular stresses and initiate responses against both abiotic and biotic stresses (SCHWARZLANDER and FINKEMEIER 2013). Abiotic factors the mitochondria are able to sense include, oxygen, calcium, heat, and ROS (SCHWARZLANDER *et al.* 2009; WOODSON and CHORY 2008). Biotic factors include the mitochondria's ability to respond to bacterial or fungal infections (CVETKOVSKA and VANLERBERGHE 2013; MAXWELL *et al.* 2002; RHOADS and SUBBAIAH 2007). These retrograde responses begin with the mitochondria sensing a stress and releasing signals that in turn leads to the expression of nuclear encoded genes.

1.7 Introduction to alternative oxidase

AOX is a pathway that can be used as a model for retrograde regulation studies because AOX is a protein that associates with the mitochondrial inner membrane, but is encoded by a nuclear gene, and its expression is affected by changes in the functional state of mitochondria. All green plants, many fungi (but not *S. cerevisiae*), some protists, some bacteria, and a few animals (but not mammals) contain the AOX pathway (MCDONALD 2008; MCDONALD and VANLERBERGHE 2006). The protein is a di-iron carboxylate protein (see section 1.7.2) that allows electron flow to bypass complex III and IV and transfers

electrons directly from the coenzyme Q pool to molecular oxygen to produce water (Figure 2) (ALBURY *et al.* 2009; BERTHOLD *et al.* 2000; BERTHOLD and STENMARK 2003; MOORE *et al.* 2008). Classical inhibitors of the sETC such as cyanide or antimycin A, can induce the AOX pathway and AOX is sensitive to salicylhydroxamic acid (SHAM), an aromatic hydroxamic acid (SCHONBAUM *et al.* 1971). ATP is produced at a lower rate when electrons flow through the AOX pathway because only complex I is a site of proton pumping and gradient formation when AOX is induced. This pathway allows for the continuation of electron flow when conditions inhibit the sETC (LAMBOWITZ *et al.* 1972).

1.7.1 Alternative oxidase is present in numerous species

Genome sequencing projects revealed that AOX is present in all kingdoms of life, except the archaebacteria (MCDONALD and VANLERBERGHE 2006). When considered in the context of mitochondrial evolution it is also of interest to note that of all extant bacterial species, AOX has only been found in the proteobacterial group (MCDONALD and VANLERBERGHE 2006). Specifically, an AOX homologue was discovered in an α-proteobacterium, which is the ancestor of mitochondria (see section 1.3). The protein is widespread in the fungal group Ascomycota, and Basidiomycota and is also observed in the more basal Zygomycota and Chytrids group (MCDONALD and VANLERBERGHE 2006). However it is absent in *S. cerevisiae* and *Schizosaccharomyces pombe* (VEIGA *et al.* 2003). This demonstrates that although AOX is widespread in nature, loss of the protein has occurred in certain lineages. For some time it was believed the Animalia kingdom also lacked AOX. However it has been discovered in 20 different animal species, representing eight different phyla, but has not been found in mammals (MCDONALD and VANLERBERGHE 2004; MCDONALD and VANLERBERGHE 2006). Putative AOXs have been found in several sponges, which is the most basal animal phylum. It has been suggested that the presence of AOX is the ancestral state because of the basal lineages the protein has been discovered in (MCDONALD and VANLERBERGHE 2006).

1.7.2 Alternative oxidase protein structure

The AOX protein in eukaryotic cells associates with the MIM (DAY and WISKICH 1995; KIRIMURA *et al.* 2006; MCDONALD 2008; VANLERBERGHE *et al.* 1998). Proper targeting of the protein to mitochondria requires the presence of a presequence at the N-terminus of the precursor protein (TANUDJI *et al.* 1999). Prokaryotic cells lack mitochondria and AOXs are instead targeted to the cellular membrane. Prokaryote's AOX lack the N-terminus region containing the targeting sequence and AOX is targeted to the cellular membrane through sequence contained within the protein (FINNEGAN *et al.* 2003). The sizes of mature AOX proteins are around 32 kDa (MCDONALD 2008).

A conserved E-X-X-H iron-binding motif was discovered amongst AOX protein sequences from several species and this motif is found in di-iron proteins; therefore AOX belongs to the di-iron family (ALBURY *et al.* 2009; SIEDOW *et al.* 1995). Di-iron proteins contain a four-helix bundle with two conserved E-X-X-H motifs. This motif coordinates the binding of iron by glutamate and histidine (SIEDOW *et al.* 1995). Early structural models, prior to 1999, based on comparisons of crystal structures of related proteins of AOX available at the time, along with hydrophobicity mapping, lead to the proposal that two transmembrane domains in the N-terminal region anchored AOX into the membrane (MOORE *et al.* 1995; SIEDOW *et al.* 1995) (Figure 4A). In this model the E-X-X-H motif found in the di-iron family was present in the carboxy-terminal hydrophobic domain of AOX. However, weaknesses of this model were that this motif was modeled into helices 1 and 4 as opposed to being found in helices 2 and 4 like other proteins from this family. At the same time the helices proposed in AOX were much shorter than those found in other di-iron proteins. Subsequently, the model was modified in 1999 to be more consistent with the crystal structures of related proteins and an expanding database of structural information for di-iron carboxylate proteins. The Andersson and Nordlund (AN) model retained the di-iron center but the anchoring transmembrane helices disappeared, the helices were longer, and the two iron binding E-X-X-H motifs were moved to helices 2 and 4 (Figure 4B). Each of helix 1 and 3 were also proposed to contain glutamate that

A

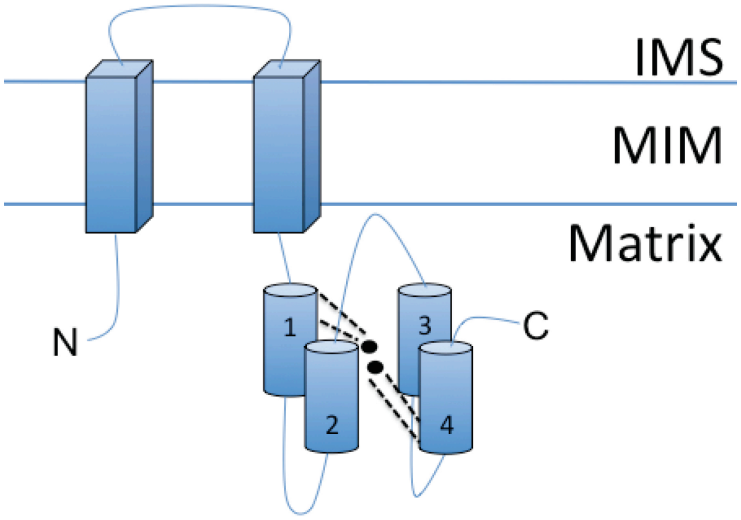

B

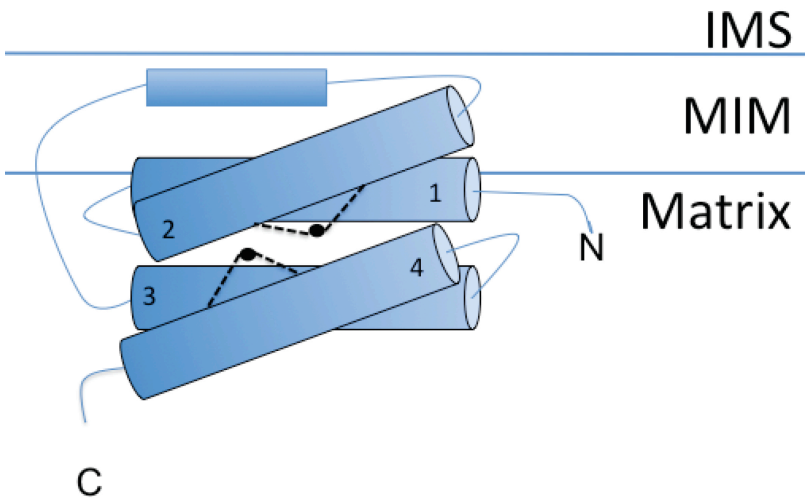

Figure 4. Structural models of AOX. A) The Siedow, Umbach and Moore model (SIEDOW *et al.* 1995). Four α-helices (cylinders) are in the matrix and the protein is anchored to the MIM by two transmembrane domains (cuboids). The E-X-X-H motifs are in helices 1 and 4 and coordinate the binding of iron (black dots). B) The modified Anderson and Nordlund model (ANDERSSON and NORDLUND 1999; BERTHOLD *et al.* 2000). Four α-helices (cylinders) are in the matrix and the protein interacts with one leaflet of the MIM through helix 1 and a hydrophobic region (rectangle). The E-X-X-H motifs that coordinate iron binding (black dots) are found in helices 2 and 4. The four α-helices are longer and this structure matches structural data of other di-iron binuclear proteins.

helped in iron binding (ANDERSSON and NORDLUND 1999). Anchoring of AOX was proposed to occur through interaction with one leaflet of the inner membrane bilayer and the hydrophobic part of the protein thereby making AOX an integral interfacial membrane protein (ANDERSSON and NORDLUND 1999; BERTHOLD *et al.* 2000). A conserved $E(X)_6Y$ motif in the third helix was shown to be required for proper AOX function in *S. guttatum* (NAKAMURA *et al.* 2005). It was confirmed that AOX contains a di-iron center through electron paramagnetic resonance spectroscopy (MOORE *et al.* 2008). More recently, the 3D structure of *Trypanosoma's* AOX, the first crystal structure of any AOX, confirmed the AN model (SHIBA *et al.* 2013). Therefore AOX is classified as a membrane-bound di-iron carboxylate protein (MCDONALD 2008).

1.7.3 Multiple gene families of AOX

A nuclear multigene family divided into two discrete gene subfamilies encodes AOX in higher plants (CONSIDINE *et al.* 2002; MCDONALD 2008; POLIDOROS *et al.* 2009). The first subfamily, termed AOX1, is only expressed in various tissues as a response to stress stimuli and has been found in both monocot and eudicot species. On the other hand, the AOX2 subfamily is constitutively expressed to carry out maintenance functions and appears to be limited to the genomes of dicots (CONSIDINE *et al.* 2002; JUSZCZUK and RYCHTER 2003; POLIDOROS *et al.* 2009). There is variation in the number of AOX genes in different plant species (CLIFTON *et al.* 2006; COSTA *et al.* 2009). In eudicot plants, there is also variation in the copy numbers of each subfamily. In the genomes of dicots usually only one of the subfamily has more than one member (POLIDOROS *et al.* 2009). Taken together, it appears as though AOX has diverged across plant families throughout evolution.

Analysis of fungal genomes has revealed that more than one AOX sequence is present, suggesting that there are gene families of AOX in these organisms (HUH and KANG 2001; MCDONALD and VANLERBERGHE 2006). *N. crassa* has one AOX gene that has a role in cyanide resistant respiration and another gene with sequence similar to this that has an unknown function (TANTON

et al. 2003). On the other hand, no animal or eubacterium has been identified that contains more than one AOX gene (MCDONALD and VANLERBERGHE 2006).

1.7.4 Regulation of alternative oxidase

In many organisms, exposure of certain chemicals or conditions leads to an increase in mRNA levels of AOX, which appears to correlate with an increase in protein or function. Antimycin A, an inhibitor of complex III of the sETC leads to an increase of the mRNA of AOX1 in tobacco and soybean; and AOX1a in *A. thaliana* (DJAJANEGARA *et al.* 2002; SAISHO *et al.* 1997; VANLERBERGHE and MCINTOSH 1996). Similarly, when *N. crassa* cells are grown in the presence of antimycin A there is an increase in *aod-1* (AOX) mRNA (BERTRAND *et al.* 1983). Therefore it appears that the metabolic state of the mitochondria controls the regulation of AOX to some degree.

Several other abiotic and biotic factors have been shown to control the expression of the AOX protein in various organisms. Treating cells with compounds that increase ROS, like H_2O_2, leads to an increase in expression of AOX1 in rice, tobacco, corn, and the fungus *Magnaporthe grisea* (LI *et al.* 2013; POLIDOROS *et al.* 2005; VANLERBERGHE and MCINTOSH 1996; YUKIOKA *et al.* 1998). Low temperature can lead to an increase of AOX1a and AOX1b expression in rice and an increase of AOX1a in *Nicotiana tabacum* (ITO *et al.* 1997; WANG *et al.* 2011). Osmotic stress, ozone and light have all been shown to affect the expression of AOX in different plant species (COSTA *et al.* 2007; EDERLI *et al.* 2006; ELHAFEZ *et al.* 2006; GIRAUD *et al.* 2008). In the blood born pathogen *Trypanosoma brucei*, the stage of development of the organism affects the expression of the AOX protein (CHAUDHURI *et al.* 2006; CHAUDHURI *et al.* 2002). Although it has been shown that many stresses affect the expression of AOX, little is known about how these signals are sensed and lead to the transcription of AOX.

Promoter regions of various AOX genes have been studied uncovering many positive and negative regulatory elements required for expression. The first AOX promoter region studied was of *S. guttatum* and the region was found to

contain a putative TATA box as well as many cis-acting transcriptional elements (RHOADS and MCINTOSH 1993; THIRKETTLE-WATTS *et al.* 2003). These cis-acting elements included presumed sequence recognition sites for zinc fingers and basic leucine zipper proteins. AOX gene families of higher plants have allowed for the comparison of the promoter regions of genes to determine if similar motifs are present (THIRKETTLE-WATTS *et al.* 2003). Soybean AOX1 and AOX2b promoter regions contain both positive and negative regulatory elements within 2 kilobasepair (kbp) of the translational start site. Positive and negative response elements are also present in the AOX1c gene of *A. thaliana* (HO *et al.* 2007). Sequence comparison of soybean's AOX2b and *A. thaliana's* AOX1c revealed many elements of interest that were also found to be functional in the other plant's promoter regions of AOX1. Therefore it is believed that there is some conservation in the control of expression of AOX (HO *et al.* 2007).

At present, few transcription factors have been found that bind to the promoter region of AOX. However, one of the best characterized deals with *N. crassa* and will be discussed below (see section 1.8). More recently, the transcription factor ABI4 was found to be a regulator of the AOX1a gene of *A. thaliana*. Using yeast one-hybrid analysis and electrophoretic mobility shift assay (EMSA), the researchers showed an interaction of ABI4 with a sequence in the promoter region of AOX1a and it was concluded that AOX1a expression is repressed by ABI4 binding (GIRAUD *et al.* 2009).

1.7.5 AOX activation

In angiosperms, AOX is present in the mitochondria either as a covalently linked or non-covalently associated homodimer (MCDONALD 2008; UMBACH and SIEDOW 1993). The linkage of subunits occurs through a disulfide bond that exists either in an oxidized or reduced form. The disulfide bond, when present, results in a less active form of the dimer, whereas when the disulfide bond is reduced a more active form of AOX is present (UMBACH and SIEDOW 1993). Two conserved cysteines (CysI and CysII) are observed in the majority of AOX proteins of angiosperms (BERTHOLD *et al.* 2000). Control of the redox state occurs through

CysI, which is located in the N-terminal region of the angiosperm AOX protein. AOX was unable to form a disulfide bond between dimers when CysI was mutated to an alanine (RHOADS *et al.* 1998; VANLERBERGHE *et al.* 1998). Therefore a mechanism of switching between covalently linked and non-covalently linked occurs through a disulfide bond conversion at CysI and AOX activation occurs when the disulfide bond is reduced.

The presence of α-keto acids, like pyruvate and glyoxylate, has been shown to increase the activation of AOX in angiosperms (MILLAR *et al.* 1993). Pyruvate activation only affects the reduced, active form of the AOX dimer and appears to occur through the CysI residue (MILLAR *et al.* 1993; UMBACH and SIEDOW 1996; VANLERBERGHE *et al.* 1998). Glyoxylate on the other hand appears to regulate AOX activation through an interaction with CysII. However this interaction only occurs if CysI is in the reduced form (UMBACH *et al.* 2006). For full AOX activity to occur the disulfide bonds of the dimer must be in the active reduced form and pyruvate must be present in the cell. The presence of the disulfide bonds between AOX dimer subunits limits the ability of CysI and CysII to bind α-keto acids.

Unlike in angiosperms, organic acids do not appear to activate AOX in other eukaryotes (JARMUSZKIEWICZ *et al.* 2005; MCDONALD 2008; UMBACH and SIEDOW 2000). In some fungi, *N. crassa* included, purine nucleoside 5' monophosphates, like GMP or AMP, appear to have an ability to activate the AOX pathway (UMBACH and SIEDOW 2000). Purine nucleoside 5' monophosphates also appear to affect the amount of AOX observed in the protists *Acanthamoeba casstellani* and *D. disccoideum* (JARMUSZKIEWICZ *et al.* 2002; JARMUSZKIEWICZ *et al.* 2005). Differences in pH optimals between the cytochrome pathway and AOX have been observed in *A. castellani* and *E. gracilis,* which has lead to the hypothesis that pH has an effect on the activation of AOX (CASTRO-GUERRERO *et al.* 2004; JARMUSZKIEWICZ *et al.* 2002). Taken together, these examples suggest that different forms of activation of AOX may be present in different species.

1.7.6 Functions of AOX

Perhaps the simplest function attributable to AOX is its ability to allow the flow of electrons to continue through an alternative pathway if there is a blockage of the sETC. In support of the hypothesis that this represents, an *in vivo* function of AOX is the observation that AOX is not sensitive to chemicals that affect the sETC. In fact, the presence of such chemicals often leads to an increase in expression of AOX (AZCON-BIETO *et al.* 1989; CASTRO-GUERRERO *et al.* 2008; DESCHENEAU *et al.* 2005; HUANG *et al.* 2002). The AOX thus enables glycolysis and respiration to continue by providing an alternative pathway of electron flow. This allows for the turnover of metabolic intermediates in the absence of a functional sETC.

AOX accepts electrons from the coenzyme Q pool and acts as a terminal quinol oxidase to produce water when there are stresses on the mitochondria. This non-proton pumping pathway wastes energy in the form of heat. The release of heat has been suggested to have a role in thermogenesis in some plants. Thermogenesis has been shown to occur in the sacred lotus through an increase in AOX activity (WATLING *et al.* 2006). The process of thermogenesis releases chemical attracts that lure pollinators to flowers (ANGIOY *et al.* 2004). These observations help explain why there is an increase of AOX in thermogenic tissues of plants but do not provide a reason for its presence in non-thermogenic tissue and organisms.

AOX is also believed to have a role in controlling the levels of ROS. The sETC is a major source of ROS. Although ROS produced by the sETC may act as signaling molecules in other parts of the cell, excess ROS can lead to oxidative damage of the mitochondria. Therefore it is believed AOX has a role in lowering the number of electrons in the sETC and thus lowering the amount of ROS generated (MCDONALD 2008; VANLERBERGHE 2013). Many examples show a relationship between an increase in activation of AOX when there is an increase in oxidative stress to a cell. When grown in the presence of H_2O_2, *E. gracilis* increases AOX activity suggesting that oxidative stress leads to the production of the protein (CASTRO-GUERRERO *et al.* 2004; MAGNANI *et al.* 2007). When grown

in the presence of compounds that lead to oxidative stress, *A. fumigatus* increases mRNA of AOX (Magnani *et al.*, 2007). Superoxide anion production is decreased in durum wheat cells expressing AOX (PASTORE *et al.* 2001). These examples all give support of AOX having a role in protecting the cell from oxidative stress.

The AOX protein has been shown to have a role in the pathogenicity of certain fungal pathogens in humans. It was observed in the human airborne pathogen *Aspergillus fumigatus* that loss of AOX led to a decrease in the ability of the fungi to resist oxidative stress *in vitro,* which led to an increase in susceptibility to macrophage killing (MAGNANI *et al.* 2008). Another human pathogen, *Paracoccidioides brasiliensis*, requires AOX, along with other parts of the respiratory chain, for the establishment of infection (MARTINS *et al.* 2011). The role of AOX in increased pathogenicity has also been observed in fungal pathogens of plants. In *Moniliophthora perniciosa* and *Sclerotinia sclerotiorum*, AOX is required for the pathogens to progress through developmental stages of infection by increasing resistance to oxidative stress (THOMAZELLA *et al.* 2012; XU *et al.* 2012).

1.8 Alternative oxidase in *Neurospora crassa*

The nuclear gene that encodes AOX in *N. crassa* is termed *aod-1*. The gene encodes a 362 amino acid protein that has a predicted molecular weight of 41.4 kDa. The size is reduced to 34.7 kDa once the mitochondrial targeting sequence is cleaved off. The AOX protein is not constitutively expressed. Instead the protein is normally expressed when the sETC is disrupted. This is achieved through chemicals, like antimycin A or cyanide that can block the flow of electrons at specific complexes or through mutations affecting proteins of the complexes of the sETC. The AOX of *N. crassa* and other fungi is found associated with the mitochondrial inner membrane as a monomer and it does not contain the N-terminal tail that is conserved in higher plants (UMBACH and SIEDOW 2000).

The first observation of the AOX polypeptide in *N. crassa* was when a radiolabeled protein around 37 kDa in size was increased in mitochondria

following growth of cells in antimycin A or oligomycin (which inhibits ATP synthase (complex V)) compared to uninduced cells (BERTRAND *et al.* 1983). Further analysis used mutants derived from a screen developed to uncover genes in the AOX pathway. Mutants were selected that were sensitive to antimycin A after growth in the mutagen *N*'-nitro-*N*-nitrosoguanidine. Many mutants were generated and these fell into two complementation groups named *aod-1* and *aod-2*. The structural gene was determined to be *aod-1* because in 19 out of the 20 strains in this complementation group, the radiolabelled protein was observed after induction in the presence of Cm, even though cyanide-resistant respiration was absent. Thus, it was assumed that missense mutations had destroyed the function of the protein, even though it was still produced. On the other hand, for strains in the *aod-2* complementation group, no protein was observed for all four strains, suggesting a regulatory role for this gene in the production of the AOX protein (BERTRAND *et al.* 1983). The presence or absence of the protein in these strains were confirmed when a monoclonal AOX antibody from *Sauromatum guttatum* was able to recognize the *N. crassa* polypeptide (LAMBOWITZ *et al.* 1989). Subsequent characterization of several strains in the *aod-1* complementation group revealed that they did have missense mutations in the coding sequence of *aod-1*. The one strain lacking a protein from the *aod-1* group had a frameshift mutation resulting in a premature stop codon and a truncated protein (LI *et al.* 1996).

Northern blot analysis revealed an increase in mRNA levels of *aod-1* when wild type cells were grown in the inducing chemicals antimycin A or chloramphenicol (Cm) (LI *et al.* 1996; TANTON *et al.* 2003). Nuclear run-on assays revealed that the *aod-1* transcript was expressed at low levels in wild type cells when grown in non-inducing conditions (TANTON *et al.* 2003). Therefore, control of the AOX pathway occurs with increased transcription in response to inducing conditions. Western blot analysis has shown no AOX protein in non-induced cultures even when Northern analysis has revealed a low level of *aod-1* mRNA in the same cells. Levels of the protein increase over time with initial presence occurring after roughly 2.5 hr of growth in inducing conditions (TANTON

et al. 2003). Interestingly, on some occasions in some strains grown in non-inducing conditions, an increase in the level of mRNA was observed that approximated the levels in wild type strains grown in inducing conditions, even though the AOX protein is not present nor is cyanide-resistant respiration (DESCHENEAU *et al.* 2005; TANTON *et al.* 2003). Therefore it was suggested that there must be control at the level of translation for AOX production although the molecular mechanism of this is not understood. The finding that several other organisms contained more than one gene encoding AOX (see section 1.7.3) and the completion of the *N. crassa* genome sequence led to the discovery of a gene encoding a protein with 55% identity to the AOX encoded by *aod-1*. The gene was termed *aod-3* (LI *et al.* 1996; TANTON *et al.* 2003). All residues predicted to be involved in iron binding are conserved in *aod-3*. However, Northern analysis using wild type cells grown in inducing or non-inducing conditions was unable to detect mRNA specific for *aod-3*. Therefore the function of *aod*-3 is currently unknown. It is possible that this gene is expressed at a different point in development or under a different stress than the ones analyzed.

Predicted regulatory elements were found conserved upstream of the *aod-1* start site (LI *et al.* 1996; TANTON *et al.* 2003). This includes a cyclic AMP responsive element (CRE) found 802 base pairs (bp) from the start codon of the *aod-1* gene. Electrophoretic mobility shift assay using whole cell extract showed an unknown protein bound to this region. However transformation of the *N. crassa* frameshift *aod-1-7* mutant with plasmids lacking the element revealed no evidence for a role in AOX induction. Deletion studies of the sequence upstream of *aod-1* revealed that the sequence within 255 bp upstream of the start codon had a role in regulating the appearance of *aod-1* mRNA. Therefore it was thought some element of transcriptional control was contained within this sequence sufficient for AOX induction (TANTON *et al.* 2003). A detailed analysis using smaller deletions and linker scanning mutagenesis revealed an alternative oxidase induction motif (AIM) sequence within the 255 bp promoter region of *aod-1*. By transforming the *aod-1* mutant with plasmids containing different lengths of the promoter sequence, a CGG repeat separated by 7 bps was discovered to be

required for efficient expression of *aod-1* (CHAE *et al.* 2007a). This motif is recognized by zinc-cluster transcription factors, which are a class of proteins unique to fungi (MACPHERSON *et al.* 2006).

In an attempt to uncover additional regulatory genes for *aod-1* production, an EMS mutagenesis screen was carried out using a reporter gene fused to 3 kbp of *aod-1* upstream sequence. Four novel genes, *aod-4, aod-5, aod-6*, and *aod-7*, along with another allele of *aod-2*, were identified in the screen as required for AOX induction (DESCHENEAU *et al.* 2005). Further work using genetic mapping coupled to gene rescue experiments led to the identification of the *aod-2* and *aod-5* genes. Both were found to encode zinc-cluster transcription factors. EMSA showed that the DNA binding domains of AOD2 and AOD5 act in concert to bind the AIM in a sequence specific manner (CHAE *et al.* 2007b). A physical interaction was confirmed through pull-down experiments and therefore it was suggested that AOD2 and AOD5 bind as a heterodimer to the AIM (CHAE and NARGANG 2009).

The *Podospora anserina* orthologs of AOD2 and AOD5 (RSE-2 and RSE-3, respectively) were shown to be required for AOX induction when it was observed that strains lacking the individual genes could not induce AOX (SELLEM *et al.* 2009). This was also the case for the AOD2 and AOD5 orthologs (AcuM and AcuK, respectively) in *Aspergillus nidulans* (SUZUKI *et al.* 2012).

The current model for the control of AOX production suggests that inefficient sETC function within the mitochondrion leads to an inducing signal being produced. Since preliminary chromatin immunoprecipitation and qPCR suggest that AOD2 and AOD5 are bound to the *aod-1* promoter in both inducing and non-inducing conditions (Z. Qi, unpublished) it seems likely that this signal (directly or indirectly) leads to AOD2 and AOD5 activation. This in turn leads to transcription of the AOX structural gene, *aod-1*. *aod-1* is transcribed, the mRNA is translated on cytosolic ribosomes, and the protein is targeted to the mitochondrion, alleviating the sETC stress. The nature of the initial signaling molecule and the number of stages to transduce it to AOD2 and AOD5 are not

known. It is also currently unknown what the gene products are for *aod-4*, *aod-6,* and *aod-7*.

1.8.1 Knockout screen for AOX mutants

The initial genes identified in *N. crassa* to play a role in AOX production were found via traditional genetic screens (BERTRAND *et al.* 1983; DESCHENEAU *et al.* 2005; EDWARDS *et al.* 1976). To identify more genes involved in AOX regulation, a new screen was undertaken using single gene knockout (KO) strains available from The Fungal Genetics Stock Center (FGSC). The KOs were created by replacement of gene sequences with a hygromycin resistance cassette in *N. crassa* strains deficient in nonhomologous end joining to ensure homologous replacement (COLOT *et al.* 2006). About 7800 different gene KOs were present in the library at the time of screening. These strains are maintained on 96 well microtiter plates. The screen was done by replica plating the strains onto normal growth medium and growth medium containing antimycin A. If strains were unable to grow or grew very slowly on antimycin A, they were considered to be possible mutants affecting AOX production. These strains were then further characterized by growth in the presence of Cm. In wild type cells, growth in the presence of Cm causes the inhibition of mitochondrial translation and the induction of AOX. Strains that did not grow in the presence of antimycin A and did not fully induce the AOX protein in the presence of Cm were considered to have a knocked out gene involved in AOX regulation.

This screen uncovered 62 genes that affect AOX production to varying extents (NARGANG *et al.* 2012). My project involves further characterizing one of the genes identified: NCU08158, which is annotated as encoding a dual specificity phosphatase (DUSP) protein. Further *in silico* analysis revealed that the predicted protein is a homologue, and likely the ortholog, of *S. cerevisiae* YVH1P (E value = 4e-52, BLASTP).

1.9 Assembly of the ribosome

S. cerevisiae's YVH1 has been suggested to have a role in a late maturation step in 60S ribosome biogenesis (discussed below in section 1.10.1) and therefore it is of importance to discuss the process of the biogenesis of the ribosome [reviewed in (GRANNEMAN and BASERGA 2004; KRESSLER *et al.* 2010; NISSAN *et al.* 2002; TSCHOCHNER and HURT 2003; WILSON and DOUDNA CATE 2012; ZEMP and KUTAY 2007). In yeast and higher eukaryotes, a translating ribosome is made up of a small 40S subunit and a large 60S subunit, which both begin assembly in the nucleus but follow distinct biogenesis pathways as they are processed and mature on their way from the nucleoplasm to the cytoplasm. Four rRNAs, and roughly 80 proteins make up these molecular machines. The creation of ribosomes is a highly complex process that requires the coordinated activity of more than 200 non-ribosomal proteins (trans-acting factors) from start to finish. Coordinated transcription by RNA polymerase I, II, and III occurs to produce a 5S rRNA, a long precursor rRNA (25S/28S, 5.8S and 18S rRNA), and the mRNA for the ribosomal proteins (r-proteins) involved in biogenesis. This activity of the RNA polymerases is tightly regulated and coordinated with the growth conditions in the cell to ensure that production of ribosomes occurs at high efficiency and accuracy. The long precursor rRNA is modified through methylation and pseudouridylation reactions and then associates with trans-acting factors and r-proteins to produce a 90S pre-ribosome in the nucleolus. The 90S pre-ribosome is cleaved through a series of endo- and exonucleolytic reactions to produce the pre-40S and pre-60S subunits of ribosomes. Once cleaved, the two subunits follow distinct and independent pathways in the process of maturation with only a few overlapping proteins. Of importance in this study is the assembly pathway of the 60S subunit and therefore the 40S pathway will not be discussed further.

1.9.1 60S formation from the nucleolus to the cytoplasm

The assembly pathway of the 60S ribosome involves numerous trans-acting factors interacting with r-proteins and rRNA [reviewed in (GRANNEMAN and BASERGA 2004; KRESSLER *et al.* 2010; NISSAN *et al.* 2002; TSCHOCHNER and

HURT 2003; WILSON and DOUDNA CATE 2012; ZEMP and KUTAY 2007). Non-ribosomal proteins process the 27S pre-rRNA into the 5.8S and 25S rRNA found in the mature functional unit. They also attach proteins that interact with the nuclear pore complex to allow for proper translocation of the pre-ribosome out of the nucleus. There are roughly 50 factors associated with the earliest intermediate isolated and more than 5 on the most mature ribosome isolated, suggesting that there are many modifications of the pre-60S subunit on its path from the nucleolus to the cytoplasm. The pre-60S ribosome completes maturation once in the cytoplasm. At this point, many of the factors are recycled back to the nucleus and must be released from the pre-60S subunit to allow it to associate with the 40S subunit and participate in translation. Once matured, ribosomes take part in translation either as free ribosomes in the cytosol or are targeted to the ER as they translate membrane or secreted proteins (EGEA *et al.* 2005; HEGDE and KEENAN 2011; MARTINEZ-GIL *et al.* 2011).

With respect to this thesis, the most important step in the biogenesis of the ribosome is the replacement of MRT4 with P0 during the formation of the ribosome stalk (Figure 5) because YVH1 is defined to have a role in this process (KEMMLER *et al.* 2009; LO *et al.* 2009). The stalk is composed of five proteins in eukaryotes; two copies each of the acidic P1 and P2 proteins and the large P0 subunit (CHIOU *et al.* 2008; LI *et al.* 2010; MAY *et al.* 2012). The N-terminal domain of P0 interacts with a GTPase associated region of the large rRNA subunit. Together with RPL12, P0 directly interacts with the 25S rRNA subunit and allows for the acidic P1 and P2 heterodimers to bind (BRICENO *et al.* 2009; CARDENAS *et al.* 2012; KROKOWSKI *et al.* 2006; LO *et al.* 2009). The C-terminal region of P0 appears to mediate this binding with the N-terminal region of the heterodimers (RODRIGUEZ-GABRIEL *et al.* 2000). Translation factors are targeted to the ribosome by the stalk and this structure is necessary for proper ribosomal function (GONZALO and REBOUD 2003; MOCHIZUKI *et al.* 2012). The stalk has been suggested to be a source of ribosome heterogeneity, which is a form of translational regulation (CARDENAS *et al.* 2012).

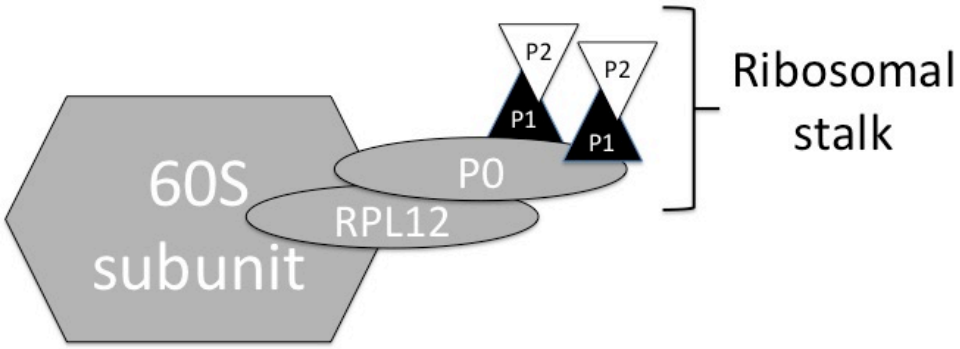

(Adapted from Lo *et al*., 2009)

Figure 5. The ribosomal stalk of the 60S subunit. The ribosomal stalk is composed of one P0 protein and two copies each of the P1 and P2 proteins, which interact with P0 as a heterodimer. P0 interacts with RPL12 and the 25S RNA of the 60S subunit to remain bound to the ribosome. The ribosomal stalk recruits translation factors to the ribosome that are required for proper function.

MRT4 is a nucleolar protein with a protein sequence very similar to that of P0 (ZUK *et al.* 1999). The N-terminal domain is conserved between the two proteins and is necessary for ribosome binding (RODRIGUEZ-MATEOS *et al.* 2009). MRT4 is found in early pre-60S subunits whereas P0 is strictly cytoplasmic and found in mature particles (COLLINS *et al.* 2007; GAVIN *et al.* 2006; KRESSLER *et al.* 2008). It is believed that nuclear MRT4 is the paralogue of cytoplasmic P0 and as the 60S subunit assembles MRT4 is replaced by P0 (RODRIGUEZ-MATEOS *et al.* 2009). The exact mechanism on how this exchange occurs is unclear but it is believed that YVH1 is involved (see below section 1.10) (KEMMLER *et al.* 2009; LO *et al.* 2009).

1.10 The YVH1 DUSP

Typical DUSP proteins are critical regulators of cellular functions. DUSPs have the ability to dephosphorylate phosphotyrosine and phosphoserine/ phosphothreonine residues located on one substrate. The proteins can be further categorized based on sequence similarity and the domains that are present (PATTERSON *et al.* 2009). The YVH1 protein contains a $HC(X)_5R$ phosphatase domain in the N-terminal region and a zinc binding domain which is made up of 7 cysteines and 1 histidine spread out over the C-terminal region (discussed further in section 1.11). The domains present lead YVH1 to be similar to the atypical subgroup of DUSP's, grouped as DUSP12 (PATTERSON *et al.* 2009)

The YVH1 protein was first identified through sequence comparison of an unidentified open reading frame in yeast to a phosphotyrosine phosphatase present in Vaccina virus termed VH1. This conservation was limited to only the phosphatase domain. The protein was found to possess phosphatase activity when expressed in *Escherichia coli.* In yeast, mRNA levels were dramatically induced by nitrogen starvation (GUAN *et al.* 1992). Nitrogen starvation of yeast leads to cells entering meiosis and sporulating. YVH1 was determined to play a role in this process when YVH1 disruption mutants were starved of nitrogen and a delay in sporulation was observed (PARK *et al.* 1996). The delay in sporulation was due to an inability of the disruption strain to synthesize ditryosine, a key component of

ascospore walls, even after a long incubation period (BEESER and COOPER 1999). The YVH1 protein was found to precede a dual specificity kinase, MCK1, in the signal transduction pathway of nitrogen starvation but it was unclear if the two proteins defined contiguous steps in the cascade (BEESER and COOPER 1999). In addition to sporulation, the YVH1 protein was also found to regulate glycogen accumulation when stationary cells lacking the protein failed to accumulate the glucose polymer. Surprisingly, the growth, sporulation, and glycogen accumulation defects were rescued by a construct lacking a catalytically active phosphatase domain suggesting that all pathways were regulated by sequence in the C-terminal domain (BEESER and COOPER 2000).

It is believed that YVH1 plays a role in the biogenesis of ribosomes in yeast. A yeast two-hybrid experiment revealed an interaction of YVH1 with NOP7 (YPH1) (SAKUMOTO *et al.* 2001). NOP7 carries out many functions during the biogenesis of the 60S ribosomal subunit including processing of the 27S pre-RNA (OEFFINGER *et al.* 2002). A study comparing microarray data sets of expression profiles from cell cycle progression, responses to external stresses, and drug treatment, showed YVH1 was expressed at the same time as ribosome biogenesis factors. The promoter region was found to contain a PAC consensus motif, which is a sequence frequently found upstream of subunits of RNA polymerase A and C (DEQUARD-CHABLAT *et al.* 1991; WADE *et al.* 2001). It is unclear if *N. crassa's* YVH1 promoter region contains this sequence. YVH1 was also found associated with purified nucleoplasmic and cytoplasmic 60S pre-ribosomal particles (NISSAN *et al.* 2002). A screen for suppressors of a defective chaperone complex involved in the folding of actin and tubulin uncovered YVH1 along with ribosomal proteins and biogenesis factors (KABIR and SHERMAN 2008). YVH1 was further characterized in its role as a novel ribosome assembly factor when it was found in a different screen looking at suppressors of misfolded membrane proteins that are properly targeted then degraded at the cell membrane. It was shown that loss of YVH1 resulted in a decrease in 60S ribosomal subunits in the cytosol, that HA-tagged YVH1 colocalized with 60S, and that the C-terminal region, not the phosphatase region, was required for normal levels of 60S

and 80S ribosomal subunits (LIU and CHANG 2009). Two separate studies showed that YVH1 localizes to both the nucleoplasm and cytoplasm of the cell and was suggested to be a shuttling protein in the process of the assembly of ribosomes (KEMMLER *et al.* 2009; LO *et al.* 2009). The protein was shown to be necessary for release of MRT4. MRT4 is a highly conserved protein in eukaryotes and its release from the stalk base during ribosome assembly allows P0 to bind and form the base of the ribosome stalk, which is required for proper ribosome activity (see section 1.9.1). Kemmler *et al.*, (2009) demonstrated that this was able to occur even when YVH1 was tethered to the cytoplasm by attachment to a strictly cytoplasmic protein, whereas Lo *et al.*, (2009) showed it could occur when YVH1 was localized to the nucleus, by addition of a nuclear localization sequence to YVH1. These two results suggested that this process could occur in either the nuclear or cytoplasm compartments. GFP-MRT4 was shown to mis-localize to the cytoplasm and remain on the 60S ribosomal subunit in the absence of YVH1 and GFP-YVH1 accumulated in the nucleus when pre-60S nuclear export was impaired. RPL12, a protein that remains bound to the 60S subunit from the early stages all the way to the end during 60S assembly, was found to be required for recruitment of YVH1 to the ribosome (Lo *et al.*, 2009). Lo *et al*. (2009) hypothesized a linear series of events for the assembly of the stalk base in eukaryotes (Figure 6). Lo *et al.*, (2009) were able to demonstrate conservation of this pathway between yeast and humans by transforming the human YVH1 (hYVH1 or DUSP12) into a yeast strain lacking YVH1 and observing the proper localization of GFP-MRT4. A suppressor of *yvh1* disruption was discovered in the *mrt4* gene and the observed phenotypes caused by deletion of *yvh1* were restored (KEMMLER *et al.* 2009; LO *et al.* 2009; SUGIYAMA *et al.* 2011). It has been suggested that the plethora of phenotypes observed in yeast due to loss of *yvh1* may be the indirect result of inefficient ribosome biogenesis.

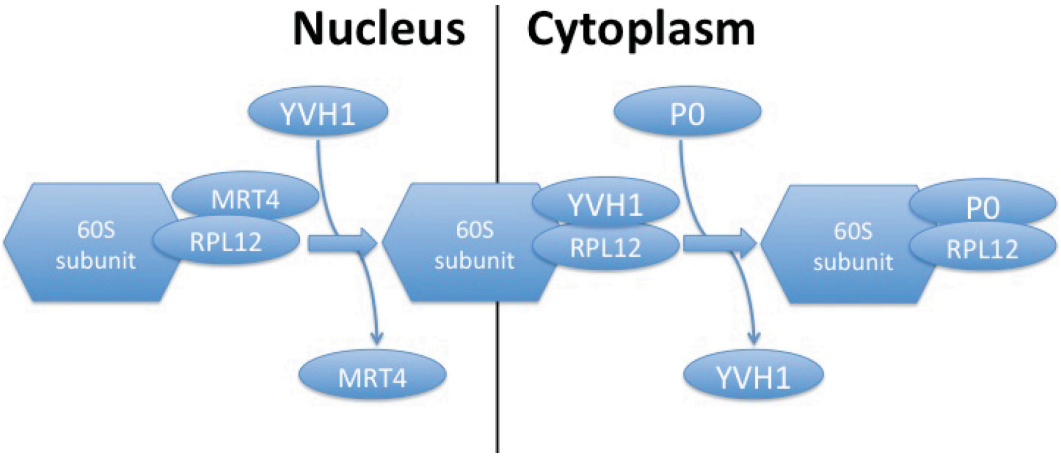

(Adapted from Lo *et al*., 2009)

Figure 6. Model for the role of YVH1 in assembling the ribosome stalk base during ribosome biogenesis. MRT4, which is believed to be a nuclear paralogue of P0, is released when YVH1 binds to RPL12. Loading of P0 (and other proteins not shown) occurs in the cytoplasm when YVH1 is displaced.

1.11 Human YVH1 (hYVH1 or DUSP12)

The human ortholog of YVH1 is not as well characterized as its yeast counterpart. hYVH1 has 33% amino acid identity with YVH1. hYVH1 has phosphatase activity *in vitro*. GFP-tagged hYVH1 localizes to the nucleus and the cytosol, and human copies missing the phosphatase domain, but not the C-terminal region, could rescue the slow growth phenotype observed in yeast lacking *yvh1* (MUDA *et al.* 1999). The C-terminal region, which contains seven conserved cysteines and one conserved histidine, can bind 2 mol of zinc per mol of protein. This region was specific for binding zinc and was termed the zinc-binding domain (MUDA *et al.* 1999). The zinc-binding domain is able to protect the catalytic cysteine in the phosphatase domain from oxidation, and therefore inactivation, in times of severe oxidative stress. The mechanism appears to require that the 2 mols of zinc are released from the zinc-binding domain allowing the protein to form intramolecular disulfide bonds in the zinc-binding domain to protect the phosphatase domain from inactivation. Therefore, it is suggested hYVH1 has an inherent redox defense mechanism capable of protecting the catalytic cysteine of the phosphatase domain from severe oxidative stress (BONHAM and VACRATSIS 2009).

hYVH1 has a role in cell cycle progression. When HEK 293 cells overexpressed FLAG-hYVH1, polyploidy increases as observed through an increase in multinucleated cells at the G_2/M. A blockage at the cell cycle stage G_0/G_1 and an increase in cellular senescence occurs when hYVH1 is knocked down by small interfering RNA. The protein localizes to the nucleus and the cytoplasm and the arrest of the cell cycle at G_0/G_1 can be rescued with the zinc-binding domain and not the phosphatase domain. Furthermore hYVH1 was phosphorylated at 3 different locations with one, Ser^{335}, required for proper localization and function (KOZAROVA *et al.* 2011).

Using a mass-spectrometry based approach, heat shock protein 70 (HSP70) was discovered to be an interacting protein with YVH1. This interaction mapped to the ATPase domain of HSP70 and to the zinc-binding domain of YVH1. Interestingly, it was shown that the phosphatase domain of hYVH1 was

required for thermal stability of hYVH1, finally suggesting a role for the domain. The YVH1 protein localized to the cytosol and upon heat stress, co-localized with HSP70 to the perinuclear region in HeLa cells (SHARDA *et al.* 2009).

1.11.1 A role of hYVH1 in human diseases

hYVH1 has been associated with some human diseases and cancers. hYVH1 is located on the chromosomal region 1q21-q22 in humans. Polymorphisms in and around this region have been linked to Type 2 diabetes across observed populations (DAS *et al.* 2006). Overexpression of hYVH1 has been associated with many forms of cancer. This includes neuroblastoma, retinoblastomas, and leukemia (BIERNACKI *et al.* 2010; GRATIAS *et al.* 2005; HIRAI *et al.* 1999). More recently, in an attempt to further elucidate the role of hYVH1 in human diseases, a cell line has been created that stably overexpresses the protein. Cells observed in this line displayed an increase in cell motility, a decrease in apoptosis, and an up-regulation of a proto-oncogene and a metastasis factor (CAIN *et al.* 2011). hYVH1's role in cell cycle progression in humans and ribosome biogenesis in yeast make it a good candidate gene for further cancer studies.

1.12 YVH1 in other organisms

Although the majority of the research on the function of YVH1 has occurred in yeast and humans, orthologs of the protein have been found in a wide range of organisms. One study in the malaria parasite *Plasmodium falciparum* showed results similar to those observed in yeast (SAKUMOTO *et al.* 2001). The protein was shown to localize to the cytoplasm during growth stages but did migrate to the nucleus during a developmental stage that involved a high amount of transcriptional and translational activity (BOZDECH *et al.* 2003). Therefore the protein was suggested to partake in nucleo-cytoplasmic shuttling. The phosphatase domain was found to be active *in vitro* and required the cysteine within the catalytic domain. Finally, the researchers were able to demonstrate that

the *P. falciparum* YVH1 interacts with the NOP7 ortholog, suggesting a role in ribosome biogenesis (KUMAR *et al.* 2004).

Another study on the opportunistic fungal pathogen *Candida albicans* revealed that the YVH1 KO had a slow rate of hyphal development and cell cycle progression. The virulence of the KO strain when injected into mice was also delayed when compared to wild type. However this delay in virulence could have been due to a delay in growth (HANAOKA *et al.* 2005).

1.13 Objective of this Study

The goal of this study was to understand the role of YVH1 in the alternative oxidase pathway of *N. crassa*. YVH1 was suggested to have a role in AOX production when it was observed that the KO strain for the *yvh1* gene was unable to induce AOX when grown in the presence of inducers of the pathway (NARGANG *et al.* 2012). In an attempt to understand the role of YVH1 in AOX production I studied the KO's response to growth in the presence of the inducers using qPCR techniques and cytochrome spectra analysis. To determine where in the cell the YVH1 protein is localized, I created *N. crassa* transformants that harbored a HA-tagged YVH1 protein either at the N- or C-terminus. Using these strains I fractionated the cell using differential centrifugation, then observed which fraction contained the HA-tagged YVH1, in both inducing and non-inducing conditions. The phosphatase domain and the zinc-binding domain of the protein were studied by mutating key amino acids of the N-HA tagged YVH1 and observing the effect on *N. crassa* cells grown in both conditions. Determining the role of YVH1 in AOX production can help to further understand the control and regulation of AOX in *N. crassa*. To my knowledge this is the first investigation of YVH1 having a role in AOX production.

2 MATERIALS AND METHODS

2.1 Handling of *N. crassa* strains

Table 1 lists the strains used in this study. Unless otherwise stated, handling and growth of the *N. crassa* strains were performed using media and techniques as previously described (DAVIS and DE SERRES 1970). Unless otherwise stated, all growth of *N. crassa* strains was performed at 30°C. To produce conidia, most strains were grown in the dark in 250 ml Erlenmeyer flasks on 50 ml of solid agar containing Vogel's salts with sucrose as the carbon source and trace elements and biotin added (VSuTB) for 48 hr (METZENBERG 2003). Flasks (referred to as "conidia flasks") were then removed from the 30°C incubator to a room temperature bench with constant light to allow formation of conidia. The *Δyvh1* strain and the strain containing mutations in the zinc-binding domain of the *yvh1* gene are deficient in conidiation. They were grown on 25 ml of solid agar VSuTB media in 125 ml Erlenmeyer flasks for 72 hr before being moved to a room temperature bench. Cm, at a final concentration of 2 mg/ml from a 200 mg/ml stock in 95% ethanol, and antimycin A, at a final concentration of 0.5 μg/ml from a 1 mg/ml stock in 95% ethanol, were added to media where indicated. Basta (glufosinate or phosphinothricin), from a 200 mg/ml stock in 95% ethanol was used at a final concentration of 200 μg/ml. Bleomycin, when required, was used at a final concentration of 1.0 μg/ml.

2.2 Measurement of growth rates

Conidia from the *N. crassa* strains being investigated were harvested in 50 ml of sterile, distilled water per conidia flask and spun in a clinical centrifuge at max speed for 2 min (International Equipment Company, Needham Heights, MA) to pellet the conidia. Conidia were washed one time in sterile, distilled water, resuspended in 1 ml of sterile, distilled water and transferred to a 1.5 ml Eppendorf tube. The concentration of conidia was determined by counting dilutions using a hemacytometer visualized under a microscope. Suspensions with final concentrations of 10^6, 10^5, and 10^4 conidia/ml were made and 10 μl of each

dilution was spotted on plates containing standard Vogel's sorbose medium (VSoTB) with or without antimycin A. Minimal media plates were incubated for 48 hr and minimal media plates containing antimycin A were incubated for 68 hr.

2.3 Transformation of *N. crassa* and isolation of working strains

DNA was transformed into conidia of *N. crassa* by electroporation using the procedure of HOPPINS *et al.* (2007b). One to two week old conidia were harvested, washed three times with 50 ml of ice cold, sterile 1 M sorbitol, and suspended at a final concentration of 2 to $2.5x10^9$ conidia/ml. The conidia were aliquoted into 40 µl (roughly $1x10^8$ conidia) samples and 2-5 µg of linearized plasmid DNA in 5 µl of water was added. The suspension was mixed and pipetted into an electroporation cuvette. Cuvettes were placed on ice for 5 min then electroporation was performed at 2.1 kV, 475 Ω, and 25 µF (ECM 630 BTX, San Diego, CA) with a time constant of roughly 11 ms. 1 ml of 1 M sorbitol was added immediately to the cuvette and the mixture was transferred to an Eppendorf tube and placed in a 30°C incubator for 30-60 min. 50 µl or 250 µl aliquots of the electroporated conidia suspension were added to 50 ml of 45ºC top agar (VSoTB containing 1 M sorbitol and the appropriate antibiotic). The solution was mixed and 10 ml was spread over plates of agar medium containing the same ingredients as the top agar except lacking the 1 M sorbitol. The plates were then incubated at 30°C until transformed colonies were visible (3-5 days). Sterile glass Pasteur pipettes were used to transfer single colonies from the plates to VSuTB agar slants containing half the concentration of antibiotic used for the initial selection, to allow for better conidiation. The slants were placed in a 30°C incubator until mycelium covered the surface of the agar and then were removed to room temperature to allow conidia to form. Conidia were streaked out onto VSoTB agar media containing the appropriate antibiotic at full strength and incubated at 30°C to obtain single colony isolates. Single colonies were then picked with sterile glass pipettes and transferred to VSuTB agar slants lacking the antibiotic and grown to obtain conidia for further analysis.

2.4 Creation of N- and C- YVH1 3xHA tagged wild type and mutant plasmids

The *yvh1*$^+$ gene (predicted size of genomic sequence is 2290 bp) was amplified through PCR from a cosmid (pMOcosX X6H9), which contains genomic sequence of *N. crassa* encompassing the *yvh1*$^+$ locus. The cosmid was obtained from the Fungal Genetics Stock Center (FGSC). The nearest genes upstream and downstream to *yvh1* are located 895 and 1066 bp away, respectively, as determined by inspection of reading frame predictions in the genome and RNA-seq data. Primers designed to amplify the predicted coding region plus 617 bp upstream from the start codon to 518 bp downstream of the stop codon of the *yvh1* gene were constructed with *AscI* restriction sites at the 5′ ends (Table 2). The insert was 2,596 bp long and contained 1 intron. The amplified fragment was digested with *AscI* and ligated into an *AscI* digested modified bluescript plasmid (pBS520-*AscI*), which also contained a bleomycin resistance gene. After screening plasmids isolated from *E. coli* through restriction analysis and sequencing of the *yvh1*$^+$ gene, plasmid p100B5-*AscI* was chosen for future work.

Primers were designed to create *NotI* sites either after the start codon at the 5′ end or before the stop codon at the 3′ end, using site directed PCR mutagenesis. Plasmids p100B5-5′*NotI* and p100B5-3′*NotI* were confirmed through sequencing and used for further work. Three repeats of the hemaglutinin (HA) epitope (YPYDVPDYA) was obtained from a plasmid (FN-*NotI*-HA3) that was synthesized by Integrated DNA Technologies (IDT, Coralvile, Iowa). The HA epitope was removed from the plasmid by digestion with *NotI* and cloned into the *NotI* digested *yvh1*$^+$ containing plasmids. The *yvh1*$^+$ coding sequence was confirmed through sequencing and the resulting plasmids were termed either p5′HA-100B5 or p3′HA-100B5. Initial attempts at transformation of *N. crassa* using bleomycin as the selectable marker were unsuccessful. Therefore the 3xHA tagged *yvh1*$^+$ was cut out of p5′HA-100B5 and p3′HA-100B5 with *AscI* and cloned into pBARSK1, which contains basta as a selectable marker (PALL and BRUNELLI 1993). Plasmids chosen for further work were pBAR-5′HA and pBAR-3′HA. Once plasmids were confirmed through sequence analysis, the HA-tagged

wild type copy of *yvh1*$^{+}$ was linearized and transformed into *N. crassa* as described above, using basta as the selectable antibiotic.

To create the phosphatase domain mutant (P-mutant) and the zinc binding domain mutant (Z-mutant), primers were designed to change the coding sequence of N-HA::*yvh1*$^{+}$ in pBAR-5′HA at specific regions via site directed PCR mutagenesis. The amino acid changes for the P-mutant were histidine 149 to glutamine (H149Q), cysteine 150 to serine (C150S), and arginine 156 to glutamine (R156Q). These changes were in the conserved $HC(X)_5R$ phosphatase domain of the protein. To create the Z-mutants, a pair of cysteines of the zinc-binding domain in the C-terminal region were mutated to serines. The cysteines are located at position 340 and 345 in the C-terminal domain of the YVH1 protein (C340S, C345S). Once the mutations were confirmed through sequencing, transformation of *N. crassa* was carried out as outlined.

2.5 Isolation of mitochondria, cytosolic, and post-mitochondrial pellet fractions

N. crassa cultures were grown for specified times at 30°C with aeration by shaking in liquid VSuTB media with or without Cm in baffled flasks. Crude mitochondria were isolated as previously described (NARGANG and RAPAPORT 2007). Mycelium was harvested onto a filter paper through vacuum filtration and weighed. Samples were ground for one minute using a mortar and pestle with sand equal to the weight of the mycelium (Sigma-Aldrich, St. Louis, MO), and SEMP isolation buffer (1 ml/g of mycelium) (0.25 M sucrose; 10 mM MOPS, pH 7.2; 1 mM EDTA; 1 mM phenylmethylsulphonyl fluoride (PMSF)) containing protease inhibitors (final concentrations of 2 µg/ml aprotinin, 1 µg/ml leupeptin and 1 µg/ml pepstatin A). After grinding, another volume of SEMP plus protease inhibitors (1 ml/g of mycelium) was added. The slurry was centrifuged at 3,600 x g (5,000 rpm) for 5 min twice, keeping the supernatant each time, using a SA-600 rotor of a Sorvall RC-5C Plus centrifuge (Sorvall, Mandel Scientific, Guelph, ON). The supernatant, which contained both cytosol and mitochondria, was pelleted by centrifuging at 21,000 x g (12,000 rpm) for 20 min, using the same

rotor and centrifuge as previous centrifugation. If required, the supernatant was saved as a crude cytosolic fraction for further use (see below). The pellet was washed by resuspending in 5 ml of SEMP and repeating the 21,000 x g centrifugation. The pellet was resuspended in 1 mL of SEMP, transferred to a microcentrifuge tube, and centrifuged at top speed in a Eppendorf tabletop centrifuge (13,000 rpm). The supernatant was poured off and the mitochondrial pellet was resuspended in SEMP plus protease inhibitor. The amount of buffer added depended on the size of the pellet but ranged from about 200 to 1000 µl. These mitochondria were classified as "crude" mitochondria.

To obtain gradient purified mitochondria for the fractionation experiments, the mitochondria were further purified through a sucrose gradient. Crude mitochondria were pelleted and resuspended in 1.5 ml of SEMP isolation buffer containing 60% sucrose and transferred to a thick wall polycarbonate ultracentrifuge tube (Beckman Instruments Inc., Palo Alto, CA). 1.5 mL of SEMP with 55% sucrose was layered over the 60% layer, and 0.75 ml of 44% sucrose SEMP was layered over the 55% layer. The sample was centrifuged at 75,000 x g (35,000 rpm) for 2 hr in a TLA110 rotor in a Beckman Optima^{TM} MAX ultracentrifuge (Beckman Instruments, Palo Alto, CA). The mitochondria were isolated from the interface of the 44% and 55% SEMP layers, placed in an Eppendorf tube, and diluted with roughly 1 ml of SEMP (enough to fill the 1.5 ml microfuge tube). The sample was then pelleted for 30 min at top speed (13,000 rpm) using a refrigerated Eppendorf tabletop centrifuge and resuspended in a volume of SEMP, which depended on the size of the pellet (usually between 200 and 1000 µl).

The crude cytosolic fraction obtained from the crude mitochondria isolation described above was further purified through centrifugation. The crude cytosolic fraction was spun twice for 30 min at 32,500 x g (15,000 rpm) in an SA-600 rotor of a Sorvall RC-5C Plus centrifuge discarding the pellet each time. This supernatant was used as the crude cytosolic sample in some experiments. For subcellular fractionation experiments this fraction was further centrifuged to isolate the cytosolic and PMP fraction, which contains fragmented endoplasmic

reticulum and other organelles. 1.5 ml of the crude cytosolic fraction was placed in a polyallomer Beckman ultracentrifuge tube (Beckman Instruments Inc., Palo Alto, CA). The sample was centrifuged at 130,000 x g (48,000 rpm) for 1.5 hours in a TLA55 rotor in a Beckman Optima^{TM} MAX ultracentrifuge. 800 µl of the supernatant was collected for the cytosolic fraction and the pellet was resuspended in 100 to 200 µl of SEMP plus protease inhibitors as the post-mitochondrial pellet (PMP). All centrifugations were performed at 4ºC.

2.6 Extraction and purification of nuclei

The isolation of nuclei was accomplished with a modified version of a previously described protocol (TALBOT and RUSSELL 1982). Strains were grown by bubbling with forced air sterilized by a filter through 1.5 L of VSuTB liquid media at 30°C and harvested through vacuum filtration. The pad of mycelium was weighed and then ground in the presence of liquid nitrogen into a very fine powder. 2 volumes (v/w) of buffer A (1 M sorbitol, 5% [w/v] Ficoll 400, 20% [v/v] glycerol, 5 mM $MgCl_2$, 10 mM $CaCl_2$, 1% [v/v] Triton-X-100, adjusted to pH 7.5) with 1 mM PMFS and protease inhibitors (describe in section 2.5) were added per gram of mycelium and the mixture was allowed to thaw at room temperature for roughly 15 min. The homogenate was then passed twice through miracloth (Calbiochem) to remove the bulk of the cellular debris. Further cellular debris was removed by centrifugation at 2,400 x g (4070 rpm) twice for 10 min using a SA-600 rotor of a Sorvall RC-5C Plus centrifuge with the supernatant being saved after each spin. To obtain crude nuclei the solution was centrifuged for 50 min at 9,000 x g (7890 rpm) using same rotor as previous centrifugation. The supernatant was carefully removed and discarded following the spin. The white pellet was resuspended in ice cold buffer B (1 M sucrose, 50 mM Tris-HCl [pH 7.5], 5 mM $MgCl_2$, 10 mM $CaCl_2$, 1% [v/v] Triton X-100) with 1 mM PMSF and the protease inhibitors (described in section 2.5). Roughly 1 ml of buffer B was added per 5 g (v/w) of starting mycelium. A Percoll:sucrose solution was created by adding 9 parts (v/v) of Percoll (GE Healthcare) to 1 part (v/v) of 2.5 M sucrose. 2 ml of Percoll:sucrose solution was added to 1 ml of nuclei suspended in

Buffer B in a 3.2 ml thick wall polycarbonate ultracentrifuge tube (1 tube per 5 g of starting mycelium) and mixed through gentle pipetting. The tubes were placed in a TLA110 rotor in a Beckman Optima^{TM} MAX ultracentrifuge and spun for 45 min at 58,000 x g (38,000 rpm). The nuclei banded in the middle of the gradient and could be seen as white bands. The bands were removed and combined to a single thick wall polycarbonate tube and spun for 2 hrs at 100,000 x g (49,000 rpm) to remove the Percoll. The white nuclei settled on top of the Percoll pellet. The nuclei were removed and added to an Eppendorf tube and washed in suspension buffer (25 mM sucrose, 50 mM Tris-HCl [pH 7.5], 5 mM $MgCl_2$, 10 mM $CaCl_2$) once by pelleting in an Eppendorf tabletop centrifuge at max speed (13,000 rpm). The final pellet was suspended in 50 to 200 µl of suspension buffer.

2.7 Whole cell extracts

Liquid media was inoculated with conidia and cultures were aerated by shaking in baffled flasks for 20 hr at 30°C. Mycelium were harvest by vacuum filtration and 1 gram of mycelium was ground with 1 gram of sand (Sigma-Aldrich, St. Louis, MO) and 1 ml of SEMP containing 2% sodium dodecyl sulfate (SDS). Samples were centrifuged for 10 min at 3600 x g (5,000 rpm) using a SA-600 rotor of a Sorvall RC-5C Plus centrifuge to remove cellular debris and sand. The supernatant was collected and protein concentrations were determined using the BCA-200 protein assay system (Pierce, Rockford, IL), which is tolerant of SDS.

2.8 Quantitative real time polymerase chain reaction (qPCR)

All qPCR data shown is based on 4 biological samples each tested in three technical replicates. Conidia from specified strains were inoculated into liquid media and were grown through aeration by shaking in baffled flasks for the specified time at 30°C with or without Cm. Bubbling of 2 L Erlenmeyer flasks containing 1.5 L of VSuTB liquid media was used to isolate mitochondria at the same time as RNA isolation for the 18 hr plus Cm samples. Roughly 100 mg of mycelium was harvested through vacuum filtration and flash frozen in liquid

nitrogen. Total RNA was isolated using the RNeasy Kit from Qiagen following the manufacture's instructions for fungi (Qiagen Inc., Santa Clarita, CA). RNA integrity was checked using a BioAnalyzer 2100 nano chip (Agilent Technologies, Mississauga) following the manufacture's instructions. cDNA was reverse transcribed from RNA (1 µg/reaction) using superscript III (Invitrogen, Carlsbad, CA) following the manufacture's directions. qPCR (StepOnePlus, Applied Biosystems, Foster City, CA) used the synthesized cDNA and PowerSYBR Green PCR master mix (Applied Biosystems, Foster City, CA) with 5 ng of cDNA template at a primer concentration of 200 nM in a total sample volume of 10 µl in a 96-well reaction plate. Samples were normalized to *gapdh*, a glycolysis enzyme (NICHOLLS *et al.* 2012), based on the ΔΔCT method.

2.9 Cytosolic ribosome isolation

Ribosomes were isolated through a combination of two previously published techniques (LO *et al.* 2009; SCHLITT and RUSSELL 1974). 5 grams of mycelium were ground in the presence of an equal weight of Sigma sand (Sigma-Aldrich, St. Louis, Mo) and 6 ml of ribosome buffer (20 mM Tris-HCl [pH 7.5], 50 mM NaCl, 10 mM $MgCl_2$, 0.25 M ultra pure sucrose) containing 1 mM PMSF and protease inhibitor (described in section 2.5) into liquid slurry. To remove cellular debris the sample was centrifuged for 3,600 x g (5,000 rpm) for 5 min using a SA-600 rotor of a Sorvall RC-5C Plus centrifuge. The supernatant was spun twice at 32,000 x g (15,000 rpm) for 20 min using a SA-600 rotor of a Sorvall RC-5C Plus centrifuge, avoiding transfer of the liquid scum at the top of the supernatant each time. 0.05 volume of 20% Triton-X-100 was added and mixed on ice for 5 min. The mixture was transferred into a polyallomer Beckman ultracentrifuge tube. A clarifying spin was done for 30 min at 70,000 x g (40,000 rpm) in a TLA55 rotor in a Beckman Optima^{TM} MAX ultracentrifuge. The pellet was resuspended in 200 to 400 µl of ribosome buffer and labeled as the clarifying spin (CS). 1 ml of the supernatant from the clarifying spin was layered over a 1 ml sucrose "cushion" (20 mM Tris-HCl [pH 7.5], 8 mM $MgCl_2$, 100 mM KCl, 1 M ultrapure sucrose) in a thick wall polycarbonate ultracentrifuge tubes for the

TLA110 rotor and ultracentrifuged at 300,000 x g (80,000 rpm) for 2 hr in a Beckman Optima™ MAX. 200 µl was taken from the top for the supernatant fraction. The rest of the liquid was removed and the sides of the tube were washed with sterile water. The clear pellet was resuspended in 50 µl of ribosome buffer and labeled as the ribosomal pellet.

The yeast RPL3 antibody developed by Jonathan R. Warner was obtained from the Developmental Studies Hybridoma Bank developed under the auspices of the NICHD and maintained by The University of Iowa, Department of Biology, Iowa City, IA 52242.

2.10 Spectral analysis

Crude mitochondria were isolated as described above after growth in the presence or absence of Cm. Final mitochondrial pellets were suspended in 1 ml of SEMP. To lyse the mitochondria an equal volume of 10 mM MOPS, pH 7.2 containing 5% sodium deoxycholate was added. The sample was gently mixed and clarified by centrifugation in an Eppendorf tabletop centrifuge at top speed (13,000 rpm) for 5 min. The supernatant was removed and placed in new microfuge tubes. Two cuvettes were filled with equal amounts of the mitochondrial solution. To oxidize the reference sample, a few crystals of potassium ferricyanide were added. The other sample was reduced with a few crystals of sodium dithionite. The samples were placed in a Biochrom Ultrospec 3100 pro spectrophotometer (GE Healthcare) and the absorbance from 500 nm to 650 nm was analyzed to create the oxidized vs. reduced spectra. Original graphs were traced with a pencil, scanned into Adobe Photoshop, and edited in Adobe Illustrator to produce the figures.

2.11 RNA-seq

The samples tested were *Δyvh1* and the control strain grown in VSuTB plus Cm for 12 hrs. Total RNA was isolated and integrity was checked as described above (section 2.8). The cDNA library was created following the Low Sample Protocol of TruSeq™ RNA Sample Preparation v2 Guide (Illumina, San

Diego, CA). The library was sequenced by Delta Genomics (Edmonton, AB) using a HiScan^{TM}SQ sequencing instrument (Illumina, San Diego, CA). Statistics were calculated by Kirsten Smith in Dr. Michael Freitag's lab at Oregon State University.

2.12 General procedures and other techniques

Standard procedures were followed for DNA agarose gel electrophoresis, transformation of *Escherichia coli*, isolation of bacterial plasmid DNA, cloning, restriction digests of plasmid DNA, and site directed PCR mutagenesis of plasmid DNA (SAMBROOK and RUSSELL 2001). Sodium dodecyl sulfate polyacrylamide gel electrophoresis (SDS-PAGE) (LAEMMLI 1970) and western blotting (GOOD and CROSBY 1989) were performed as previously described. Proteins were prepared for SDS-PAGE by dissolving in cracking buffer (0.06 M Tris-HCl, pH 6.8; 2.5% SDS; 5% sucrose; 5% β-mercaptoethanol). Western blot detection used the LumiGLO chemiluminescent substrate system (Mandel Scientific Company Inc., Guelph, ON). Protein concentration was determined using the colourimetric Bio-Rad protein assay kit (Bio-Rad, Hercules, CA). For automated sequencing, a BigDye Terminator cycle sequencing kit (Version 3.1) was used. The reactions were analyzed using a model 3730 DNA Analyzer (Applied Biosystems, Foster City, CA) in the Molecular Biology Service Unit (MBSU) of the Department of Biological Sciences. Bacterial plasmid DNA was isolated using Qiagen mini-prep column spin kits (Qiagen Inc., Santa Clarita, CA) following the manufactures manual.

2.13 Oligonucleotides and plasmids

Table 2 and table 3 list the oligonucleotides and plasmids used, respectively, in this study.

Table 1. Strains used in this study

Strain	Comments	Origin
NCN251	Mating type A; laboratory wild type strain	FGSC #2489
Δyvh1	Mating type A; a 1949 bp deletion of *yvh1*$^+$ by replacement with a hygromycin resistance cassette	FGSC #19644
N-HA YVH1	*Δyvh1;HA::yvh1*$^+$*(EC)* Contains an ectopic copy of genomic *yvh1*$^+$ with an N-terminal 3xHA tag. Created by transformation of *Δyvh1* with linearized plasmid pBAR-5′HA (see Table 3). Also basta and hygromycin resistant. Isolate #2	This study
C-HA YVH1	*Δyvh1;HA::yvh1*$^+$*(EC)* Contains an ectopic copy of genomic *yvh1*$^+$ with a C-terminal 3xHA tag. Created by transformation of *Δyvh1* with linearized plasmid pBAR-3′HA (see Table 3). Also basta and hygromycin resistant. Isolate #1	This study
N-HA YVH1 Phosphatase mutant (N-HA P-8)	*Δyvh1;HA::yvh1*$^{P\text{-}mut}$*(EC)* Contains an ectopic copy of genomic *yvh1* with amino acids H149, C150, and R156 in the $HC(X)_5R$ dual specificity phosphatase domain mutated to $QS(X)_5Q$. Created by transformation of *Δyvh1* with linearized plasmid pBAR-5′HA-P-mut. Isolate #8	This study
N-HA YVH1 Zinc binding mutant (N-HA Z-9)	*Δyvh1;HA::yvh1*$^{Z\text{-}mut}$*(EC)* Contains an ectopic copy of genomic *yvh1* with cysteine 340 and 345 of the zinc binding domain mutated to serine. Created by transformation of *Δyvh1* with linearized plasmid pBAR-5′HA-Z-mut. Isolate #9	This study

Table 2. Oligonucleotides

Primer name	**Sequence (5′ - 3′)**	**Comments**
bdNCU08158-F	GATTTATAGGCGC GCCGCCCTGGGCC ATCCCCTCTGTTA TCCCGTCG	Forward primer used to amplify *yvh1*$^{+}$ including 617 bp of 5′ region upstream of start codon. *AscI* site in 5′ end
bdNCU08158-R	TTCTAGATGGCGC GCCCGGAGGGAA ACTGAAGCATCAA AGGGCC	Reverse primer used to amplify *yvh1*$^{+}$ including 518 bp of 3′ region downstream of stop codon. *AscI* site in 5′ end
5′not1NCU08158bd	/5Phos/GCCCGGAG AGACCGGTCGCAA TGGCGGCCGCGCG CTAAATCGCATCA ATGG	Insert *NotI* site into *yvh1*$^{+}$ coding region after the start codon
3′not1NCU08158bd	/5Phos/GGTGGACC TAAGGAGAACCTA GCGGCCGCTGAAT GGATTCTTCTTTTG TGGG	Insert *NotI* site into *yvh1*$^{+}$ coding region before the stop codon
(1)bdseqNCU08158	ACGAGCAACCCGC CTT	*yvh1* sequencing
(2)bdseqNCU08158	CGTGGAGGAGGCC GAT	*yvh1* sequencing
(3)bdseqNCU08158	CAGGAGACGACG CGGT	*yvh1* sequencing
(4)bdseqNCU08158	ATGAGGCGACGTC GGC	*yvh1* sequencing
phosphatasedomain	/5Phos/AACCCGGC GCCGTCCTAGTCC AGAGCGCCATGGG CAAATCTCAATCC GTCTCCGCCATCG TCGCCTAC	*yvh1* phosphatase domain mutations H149Q, C150S, R156Q
NCU08158 C340,345/S	/5Phos/GAGCTGGA GGGCAGACTAACG TCTCCGAACCAAA AGTCTCTGGCGTC CGTGGGGAGGTA	*yvh1* zinc binding domain mutations C340S, C345S

aod-1 (θ *aod-3*) forward qPCR.	CCACTTCCTTACA TCCAACACAGA	*aod-1*$^{+}$ qPCR forward primer. Base 116 to 139. Designed to not align with *aod-3* sequence
aod-1 (θ *aod-3*) reverse qPCR;	TCAGTCGAGTAAC GCTTGTTGTC	*aod-1*$^{+}$ qPCR reverse primer. Base 174 to 196. Designed to not align with *aod-3* sequence
gapdh forward qPCR	CATTGAGCACGAT GACATCCA	*gapdh*$^{+}$ qPCR forward primer. Base 63 to 83.
gapdh reverse qPCR	GGAGCATGTAAGC AGCGTACTTG	*gapdh*$^{+}$ qPCR reverse primer. Base 117 to 139

Table 3. Plasmids used in this study

General Plasmids

Plasmid name	**Origin or source**	**Comments**
pMOcosX X6H9	FGSC	Cosmid containing *N. crassa* genomic sequence including *yvh1*$^{+}$; Hygromycin and ampicillin resistance
pBS520-*AscI*	Frank Nargang	Modified Bluescript with *NotI* site mutated to *AscI*; Bleomycin and ampicillin resistance
pBARSK1	FGSC	Modified pUC with polylinkers from pGEM and Bluescript vectors; Basta and ampicillin resistance (PALL and BRUNELLI 1993)
pBARSKI-*AscI*	Frank Nargang	*NotI* sites mutated to *AscI* in pBARSK1; Basta and ampicillin resistance
FN-*NotI*-HA3	IDT Technologies	Modified pUC that contains three repeats of hemagglutinin (HA) epitope (YPYDVPDYA) flanked by *NotI* sites; Kanamycin resistance

yvh1 containing plasmids

Plasmid name	**Origin or source**	**Comments**
p100B5-*AscI*	This study	*yvh1*$^{+}$ fragment amplified from pMOcosX X6H9 using primers bdNCU08158-F and bdNCU08158-R cloned into pBS520-*AscI*
p100B5-5′*NotI*	This study	*NotI* site introduced after start codon of *yvh1*$^{+}$ in pBS520-*AscI*
p100B5-3′*NotI*	This study	*NotI* site introduced before stop codon of *yvh1*$^{+}$ in pBS2520-*AscI*

p100B5-5′HA	This study	*NotI* digested 3xHA epitope from FN-*NotI*-HA3 cloned into *NotI* digested p100B5-5′*NotI*
p100B5-3′HA	This study	*NotI* digested 3xHA epitope from FN-*NotI*-HA3 cloned into *NotI* digested p100B5-3′*NotI*
pBAR-5′HA	This study	5′HA::*yvh1*$^{+}$ plus upstream and downstream regulatory sequence cut out of p100B5 5′HA using *AscI* and cloned into *AscI* digested pBARSKI-*AscI*
pBAR-3′HA	This study	3′HA::*yvh1*$^{+}$ plus upstream and downstream regulatory sequence cut out of p100B5-3′HA using *AscI* and cloned into *AscI* digested pBARKS1-*AscI*
pBAR-5′HA-P-mut	This study	Coding sequence of phosphatase domain of *yvh1* in pBAR-5′HA mutated so amino acid changes are H149Q, C150S, R156Q
pBAR-5′HA-Z-mut	This study	Coding sequence of zinc-binding domain of *yvh1* in pBAR-5′HA mutated so amino acid changes are C340S and C345S

3 RESULTS

3.1 A dual specificity phosphatase protein has a role in AOX production in *N. crassa*

The protein coding sequence of *N. crassa yvh1* is 1317 bp long, is made up of two exons, and encodes a 439 amino acid, 47.2 kDa protein (Figure 7A). *N. crassa* YVH1 shares 31% amino acid sequence identity with *S. cerevisiae* YVH1 (E value = 4e-52, BLASTP) and 29% identity with DUSP12 or hYVH1, the *Homo sapiens* ortholog (E value = 1e-31, BLASTP) (Figure 7B). As described in the Introduction, the *yvh1* KO strain (*Δyvh1*; Table 1) was identified in a screen of the *N. crassa* KO library as having defects in AOX production. To further examine this defect I grew the strain in the presence of the AOX inducer Cm (see section 1.8.1) over the course of various time points and analyzed for the presence of AOX through western analysis. The control strain (NCN251; Table 1) had similar levels of AOX at all time points tested from 16 to 48 hr. On the other hand, AOX was not observed in *Δyvh1* until between 20 to 24 hr (Figure 8A). The level of the protein slowly increased over the time points examined but the amount never fully reached the same level as the control at 48 hr of growth. To examine the ability of *Δyvh1* to grow using AOX for respiration, conidia were spotted on media containing antimycin A, which blocks the sETC at complex III. Relative to a negative control lacking AOX, *Δyvh1* exhibited a small amount of growth in the presence of antimycin A. However the growth rate was much slower than the wild type control strain (Figure 8B).

3.2 *aod-1* transcript levels in the *Δyvh1* strain

YVH1 has been shown to be a protein involved in the late maturation step of ribosome biogenesis in *S. cerevisiae* (KEMMLER *et al.* 2009; LO *et al.* 2009). Therefore, I hypothesized that under inducing conditions there might be a delay of translation of *aod-1* transcripts leading to the AOX deficiencies described above. If this were the case, levels of the *aod-1* transcript might be expected to be similar to those in a control grown under the same conditions. qPCR was performed to

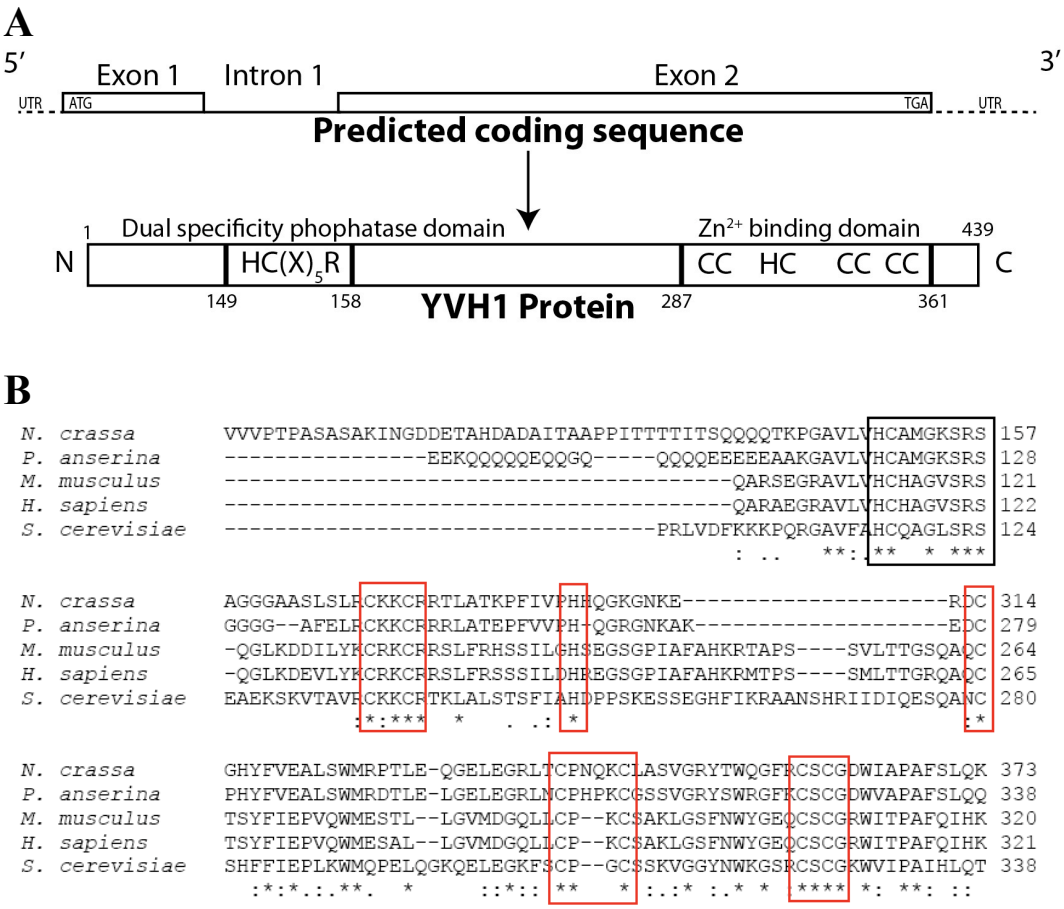

Figure 7. Structure of the *yvh1* predicted coding sequence and protein. A) The *yvh1* gene is located on the 7th chromosome in the *Neurospora crassa* genome. The protein coding sequence is 1317 nucleotides long and is composed of 2 exons that are separated by 1 intron in the genomic sequence. The protein encoded is 439 amino acids long and contains a $HC(X)_5R$ dual specificity phosphatase domain located in the N-terminal region and a zinc-binding domain containing seven Cys and one His residues in the C-terminal region. B) Amino acid similarity between the functional domains of YVH1 proteins. The amino acid sequence of YVH1 of *Neurospora crassa* was aligned to *Podospora anserina* (E value = 3e-156, BLASTP), *Mus musculus* (E value = 1e-33, BLASTP), *Homo sapiens* (E value = 1e-31, BLASTP), and *Saccharomyces cerevisiae* (E value = 4e-52, BLASTP) using the online ClustalW tool of European Bioinformatics Institute. E values are based on whole protein alignment of YVH1 orthologs. The alignment shows only the portion of the proteins that contain the two functional domains shown in panel A. The amino acids that make up the phosphatase domain in the N-terminal region are highlighted in the black box. The seven Cys and one His that make up the zinc-binding domain of the COOH region are shown in red boxes. The "*" shows identical residues in all the seqences compared. The ":" shows conserved substitution of residues with the same physiochemical properties. "." shows semi-conserved substitution between residues of a the aligned protein.

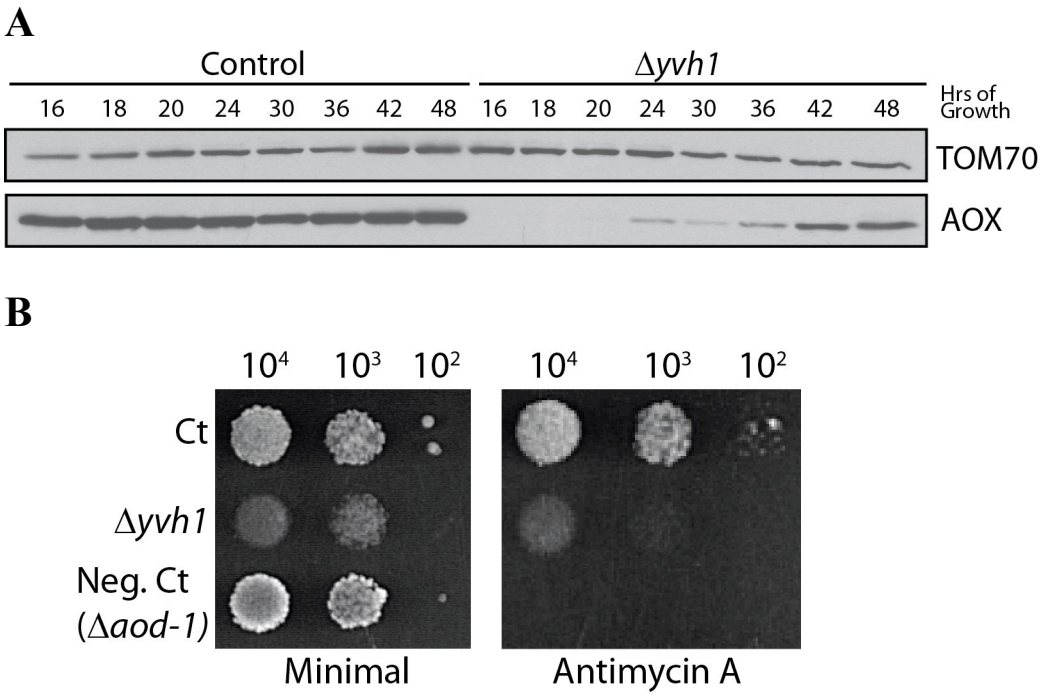

Figure 8. Induction of AOX and growth of *Δyvh1*. A) Western blot analysis for the timing of induction of AOX. Mitochondrial fractions were isolated from the control strain (NCN251) and *Δyvh1* after growth in Cm for the specified times. Proteins were separated by SDS-PAGE, blotted to nitrocellulose membrane and probed with antibodies as indicated on the right. TOM70, an outer mitochondrial membrane protein, was used as a loading control. B) Growth rate of *Δyvh1*. Ten fold serial dilutions of conidia (indicated at top of panel) from a control strain (Ct; NCN251), a negative control strain (*Δaod-1*) and *Δyvh1* were spotted and incubated at 30°C for 48 hr on minimal media and 68 hr on medium containing antimycin A.

determine the levels of the *aod-1* transcript in a control and *Δyvh1* strain when grown in the presence or absence of the AOX inducer Cm. RNA was isolated from four biological replicates of each strain under each condition following growth for 18 hr. To compare AOX protein levels to transcript levels, mitochondria were also isolated from the biological replicates of both the control and *Δyvh1*. As predicted from the previous results (Figure 8A), after 18 hr of growth in Cm, the *Δyvh1* strain had no detectable AOX protein while the control strain did (Figure 9A). When the control strain was grown for 18 hr in inducing conditions (+ Cm), the *aod-1* transcript levels increased about 25 fold compared to the control without the inducer (Figure 9B). When the *Δyvh1* strain was grown for 18 hr without the inducer, transcript levels of *aod-1* were only about 20% of the control levels grown without the inducer (Figure 9C). When the *Δyvh1* strain was grown in the presence of the inducer, the transcript levels were increased to about the control levels grown without inducer (Figure 9C). Thus, there was an increase in *aod-1* transcript levels in the *Δyvh1* cells when grown in Cm, but only about 5 fold over *Δyvh1* without Cm (Figure 9D) and about 25 fold less than the control grown in the presence of inducer (Figure 9B). These results show that *aod-1* transcript levels are severely reduced in *Δyvh1* compared to control cells grown in Cm (about 3.2%) and therefore do not support the hypothesis that inhibition of translation accounts for the deficiency of AOX in the mutant strain. The data also suggest that in the 18 hr *Δyvh1* culture grown without Cm, the basal level of transcription is reduced. In the *Δyvh1* cells grown in the presence of Cm, some induction occurs, but this falls well below the level of that observed in control cells grown under similar conditions. Together these data suggest that both the basal level of *aod-1* transcription and the ability to respond to the inducing signal are deficient in *Δyvh1* cells.

To determine if the level of *aod-1* transcripts increased in *Δyvh1* in older cultures, the experiment was repeated for cells grown for 36 hr in the presence of Cm. In the control strain, the fold change between uninduced and induced cells was roughly the same as for 18 hr cultures (Figure 9E). For *Δyvh1*, the level of

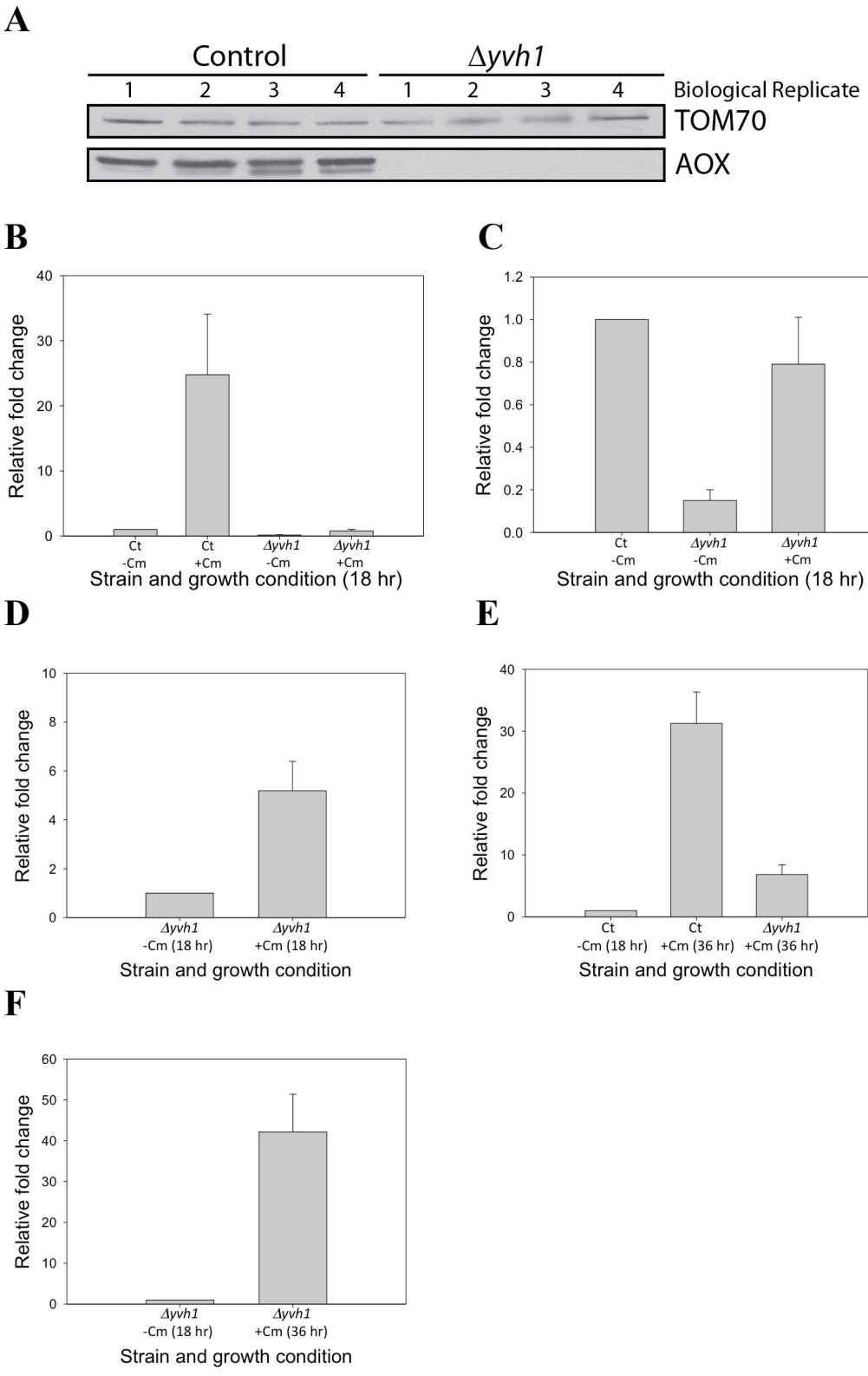
A
Control
Δyvh1
1 2 3 4 1 2 3 4
Biological Replicate
TOM70
AOX
B
Relative fold change
Ct -Cm
Ct +Cm
Δyvh1 -Cm
Δyvh1 +Cm
Strain and growth condition (18 hr)
C
Relative fold change
Ct -Cm
Δyvh1 -Cm
Δyvh1 +Cm
Strain and growth condition (18 hr)
D
Relative fold change
Δyvh1 -Cm (18 hr)
Δyvh1 +Cm (18 hr)
Strain and growth condition
E
Relative fold change
Ct -Cm (18 hr)
Ct +Cm (36 hr)
Δyvh1 +Cm (36 hr)
Strain and growth condition
F
Relative fold change
Δyvh1 -Cm (18 hr)
Δyvh1 +Cm (36 hr)
Strain and growth condition

Figure 9. AOX protein and transcript levels in the control (Ct) and the *Δyvh1* strain. A) Western blot analysis of four biological replicates of the control strain (Ct; NCN251) and *Δyvh1* grown in the presence of Cm for 18 hr. Mitochondrial were isolated from the biological replicates. Proteins were separated by SDS-PAGE, blotted to nitrocellulose membrane and probed with antibodies as indicated on the right. B) C) D) and E) qPCR of *aod-1* transcript levels in control (Ct) and *Δyvh1* grown in the presence or absence of Cm for 18 hr (B, C, D) or 36 hr (E). Error bars represent 95% confidence intervals. Fold change values were relative to the control (B, C, E) or *Δyvh1* (D) grown in the absence of the inducer Cm for 18 hr. Graphs B, C, and D are all created from the same data but emphasizes different aspects of the comparison. Samples were normalized to *gapdh* based on the ΔΔCT-method. F) Fold change of *Δyvh1* grown in Cm for 36 hr relative to *Δyvh1* grown for 18 hr in the absence of Cm. Error bars represent 95% confidence intervals. Samples were normalized to *gapdh* based on the ΔΔCT-method. Graph F uses the same data as in panel E for *Δyvh1* plus Cm, 36 hr but compares the values to *Δyvh1* minus Cm 18 hr growth from panel B.

aod-1 transcript in the 36 hr plus Cm culture increased roughly 6 fold compared to the 18 hr minus Cm control (Figure 9E). This level is about 15-20% of the control level following growth in the presence of Cm and probably accounts for the presence of the protein in older *Δyvh1* cultures grown in Cm (Figure 8A) even though it is still at reduced levels relative to the control. The mechanism by which the age of the culture influences AOX expression is not currently understood. The level of change between 18 hr *Δyvh1* minus Cm and 36 hr *Δyvh1* plus Cm was about 40 fold (Figure 9F) and was roughly equal to the fold change of 30 observed in the control at 36 hr. However the overall level in *Δyvh1* was still reduced compared to the control.

3.3 Analysis of cytochrome spectra for efficiency of Cm inhibition

It was conceivable that the inefficient production of AOX in *Δyvh1* was because Cm was not effectively inhibiting mitochondrial protein synthesis in this strain. This possibility was investigated by examining the cytochrome spectra of the mitochondria. Cm enters the mitochondria and inhibits translation by mitochondrial ribosomes (MCKEE *et al.* 2006). Mitochondrial translation products include cytochrome *b* of complex III and three proteins of cytochrome aa_3, which is complex IV of the sETC. Cytochrome *c* is a single polypeptide that is encoded in the nucleus, translated on cytosolic ribosomes and imported into the mitochondria (BOTTORFF *et al.* 1994). Thus, when grown under non-inducing conditions the control has distinguishable peaks for cytochrome *c*, cytochrome *b*, and cytochrome aa_3 (Figure 10A). However, when grown in the presence of Cm, the peaks for cytochrome *b* and cytochrome aa_3 become severely reduced (DESCHENEAU *et al.* 2005). Levels of cytochrome *c* in Cm grown cultures are found to be higher than those in normal cultures, possibly due to a response to the decreased mitochondrial function that results from the action of Cm (BERTRAND and PITTENGER 1969).

When grown in non-inducing conditions, *Δyvh1* had the same peaks as observed in the control strain grown in non-inducing conditions suggesting that the normal sETC is present (Figure 10B). However, when the *Δyvh1* strain was

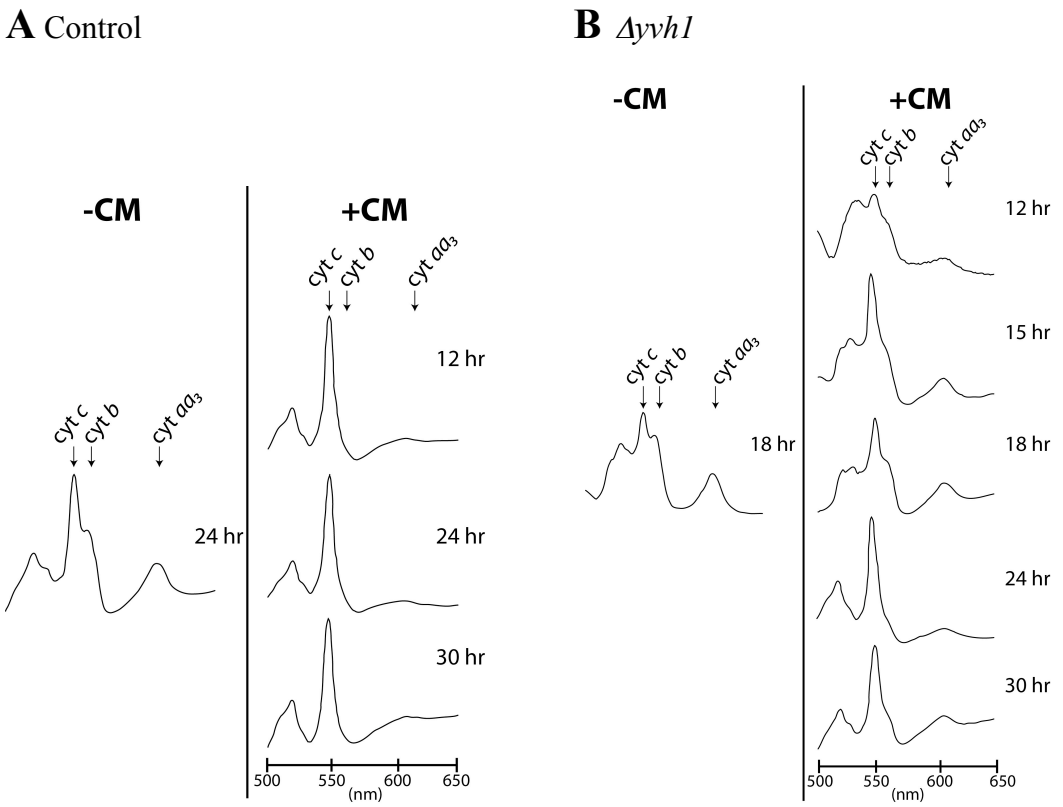

Figure 10. Qualitative cytochrome spectra of the NCN251 control strain (A) and *Δyvh1* (B). The cytochrome content of the cultures was determined by scanning a reduced sample vs. an oxidized reference from 500 nm to 650 nm. Cultures were grown for the indicated times in either non-inducing conditions (-Cm) or in the presence of Cm (+Cm). The peaks indicated on the spectrum correspond to cytochromes *aa₃* (605 nm), *b* (560 nm) and *c* (550 nm). The time of growth is indicated for each spectrum. Original output scans were traced with a pencil, scanned into Adobe Photoshop, and edited in Adobe Illustrator to produce the above images.

grown in the presence of Cm, the peaks for cytochrome aa_3 and cytochrome *b* were reduced but not to the extent observed in the control plus Cm cultures, suggesting these proteins were still being translated by mitochondrial ribosomes when the cell was grown in the presence of Cm (Figure 10B). These observations suggest that Cm may be affecting *Δyvh1* mitochondrial translation to a lesser extent than in the control. This could help explain the slow rate of AOX induction in *Δyvh1* (Figure 8A) since decreased retrograde signaling from mitochondria would be expected if the effects of Cm were reduced.

3.4 A construct expressing an HA-tagged version of YVH1 restores expression of AOX in *Δyvh1*

To determine the subcellular localization of the YVH1 protein, *N. crassa* transformants that express an N- or C-terminal HA-tagged copy of the gene were created in a vector that encoded basta resistance. This was done by cloning a 3xHA epitope tag into either the 5' (i.e. immediately following start codon) or 3' (i.e., immediately prior to the stop codon) end of the *yvh1* coding sequence. This would allow for determining where in the cell HA-YVH1 was located by using a commercially available HA antibody that recognizes the HA epitope, and differential centrifugation. Constructs with tags at either end of the protein were used in case of the possibility of a tag at one end of the protein resulting in altered function or mislocalization. These constructs were then transformed into the *Δyvh1* strain. Transformants were selected on basta containing medium and then screened for their ability to induce AOX when grown in the presence of Cm. As shown in western blots on isolated mitochondria, both N- and C-terminal HA tagged transformants were able to induce AOX to various levels (Figure 11A, B). At the time these mitochondrial fractions were isolated, I also kept the post-mitochondrial supernatant, which should contain the cytosol and other organelles of the cell except the nucleus and mitochondria. When this fraction was analyzed by western blotting, an HA-tagged protein was observed in all the transformants (Figure 11A, B), at roughly the position predicted as the size for the *N. crassa* 3xHA YVH1 protein, 50.4 kDa. This band was not present in either the *Δyvh1*

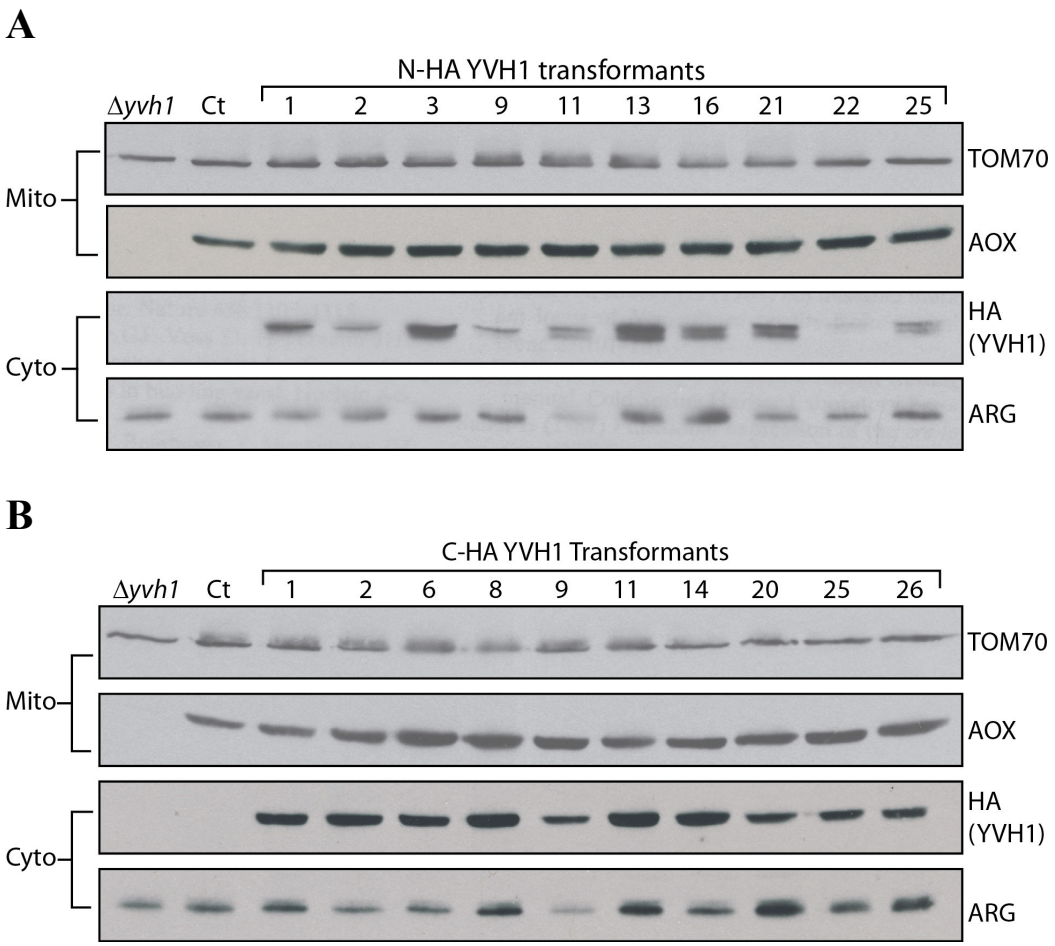

Figure 11. Western blot analysis of N- and C-terminal HA tagged YVH1 containing strains. Mitochondria (Mito) and cytosolic (Cyto) fractions (indicated on left) were prepared from ten N-HA (A) and ten C-HA (B) tagged YVH1 transformants, the control strain (Ct; NCN251), and the *Δyvh1* strain. Cultures were grown in the presence of Cm for 20 hr. Proteins were separated by SDS-PAGE, blotted to nitrocellulose membrane and probed with antibodies as indicated on the right. Crude cytosolic fractions were examined for arginase (ARG), a known cytosolic enzyme in *N. crassa* (Marathe *et al.* 1998; Turner and Weiss 2006), as a loading control and HA for the tagged YVH1. The mitochondrial fractions were analyzed for AOX and the outer mitochondrial membrane protein TOM70 as a loading control.

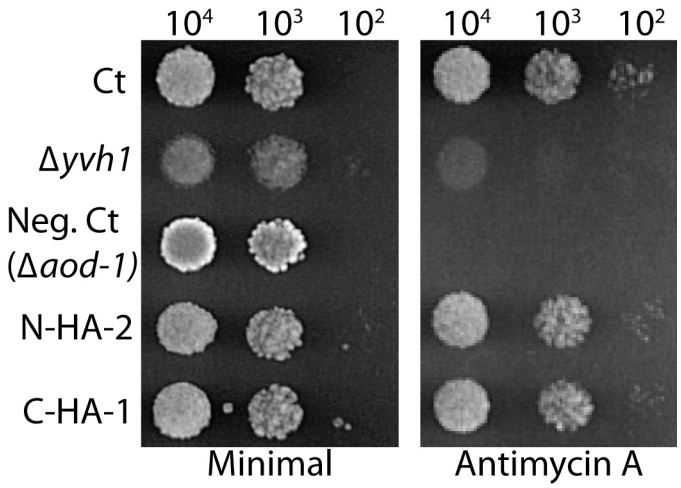

Figure 12. Growth rate of N-HA-2 and C-HA-1 YVH1 transformants. Conidia from the indicated strains were spotted and incubated at 30°C for 48 hr on minimal medium or 68 hr on antimycin A containing medium. Ct = control (NCN251).

strain or the control strain. This showed that rescue of AOX expression was concomitant with the presence of the HA tagged *yvh1* gene.

N-HA and C-HA transformants expressing the tagged YVH1 protein showed variability in the expression of the HA-tagged YVH1 protein. This could be due to position effects on expression of the HA-tagged *yvh1* in the *Δyvh1* genome as insertion of transformed DNA occurs at random locations through non-homologous end joining (NINOMIYA *et al.* 2004; PAIETTA and MARZLUF 1985). Although the levels of AOX in the different transformants were not always similar to the control on the gels for screening transformants, subsequent work showed AOX levels similar to the control in strains N-HA-2 and C-HA-1 (see below, section 3.5). In both N-HA-2 and C-HA-1 the growth rate of the *Δyvh1* strain was restored to the control levels on minimal medium and medium containing antimycin A (Figure 12). For these reasons, and because expression levels of the tagged YVH1 appeared to be about average among transformants, these strains were used for further work.

3.5 The HA tagged YVH1 protein localizes to the nuclear and PMP fractions of the cell

Using GFP tagged proteins and fluorescent microscopy, YVH1 has been shown to localize to the nuclear and cytoplasmic regions of the cell in yeast and humans (KEMMLER *et al.* 2009; MUDA *et al.* 1999). KUMAR *et al.* (2004) used fluorescent microscopy to observe the shuttling of YVH1 between the nucleus and cytoplasm in the malaria parasite, *P. falciparum*. They also isolated nuclear and cytosolic protein fractions through differential centrifugation from three growth stages of the parasite and used western blotting to observe the localization of YVH1 to the cytosol and nucleus.

I examined the localization of the *N. crassa* protein using a sub-cellular fractionation approach. In both the N-HA-2 and C-HA-1 tagged transformants, AOX levels were found to be at control levels in gradient purified mitochondrial fractions of cells grown under inducing conditions (Figure 13A, B). AOX was not found in any other fraction (Figure 13A, B). The HA tagged protein was shown to

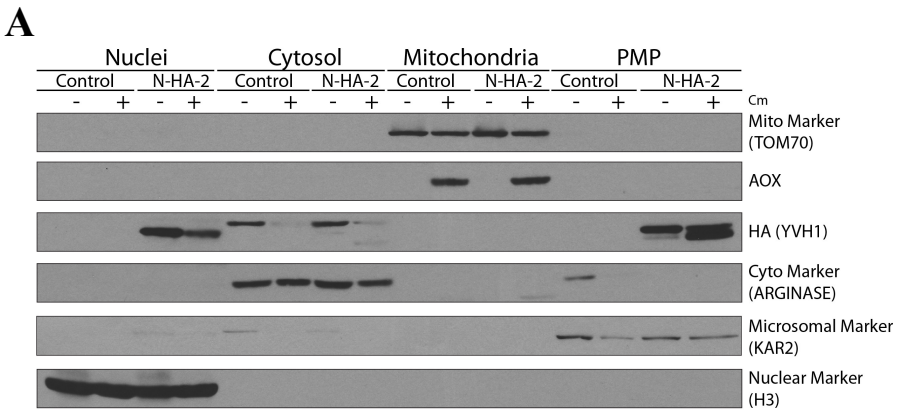
A
Nuclei
Cytosol
Mitochondria
PMP
Control
N-HA-2
Control
N-HA-2
Control
N-HA-2
Control
N-HA-2
- + - + - + - + - + - + - + - +
Cm
Mito Marker
(TOM70)
AOX
HA (YVH1)
Cyto Marker
(ARGINASE)
Microsomal Marker
(KAR2)
Nuclear Marker
(H3)

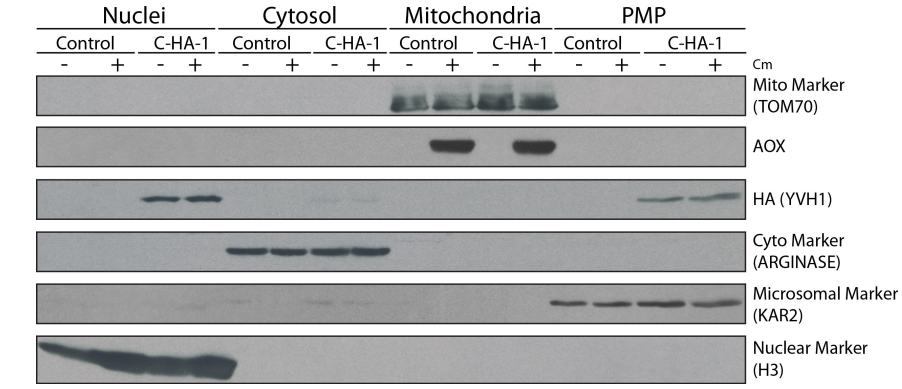
B
Nuclei
Cytosol
Mitochondria
PMP
Control
C-HA-1
Control
C-HA-1
Control
C-HA-1
Control
C-HA-1
- + - + - + - + - + - + - + - +
Cm
Mito Marker
(TOM70)
AOX
HA (YVH1)
Cyto Marker
(ARGINASE)
Microsomal Marker
(KAR2)
Nuclear Marker
(H3)

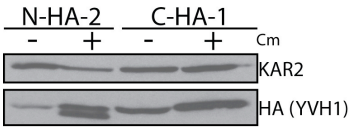
C
N-HA-2
C-HA-1
- + - +
Cm
KAR2
HA (YVH1)

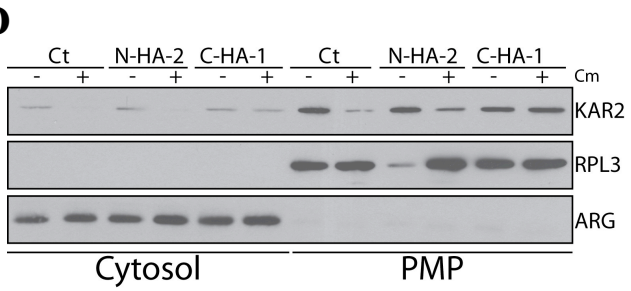
D
Ct
N-HA-2
C-HA-1
Ct
N-HA-2
C-HA-1
- + - + - + - + - + - +
Cm
KAR2
RPL3
ARG
Cytosol
PMP

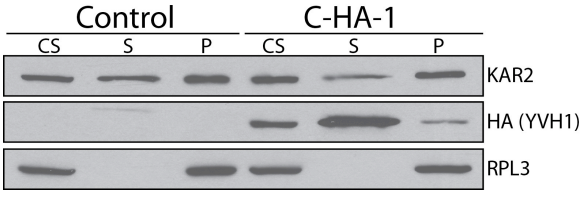
E
Control
C-HA-1
CS
S
P
CS
S
P
KAR2
HA (YVH1)
RPL3

Figure 13. Subcellular localization of YVH1. A, B) Western blot analysis of subcellular fractionation experiment from N- and C- terminal HA tagged YVH1 strains. Nuclei, cytosol, mitochondria, and PMP fractions were isolated from N-HA-2 (A) and C-HA-1 (B) tagged YVH1 transformants as well as the control strain (NCN251) as described in the Material and Methods (section 2.5 and 2.6). Cultures were grown in the absence (-) or presence (+) of Cm. Proteins were separated by SDS-PAGE, blotted to nitrocellulose membrane and probed with antibodies as indicated on the right. Antibodies that served as controls for the different fraction were KAR2, a known ER protein of *N. crassa* (Addison 1998) as a microsomal marker. Histone 3 (H3) was used as a nuclear marker, arginase as a cytosolic marker, and Tom70 as a mitochondrial marker. C) Comparative western blot analysis of the HA tagged bands in the PMP fraction of the N-HA-2 and C-HA-1 transformants. PMP fractions were isolated from N-HA-2 and C-HA-1 grown in the absence (-) or presences (+) of Cm. Proteins were separated by SDS-PAGE, blotted to a nitrocellulose membrane, and probed for the proteins indicated on the right. D) Western blot analysis of cytosol and PMP fractions from fractionation experiments of Figure 13A and B. Proteins were separated by SDS-PAGE, blotted to a nitrocellulose membrane, and probed for the proteins indicated on the right. Ct = control strain (NCN251). E) Ribosome isolation. Ribosomes were isolated from the control strain (NCN251) and C-HA-1 grown in the absence of Cm by centrifugation of whole cell extract through a 1 M sucrose cushion (20 mM Tris-HCL, pH 7.5; 8 mM $MgCl_2$; 100 mM KCL; 1M ultra-pure sucrose). The pellet (P) and supernatant (S; top 200 µl of supernatant after centrifugation to pellet ribosomes) were subjected to SDS-PAGE, blotted to nitrocellulose, and probed for the proteins on the right. A yeast RPL3 antibody was used as a ribosomal protein marker. A clarifying spin was performed after the addition of the detergent Triton-X-100 to remove insoluble material. The supernatant from the clarifying spin was layered onto the sucrose cushion for centrifugation. The pellet from the clarifying spin was suspended in cracking buffer and electrophoresed with the other samples (labeled on gel as CS (see section 2.9 of Materials and Methods)). 30 µg of protein was loaded in each lane.

localize with markers for both nuclei and the PMP fractions. The PMP fraction contains fragmented endoplasmic reticulum and other organelles. A double band was observed in the N-terminal HA tagged mutant in the PMP fraction from Cm induced cells. The smaller form is likely the result of protein degradation at the C-terminus. I have shown that the band observed for the C-terminal tagged protein is equivalent to the larger form of the N-terminal tagged protein (Figure 13C**)**. Thus, it is unclear if the C-terminal tag offers protection from proteolytic attack or if proteolysis does occur and the fraction of the protein affected is simply not detectable due to loss of the C-terminal tag.

The finding that a large amount of YVH1 was present in the PMP (Figure 13A, B) and the fact that the yeast YVH1 protein is involved in ribosome assembly, led me to ask if our PMP isolation protocol led to the pelleting of ribosomal particles. An antibody to *S. cerevisiae* RPL3, which has 75% identity with its *N. crassa* ortholog, was obtained from the Developmental Studies Hybridization Bank. The PMP and cytosol (i.e. the post PMP supernatant) were examined with this antibody as well as markers for the ER and cytosol. As shown in Figure 13D, it appears that ribosomal subunits are present in the PMP but not the cytosol, as was the tagged YVH1 (Figure 13A, B). Given the function of YVH1 in *S. cerevisiae*, this implied that the protein was associated with ribosomal subunits even after they had left the nucleus. To examine this point further, I isolated ribosomes in the presence of a high concentration of Triton-X-100 (1%) from a whole cell extract of strain C-HA-1. Ribosomes were pelleted through a 1 M sucrose cushion and both the pellet and supernatant (material above the cushion) were examined by western blot analysis. In this case the majority of *N. crassa* YVH1 was not found associated with ribosomes but was found as a soluble protein in the supernatant (Figure 13E). Taken together, these data support that in our PMP fraction from subcellular localization, YVH1 is associated with a pelleted complex (most likely ribosomes given its known function in *S. cerevisiae*). However, in the procedure for purification of ribosomes, the interaction is broken. Conceivably the presence of 1% Triton-X-100, could be responsible.

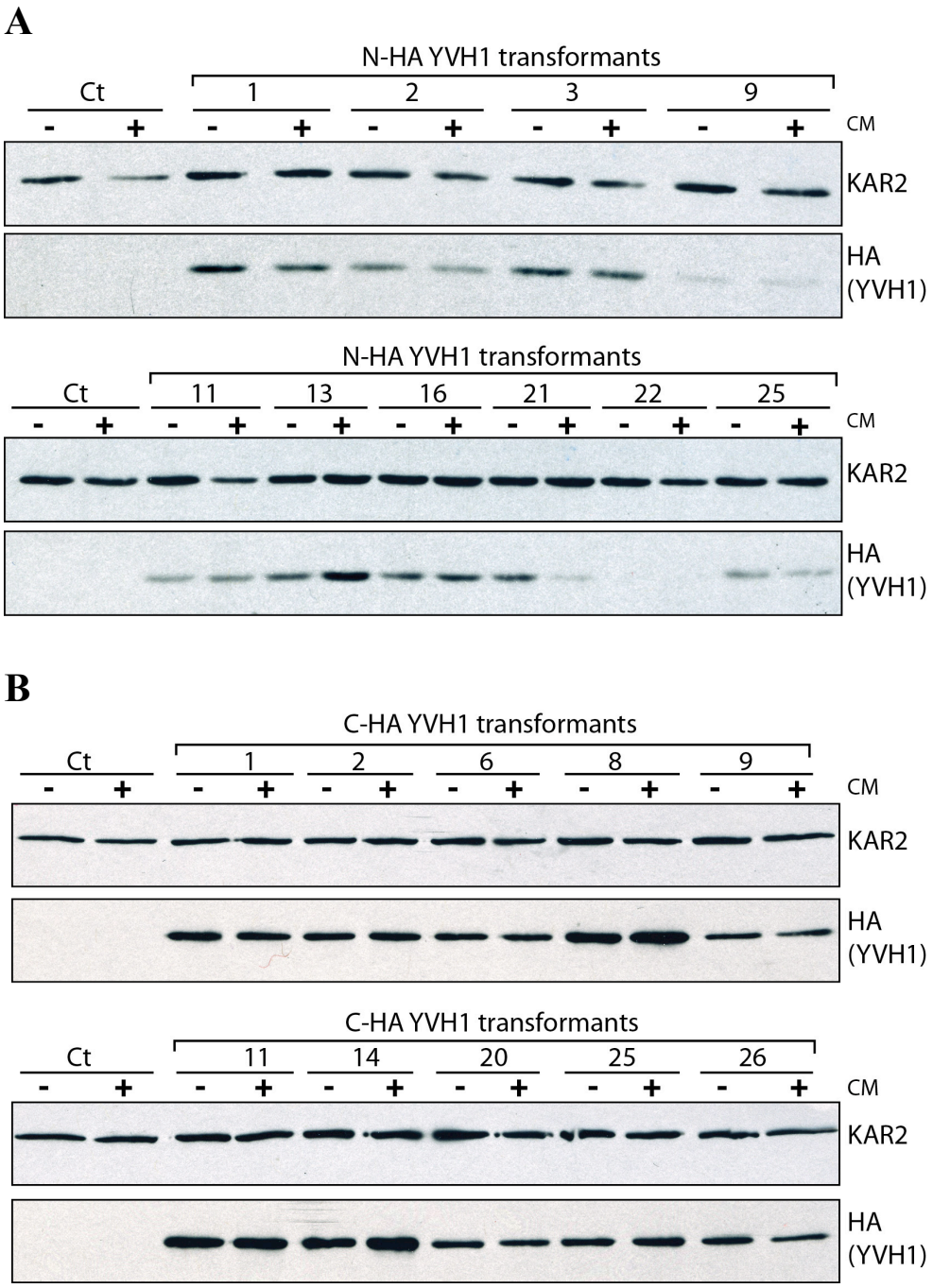

Figure 14. Western blot analysis of N- and C- terminal HA tagged YVH1 strains derived by transformation of *Δyvh1*. PMP fractions were isolated from ten N-HA tagged (A) and ten C-HA tagged (B) *Δyvh1* transformants, (identified by transformant number) and the control strain (Ct; NCN251). Cultures were grown in the absence (-) or presence (+) of Cm. Proteins were separated by SDS-PAGE, blotted to nitrocellulose membrane and probed with antibodies as indicated on the right. The fractions were analyzed for KAR2 as a loading control, and HA for the tagged YVH1 protein.

The HA-tagged protein levels in strains N-HA-2 and C-HA-1 in the PMP fraction under both inducing and non-inducing conditions appeared to be roughly equal (Figure 13A, B). To confirm if this was also true for other transformants, I examined the PMP fraction of ten N-HA and ten C-HA YVH1 transformants in both inducing and non-inducing conditions (Figure 14A, B). Although a few transformants showed different levels of expression of YVH1 between plus Cm and minus Cm conditions (N-HA-1, -13, -21 and C-HA-8, -14, -26), the YVH1 protein levels in the majority of transformants remained unchanged suggesting that YVH1 levels are unaffected by growth in Cm. It should also be noted that in those isolates showing a different level in the presence or absence of Cm that there was no consistency with respect to the higher level being seen in either minus Cm or plus Cm. Differences in expression may be due to position effects as discussed in section 3.4.

3.6 AOX expression requires a functional zinc binding domain but not the phosphatase domain of YVH1

Although YVH1 contains a DUSP domain that has been shown to have activity *in vitro* and is required for interaction with Hsp70 in mammalian cells (MUDA *et al.* 1999; SHARDA *et al.* 2009), all examined negative phenotypes seen in YVH1 mutants in yeast can be restored to wild type by rescue with a gene encoding a protein containing the functional zinc-binding domain but lacking a functional phosphatase domain (BEESER and COOPER 2000; KEMMLER *et al.* 2009; LO *et al.* 2009; MUDA *et al.* 1999). Since AOX is not present in either *S. cerevisiae* or mammals, I wanted to determine if either or both domains were required for AOX expression. Therefore, I created mutants of each domain in the N-terminal HA tagged protein and transformed the constructs encoding them into the *Δyvh1* strain. The constructs contained a basta resistance gene and working isolates were selected for growth on basta. These were then screened for their ability to induce AOX. The phosphatase domain mutants (P-mutants) have the $HC(X)_5R$ dual specificity phosphatase domain mutated to $QS(X)_5Q$ (Figure 15A, top). The zinc binding domain mutants (Z-mutants) have the 3rd pair of cysteines

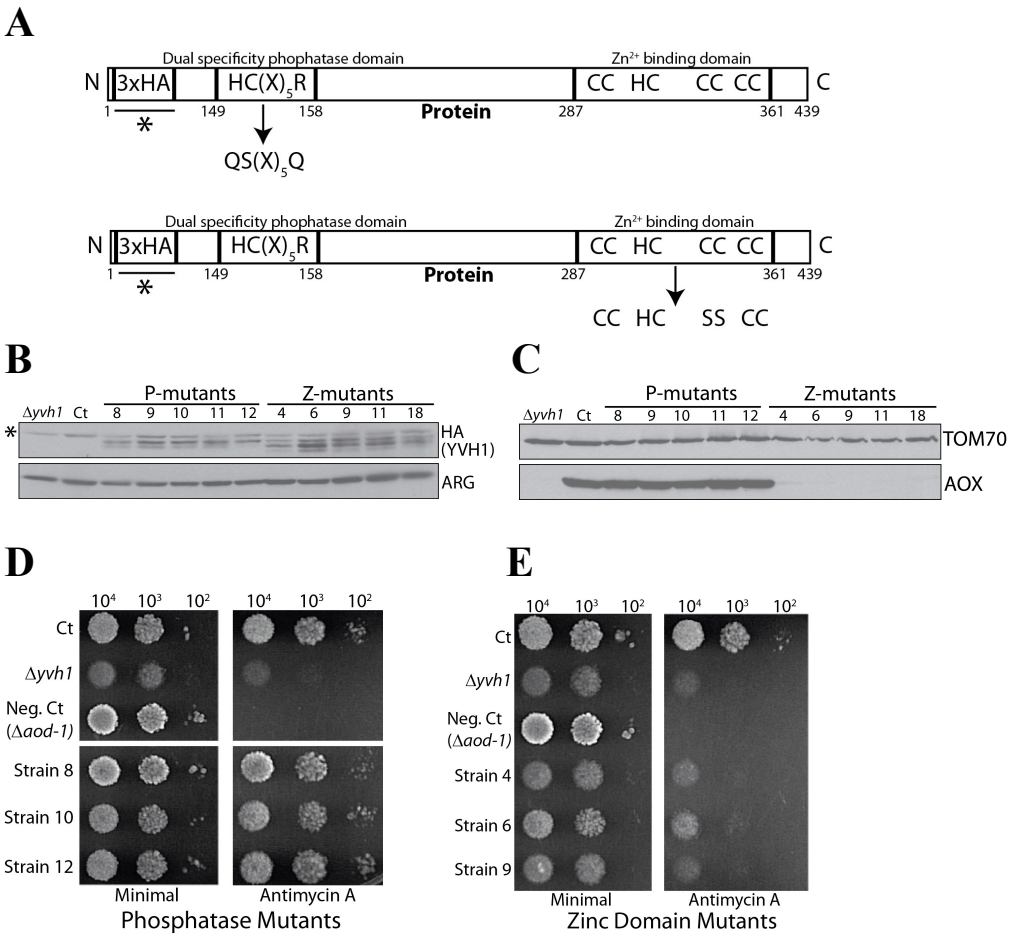

Figure 15. Analysis of phosphatase domain and zinc binding domain mutants. A) Representation of the position of amino acid changes introduced into *N. crassa* YVH1 to create the mutated phosphatase (P-mutants) and zinc-binding (Z-mutants) domains. The amino acid changes in the P-mutant are H149/Q, C150/S, and R156/Q. The amino acid changes in the Z-mutant are C340/S and C345/S in the zinc binding C-terminal region. The * shows that the HA tag was not considered in the numbering of the amino acids. B, C) HA and AOX protein levels in the P- and Z-mutants. Proteins were separated by SDS-PAGE, blotted to nitrocellulose membrane and probed with antibodies indicated on the right. B) Whole cell extracts were prepared from cells grown for 20 hr in the presence of Cm. The whole cell extract was examined for HA and the loading control arginase (ARG). The * symbol shows non-specific binding to an unknown protein by the HA antibody in whole cell extract fractions. C) Mitochondrial fractions were isolated from strains grown for 20 hr in the presence of Cm. The mitochondrial fractions were analyzed for AOX and TOM70 as a loading control. D, E) Growth rate of selected N-terminal HA tagged YVH1 P-mutant (D) and Z-mutant (E) transformants. Conidia from the indicated strains were spotted on each plate and incubated at 30°C for 48 hr on minimal medium and 68 hr on antimycin A containing medium. Some irrelevant rows were removed electronically. Ct = control (NCN251).

involved in zinc binding mutated to serines (Figure 15A, bottom). Several isolates of each transformant were examined for the presence of the HA-tagged protein and the ability to produce AOX when grown in the presence of Cm. All transformants I examined were shown to express the HA-tagged YVH1 protein (Figure 15B). The P-mutants were able to restore AOX to control levels while the Z-mutants could not (Figure 15C). When the different mutants were tested for growth, the phosphatase domain mutants grew at the same rate as the wild type control on both minimal media and media containing antimycin A (Figure 15D). However the zinc domain mutants were not rescued and grew at the *Δyvh1* rate on both types of media (Figure 15E). This suggested that the mutated cysteine pair in the zinc-binding domain is required for proper growth and AOX expression.

3.7 Localization of mutant YVH1 protein

For further analysis, I used the P-mutant strain 8 (N-HA P-8) in subcellular fractionation experiments to determine the localization of the protein. The protein was found in the nuclear and PMP fractions (Figure 16A), as was the case for the tagged wild type YVH1 (Figure 13A, B). AOX levels in the gradient purified mitochondrial fraction were similar to the control when the cells were grown in the presence of Cm. These data reinforce the idea that YVH1 doesn't require a functional phosphatase domain to express AOX to control levels when grown in the presence of Cm.

Subcellular fractionation of the zinc mutant, N-HA Z-9, revealed that the protein only appears in the nuclear fraction following either 20 or 48 hr growth in Cm (Figure 16B, C). This suggests a possible role of the domain in shuttling out of the nucleus (see discussion section 4.3). Also, at 20 hr of growth, AOX was not detectable as in *Δyvh1*. After 48 hr of growth, levels of AOX appeared to be at the control levels in the Z-9 mutant (Figure 16C). This was unexpected since AOX levels in the deletion mutant never reach the control levels (Figure 8A). This result suggested the possibility that in the absence of a functional Z-domain, the phosphatase domain might play a role in allowing full restoration of AOX levels at longer growth time in Cm. To test this further, mitochondria were

A

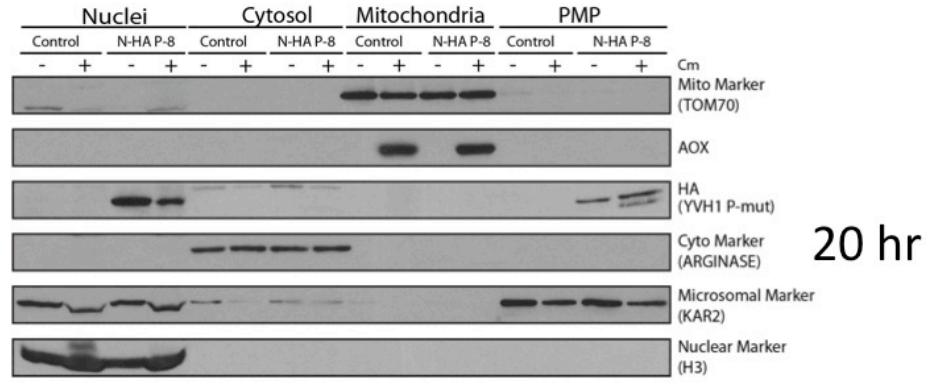
Nuclei
Cytosol
Mitochondria
PMP
Control
N-HA P-8
Cm
Mito Marker (TOM70)
AOX
HA (YVH1 P-mut)
Cyto Marker (ARGINASE)
Microsomal Marker (KAR2)
Nuclear Marker (H3)
20 hr

B

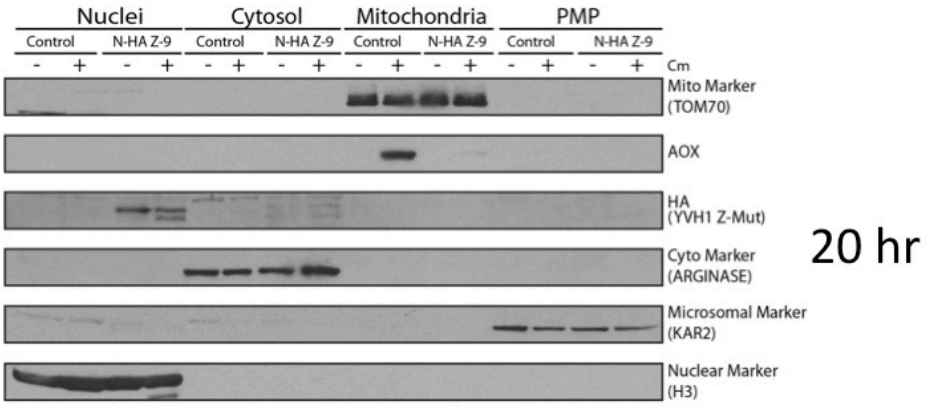
Nuclei
Cytosol
Mitochondria
PMP
Control
N-HA Z-9
Cm
Mito Marker (TOM70)
AOX
HA (YVH1 Z-Mut)
Cyto Marker (ARGINASE)
Microsomal Marker (KAR2)
Nuclear Marker (H3)
20 hr

C

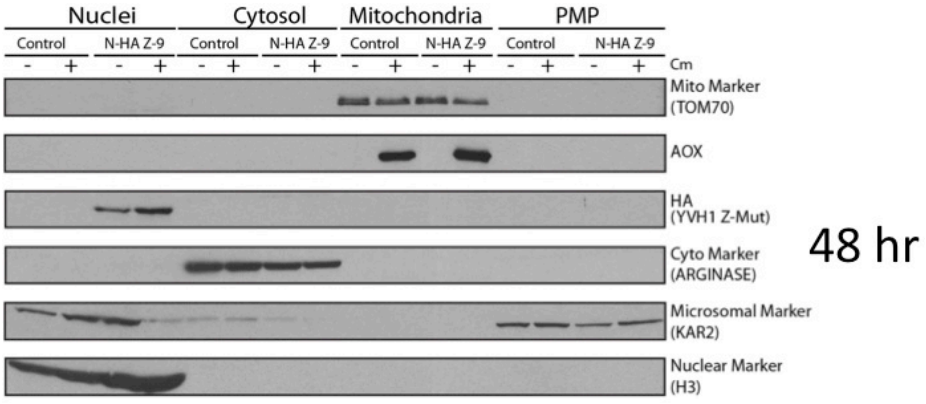
Nuclei
Cytosol
Mitochondria
PMP
Control
N-HA Z-9
Cm
Mito Marker (TOM70)
AOX
HA (YVH1 Z-Mut)
Cyto Marker (ARGINASE)
Microsomal Marker (KAR2)
Nuclear Marker (H3)
48 hr

D

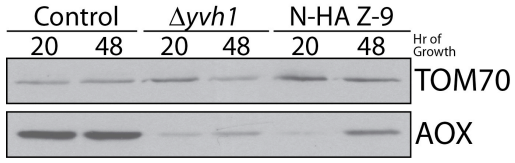
Control
Δyvh1
N-HA Z-9
20
48
Hr of Growth
TOM70
AOX

Figure 16. Subcellular fractionation of N-HA tagged P- and Z-mutant YVH1 strains. Nuclei, mitochondria, cytosol, and PMP fractions were isolated as described in the Materials and Methods (section 2.5 and 2.6) from phosphatase domain mutant strain 8 (N-HA P-8) (A) following 20 hr of growth and from the zinc-binding domain mutant strain 9 (N-HA Z-9) for 20 hr (B) and 48 hr of growth (C). The control strain was NCN251. Cultures were grown in the absence (-) or presence (+) of Cm. Proteins were separated by SDS-PAGE, blotted to nitrocellulose membrane and probed with antibodies as indicated on the right. The fractions were analyzed for KAR2 as a PMP marker, H3 as a nuclear marker, arginase as a cytosolic marker and Tom70 as a mitochondrial marker. D) Western blot analysis of the timing of induction of AOX when the control (NCN251), *Δyvh1* and N-HA Z-9 are grown in the presence of Cm. Mitochondrial fractions were isolated from growth in Cm for the specified times. Proteins were separated by SDS-PAGE, blotted to nitrocellulose membrane and probed with antibodies indicated on the right.

isolated from another biological replicate of N-HA Z-9 following 20 and 48 hr of growth. In this sample AOX levels appeared more similar to *Δyvh1* and not to the control especially with respect to the loading control Tom70. (Figure 16D). The differences between AOX levels in the Z-mutant in Figures 16C and 16D are not readily explainable but it should be noted that mitochondria used Figure 16C had been gradient purified while those in Figure 16D were crude mitochondrial preparations. It is conceivable that there could be two populations of mitochondria in the mutant with different densities and AOX levels. In this case, mitochondria lacking AOX might be lost during isolation of gradient purified mitochondria.

3.8 RNA-Seq analysis of *Δyvh1* and the control grown in the presence of Cm for 12 hr

A number of phenotypes have been associated with loss of the YVH1 protein in yeast and mammals (BEESER and COOPER 2000; CAIN *et al.* 2011; KOZAROVA *et al.* 2011; LO *et al.* 2009; SAKUMOTO *et al.* 2001; SHARDA *et al.* 2009; SUGIYAMA *et al.* 2011). The finding that the primary function of the protein is likely to be in ribosome assembly suggests that other effects are secondary. Nonetheless, it is curious that production of AOX under normal inducing conditions is reduced. The mechanism by which this is achieved remains unknown. In an attempt to gather more information regarding the status of *Δyvh1* cells in the presence of Cm, I performed an RNA-seq experiment. Total RNA was isolated from *Δyvh1* and the control strain grown in Cm for 12 hr. Preliminary analysis suggested that roughly 1200 genes were down-regulated and 500 genes were up-regulated by at least 2-fold in *Δyvh1* when grown in Cm for 12 hr compared to the control grown under similar conditions. This would represent altered regulation of about 17% of the total 10,000 genes predicted in *N. crassa*. Table 4 and 5 show the top 20 down-regulated and top 20 up-regulated genes, respectively, in *Δyvh1* when grown in the presence of the inducer Cm for 12 hr. Gene product names were retrieved from the online Broad Institute *Neurospora crassa* database by using the NCU numbers. Proteins that have no similarities to other proteins or known functional domains are termed hypothetical proteins.

Preliminary results suggest no observable pattern to the types of genes affected by loss of *Δyvh1*. The gene under study here as the KO gene (NCU08158) was the 2nd most lowest expressed gene in *Δyvh1* compared to the control gene giving good evidence that the strain analyzed was genotypically correct. It is of interest that AOX is among the top 20 down-regulated (Figure 17A) and that phosphoenolpyruvate carboxykinase (PCK) is also in this group (Figure 17B). It has been shown in *A. nidulans* and *P. anserina* that both of these genes are controlled by the AOD2 and AOD5 orthologs in these organisms (SELLEM *et al.* 2009; SUZUKI *et al.* 2012). Similarly, Z. Qi in our lab has preliminary evidence that the PCK promoter binds the AOD2 transcription factor. It is interesting to note that neither the *aod-2* nor *aod-5* transcript level seems to be affected in the *Δyvh1* (Figure 17C, D). This suggests that the effect of *Δyvh1* on AOX and PCK production is either at the level of translating those transcription factors or in the generation/delivery/interpretation of the normal induction signal. The up-regulation of the ABC drug exporter AtrF is also of interest (Figure 17E). The yeast ortholog, Pdr5, has been shown to be required for resistance to Cm. When yeast cells lack Pdr5, an increase in sensitivity to Cm has been observed (RUTLEDGE *et al.* 2011). Up-regulation of the AtrF protein in the *N. crassa Δyvh1* strain, could lead to an increase resistance to Cm. This suggestion is supported to some extent by the cytochrome spectra analysis (section 3.3). This could lead to a delay in the expression of AOX when *Δyvh1* is grown in Cm (see discussion).

A

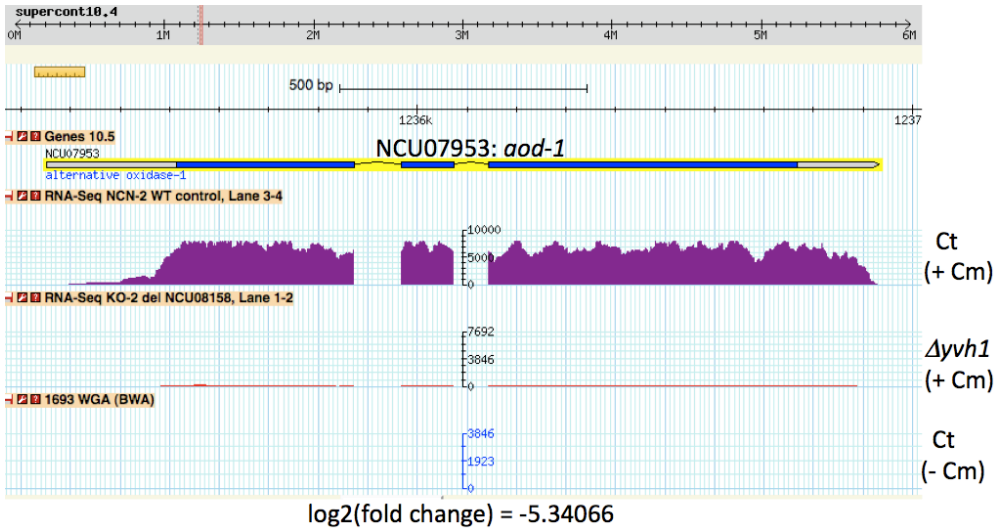

log2(fold change) = -5.34066

B

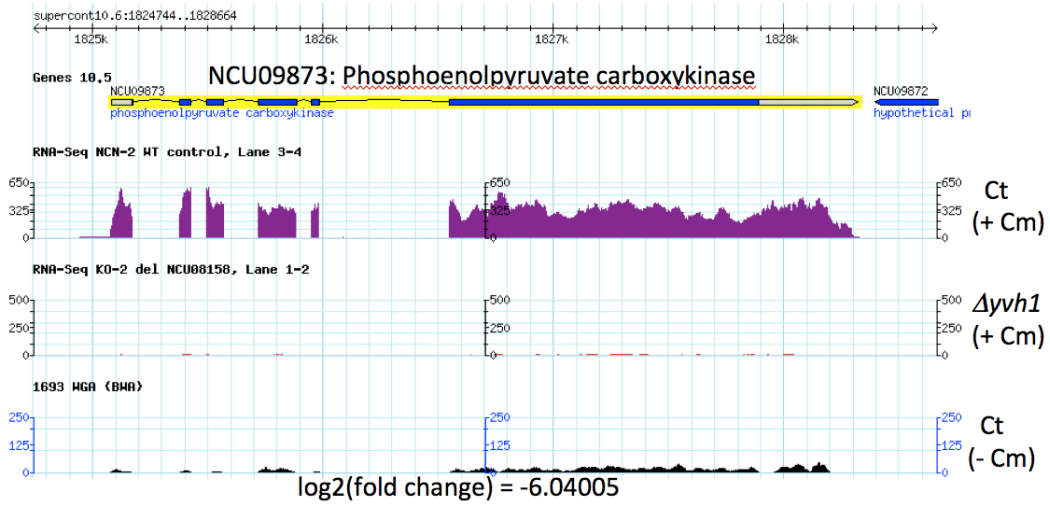

log2(fold change) = -6.04005

C

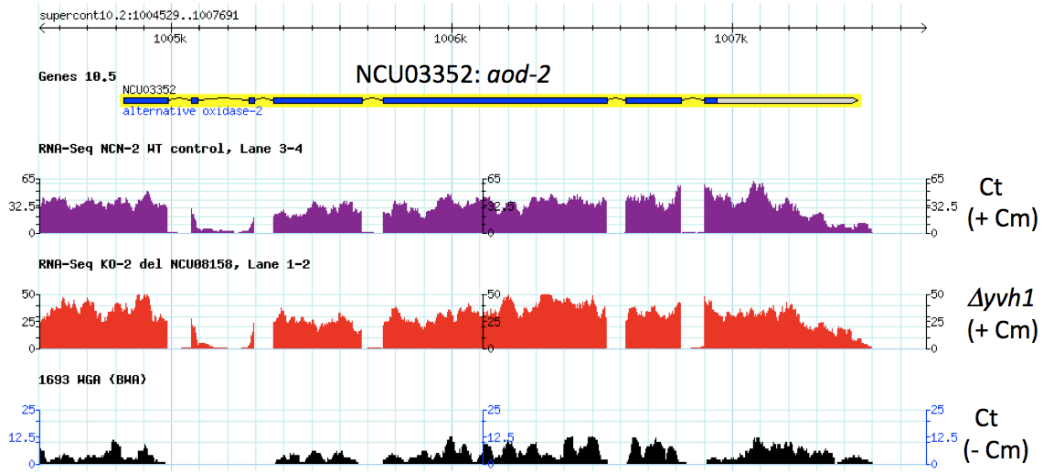

D

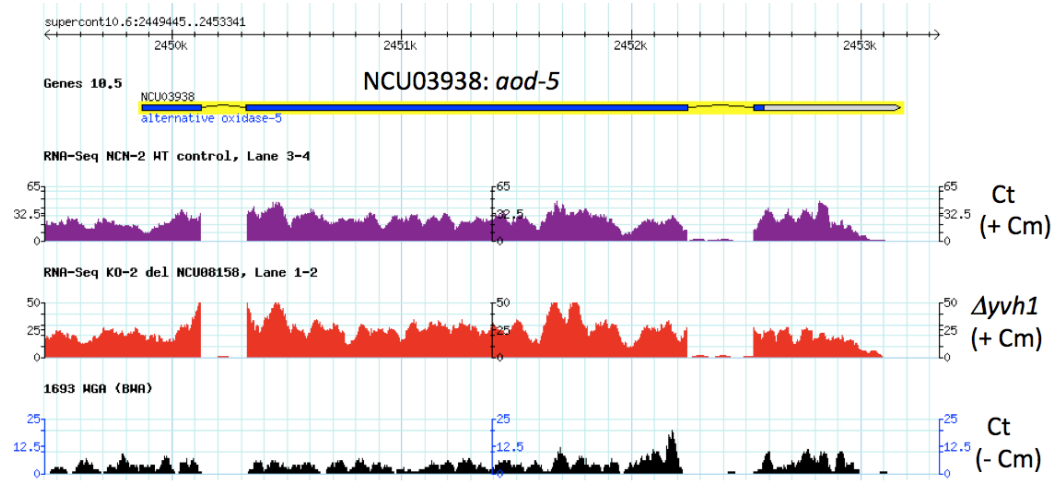

E

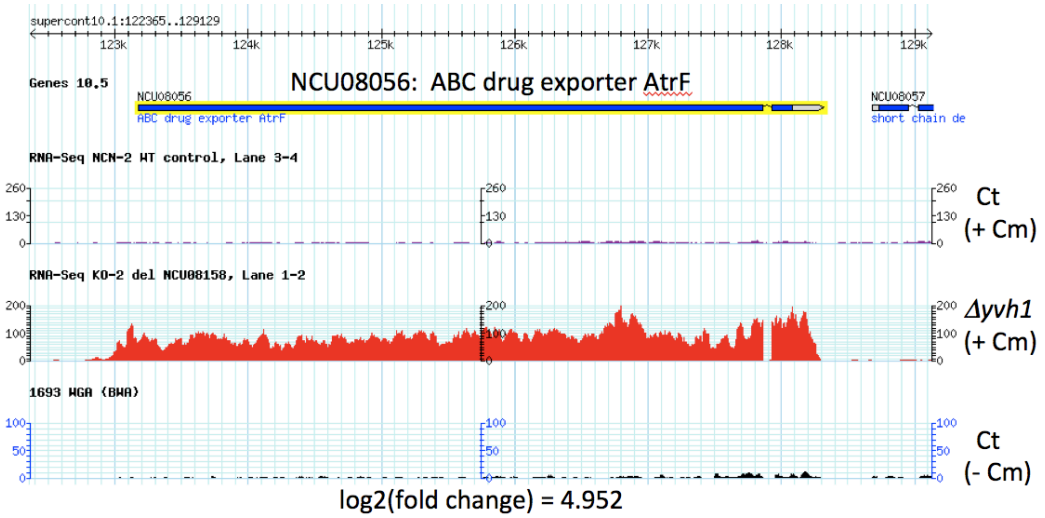

Figure 17. Data from RNA-seq. Total RNA was isolated from the control strain and the *Δyvh1* strain each grown in Cm for 12 hr. mRNA libraries were prepared and sequenced using the Illumina platform by Delta Genomics. Initial data analysis was done by collaborators K. Smith and M. Freitag (Oregon State University). An example of a gene down-regulated in *Δyvh1* is *aod-1* (A) phosphoenolpyruvate carboxykinase (B). Example of genes expressed at similar levels in the control and *Δyvh1* are shown by *aod-2* (C) and *aod-5* (D). A gene up-regulated in *Δyvh1* is the ABC drug exporter AtrF (E). Gene structure is highlighted in yellow. The number of reads at each position is represented by purple in the control strain and red in *Δyvh1*. The Y-axis has been adjusted to give a ratio corresponding to the number of mappable reads in each experiment. Fold change values are calculated between *Δyvh1* (+ Cm) and Ct (+ Cm). Ct = NCN251. The NCN251 control experiment was done at same time as the *Δyvh1* experiment. Ct (- Cm) is a RNA-seq experiment in the same control strain grown in the absence of Cm, but done several years ago in the Freitag lab.

NCU number	Gene Product Name	log2(fold change)
NCU04697	cyanide hydratase	-12.1762
NCU08158	dual specificity phosphatase	-10.8212
NCU05914	hypothetical protein	-8.52216
NCU09969	hypothetical protein	-8.44373
NCU00665	Ser/Thr protein phosphatase	-7.56216
NCU09045	heterokaryon incompatibility protein	-6.84228
NCU04591	pentachlorophenol monooxygenase	-6.65876
NCU04028	hypothetical protein	-6.53871
NCU09873	phosphoenolpyruvate carboxykinase	-6.04005
NCU12151	hypothetical protein	-6.0386
NCU07351	alpha-glucuronidase	-5.93435
NCU12050	hypothetical protein	-5.60153
NCU06940	hypothetical protein	-5.43363
NCU00732	trichothecene C-15 hydroxylase	-5.3862
NCU07474	ergot alkaloid biosynthetic protein A	-5.37075
NCU07352	hypothetical protein	-5.36257
NCU07953	alternative oxidase-1	-5.34066
NCU09273	hypothetical protein	-5.31326
NCU02904	alpha/beta hydrolase fold protein	-5.15451
NCU09274	hypothetical protein	-5.13836

Table 4. Top 20 down-regulated genes as determined from RNA-seq. Transcript levels of *Δyvh1* and the control (NCN251) grown in the presence of Cm for 12 hr were compared. The NCU number was used to obtain the gene product name from the Broad Institute Neurospora crassa database. Proteins with no similarities to other known proteins of known function are termed hypothetical proteins. The log2 (fold change) was calculated by the difference in expression of transcripts between the control and *Δyvh1*.

NCU number	Gene Product Name	log2(fold change)
NCU05230	hypothetical protein	6.86272
NCU00079	hypothetical protein	6.57099
NCU08852	polymerase 2 ADP-ribosyltransferase 2	6.19755
NCU08531	hypothetical protein	5.54718
NCU03376	hypothetical protein	5.3992
NCU05183	hypothetical protein	5.22296
NCU05277	hypothetical protein	5.13665
NCU09698	hypothetical protein	5.13127
NCU08056	ABC drug exporter AtrF	4.95222
NCU02275	hypothetical protein	4.93374
NCU11050	DUF455 domain-containing protein	4.66729
NCU05822	hypothetical protein	4.63103
NCU04583	acetyltransferase	4.48361
NCU04963	high-affinity glucose transporter	4.38166
NCU07789	hypothetical protein	4.26376
NCU07812	hypothetical protein	4.07211
NCU00943	trehalase	4.05434
NCU08473	alpha-1,3-glucanase	3.98804
NCU02080	hypothetical protein	3.968
NCU07224	monooxygenase	3.96339

Table 5. Top 20 up-regulated genes as determined from RNA-seq. Transcript levels of *Δyvh1* and the control (NCN251) grown in the presence of Cm for 12 hr were compared. The NCU number was used to obtain the gene product name from the Broad Institute Neurospora crassa database. Proteins with no similarities to other proteins with known function are termed hypothetical proteins. The log2 (fold change) was calculated by the difference in expression of transcripts between the control and *Δyvh1*.

4 DISCUSSION

4.1 Growth and AOX protein levels in *Δyvh1*

The *yvh1* gene was originally characterized as having a role in AOX production in a screen of the *N. crassa* KO library. The strain was unable to grow in the presence of the sETC inhibitor antimycin A, and was found to have no AOX protein on a western blot after mitochondria were harvested from strains grown for 24 hr in Cm. However, the strain did express the AOX protein after 48 hr of growth (NARGANG *et al.* 2012). Therefore, a finer analysis of the time points of AOX production was performed in attempt to understand the production of AOX in *Δyvh1*. I have shown that AOX typically begins to appear after 20 to 24 hr of growth in the presence of Cm and does not reach a level equal to the control even after 48 hr of growth in Cm. In addition, the *Δyvh1* strain on normal media lacking inhibitors has a slow growth phenotype. This has also been observed in other species lacking *yvh1* (BEESER and COOPER 1999; GUAN *et al.* 1992; HANAOKA *et al.* 2005; KEMMLER *et al.* 2009; LIU and CHANG 2009; MUDA *et al.* 1999; SUGIYAMA *et al.* 2011), but there have been no previous reports regarding effects on AOX.

Previously it was determined that *Δyvh1* was unable to grow in the presence of antimycin A, although this result was observed after 48 hr of growth in the presence of the chemical (NARGANG *et al.* 2012). In the present study, the strain was allowed to grow for 63 hr and a small amount of growth was observed under these conditions. The delay in growth on antimycin A probably correlates to the delay in the expression of the AOX protein. In *N. crassa*, the AOX protein has been observed after only 2.5 hr of growth in the presence of antimycin A (TANTON *et al.* 2003), and respiration via AOX has been observed after 30 min of exposure to Cm (EDWARDS *et al.* 1974). Therefore induction of the pathway occurs relatively quickly in the control strain but there is a delay in the response of *Δyvh1* to growth in chemicals that induce the AOX pathway.

The low level of the AOX protein observed in the *Δyvh1* strain appears to be due to a low level of *aod-1* transcript produced when the cell was grown in

inducing conditions. In the Δ*yvh1* strain, there was a slight increase in *aod-1* transcript level over time, correlating to the observed increase in AOX protein levels over time. However, even after 36 hr of growth in Cm, the amount of *aod-1* transcript in *Δyvh1* is only about 15-20% of the control levels.

Although the relative amount of transcript levels in the Δ*yvh1* were very low compared to the control under all conditions, and there was only roughly a 5 fold increase when comparing the 36 hr Δ*yvh1* plus Cm to the 18 hr control minus Cm, there was still induction over the basal level of transcription occurring within Δ*yvh1* that was equal to the induction observed in the control (i.e. 40 fold in *Δyvh1*, 30 fold in Ct, after 36 hr growth in Cm). Although the fold change within Δ*yvh1* was roughly equal to that of the control, the overall transcript and protein levels are still considerably lower.

This result was unexpected based on the original hypothesis in section 3.2. that stated there would be an equal amount of *aod-1* transcript - but not protein - between the control and *Δyvh1* because the *yvh1* gene has been suggested to have a role in ribosome biogenesis (KEMMLER *et al.* 2009; LIU and CHANG 2009; LO *et al.* 2009). This hypothesis is refuted because we do not observe equal amounts of *aod-1* transcript between the control and *Δyvh1*. These data strongly suggest that lack of the AOX protein is not directly due to a specific defect in translating of the AOX mRNA.

Preliminary RNA-seq data analysis has revealed that *N. crassa* cells may be unable to process the signal required for AOX induction. The AOD2 and AOD5 transcription factors are expressed to roughly the same levels between the control strain and the *Δyvh1* strain grown in the presence of Cm (Figure 17C, D). In the *Δyvh1* cell, the AOD2/5 transcription factors are expressed at roughly control levels, but cannot induce the *aod-1* transcript to control levels. Therefore, an alternative hypothesis to the one refuted above would be that the *Δyvh1* cells are unable to generate, deliver, or interpret the inducing signal correctly. This would lead to the very low levels of the *aod-1* transcript and AOX protein induced when grown in Cm.

One observation suggests that generation of the signal may be reduced in *Δyvh1* since the cytochrome spectra analyses revealed that Cm is not as effective in Δ*yvh1* as in the control. One explanation for this could be that Cm is not accumulating in the mutant mitochondria to the same extant as the control or that Δ*yvh1* has somehow become resistant to the effects of Cm. In either case, more synthesis of mitochondria encoded sETC proteins would occur and the stress on the cell to induce AOX would be lowered. However, over time Cm has an increased effect on the cell because the peaks observed for cytochrome aa_3 and *b* slowly decrease (Figure 10B). This delay in the effects of Cm may be what leads to the delay in induction of transcript and AOX protein in Δ*yvh1* cells.

The ability of the *Δyvh1* cell to resist the effects of Cm may be due in part to the increase of the ABC drug exporter AtrF mRNA, observed from the RNA-seq experiment (Figure 17E). Some proteins with the ABC transport domain can be efflux pump membrane proteins involved in shuttling substrates across membranes, including drugs like Cm (HIGGINS 2001; RUTLEDGE *et al.* 2011). The *N. crassa* protein has 35% identity (E value = 0; BLASTP) with the yeast protein Pdr5. Loss of Pdr5 in yeast leads to an increase in sensitivity to Cm because of an inability to remove the drug from cells (LEONARD *et al.* 1994). Expression of the *C. albicans* ortholog of Pdr5, Cdr1, in a *S cerevisiae pdr5* null mutant imparted resistance of the yeast strain to Cm (PRASAD *et al.* 1995). Overexpression of the protein leads to an increased resistance to multiple drugs, including Cm (Meyers *et al.* 1992). It is possible that, due to the increase of a drug efflux pump, the *Δyvh1* strain has become at least partially resistant to the effects of Cm. Because the ABC drug transporter is up-regulated, the cell may be expelling more Cm than the control so that the effects on mitochondrial translation are reduced resulting in reduced signals for AOX expression. Over time it appears that this effect decreases because an increase in *aod-1* transcript and AOX protein is observed the longer the cell is in the presence of Cm. If AtrF is a Cm efflux pump, it is unclear why it is expressed to a higher level in *Δyvh1* grown in Cm compared to the control grown in Cm (Figure 17E). It is conceivable that deficient AOX induction in *Δyvh1* results in increased expression of the efflux pump. One way to

test this model would be to follow AOX induction in a *Δyvh1 ΔAtrf* double mutant strain. Alternatively monitoring AOX induction in *Δyvh1* cells where a different inducer of AOX, such as a sETC mutation, could be tried. Finally, it should be noted that the possible effects of Cm efflux mediated by AtrF cannot entirely explain the AOX phenotype, since *aod-1* transcript levels are also reduced in the absence of Cm in the *Δyvh1* strain.

Taken together these results suggest that there is an overall delay in *Δyvh1* of growth and AOX expression in both inducing and non-inducing conditions. AOX protein expression is slower in *Δyvh1* than in the control and transcript levels of *aod-1* never reach the same levels as the control. There also appears to be a reduction in the effects of Cm on mitochondrial ribosome translation, due to an increase in the expression of a drug efflux pump when *Δyvh1* cells are grown in the presences of Cm. It seems likely that the effects observed are secondary to ribosome assembly problems (LIU and CHANG 2009; SUGIYAMA *et al.* 2011). However it remains unclear as to why specific aspects of AOX regulation would be affected.

4.2 YVH1 localization

Rescued transformants of *Δyvh1* were produced by introduction of $yvh1^{+}$ genes carrying HA tags at their N- or C-terminus. Of the transformants screened, N-HA-2 and C-HA-1 were chosen for further work based on the levels of expression of the HA-tagged protein being roughly average among the 20 transformants and on the level of expression of AOX in the transformants after 20 hr of growth in the presence of Cm being equivalent to the control. The chosen transformants also grew at control rates on medium with and without antimycin A. The rescue of the slow growth phenotype associated with loss of *yvh1,* with a wild type copy of *yvh1*, has also been observed in yeast and human cell lines (BEESER and COOPER 1999; GUAN *et al.* 1992; HANAOKA *et al.* 2005; KEMMLER *et al.* 2009; LIU and CHANG 2009; MUDA *et al.* 1999; SUGIYAMA *et al.* 2011). In the present study, levels of the HA-tagged protein in the transformants do not seem to vary between the two growth conditions of plus Cm or minus Cm (Figure 14). In

yeast, mRNA levels of *yvh1* were initially increased when the cells were placed under nitrogen starvation conditions (MUDA *et al.* 1999). Western analysis of the different growth stages of *P. falciparum* showed that YVH1 was constitutively expressed in all stages (KUMAR *et al.* 2004)

The *N. crassa* protein was found to localize to the nuclear fraction and the PMP fraction in both inducing and non-inducing conditions. In yeast, the protein has been shown to localize to the nucleus and the cytoplasm through fluorescent microscopy techniques (KEMMLER *et al.* 2009; LIU and CHANG 2009; LO *et al.* 2009; MUDA *et al.* 1999). The PMP fraction is composed of fragmented ER, other organelles, and any complex or aggregate that would be pelleted at 130,000 x g for 1.5 hr. I demonstrated that the PMP also contained ribosomes using Western blots and an antibody to *S. cerevisiae* RPL3. Furthermore, there was no evidence for ribosomes remaining in the cytosol fraction

Although the subcellular fractionation experiments revealed that YVH1 was in the same fraction as the ribosome marker, isolation of ribosomes in the presences of 1% Triton-X-100 showed that a very low amount was found in the ribosome pellet, with the majority present in the supernatant as a free protein. This could suggest that the interaction between YVH1 and ribosomes in the cytosol is not a strong one and is disrupted by the detergent. Thus, differences in experimental protocols likely explain why YVH1 pelleted with RPL3 in the PMP fraction of the fractionation experiment but did not pellet in the sucrose cushion ribosome isolation experiment. In the ribosome isolation, Trition-X-100 was added to dissolve organelle membranes and release any membrane bound ribosomes. A clarifying spin was also done to ensure any aggregates that are not dissolved by the detergent are removed. Our procedure was a modification of LO *et al.* (2009). In their ribosome isolation experiments they found YVH1 in the ribosome pellet and not in the supernatant. However, we used a higher detergent concentration (1% versus 0.1%) and also a clarifying spin. In their materials and methods (LO *et al.* 2009), they do not explicitly state that they carried out a clarifying spin and this may be the difference between the two studies. Another

simple explanation might be that the YVH1 protein in *N. crassa* may associate more loosely with ribosomes than in *S. cerevisiae*.

4.3 Functional domain of YVH1

Mutations of the phosphatase domain that change the cysteine of the $HC(X)_5R$ catalytic domain to serine have been shown to inactivate the phosphatase domain in yeast YVH1 (BEESER and COOPER 2000). I made an identical mutant in the *N. crassa* protein as well as changing the histidine and arginine both to glutamine to inactivate the phosphatase domain. The cysteines of hYVH1 zinc-binding domain have been shown to bind 2 mols of zinc per molecule with 4 amino acids interacting to bind each metal ion (BONHAM and VACRATSIS 2009; MUDA *et al.* 1999). I mutated a pair of cysteines in the zinc-binding domain, to inactivate this domain. The mutant constructs were used to transform *Δyvh1* and transformants with only one working domain were isolated. These were used to determine if both or either of the domains had a role in AOX production in *N. crassa*.

My results showed that *N. crassa* cells could not produce AOX when the two cysteines of the zinc-binding domain were mutated to serines. On the other hand, when the phosphatase domain was mutated, localization of the protein was unaffected and AOX expression occurred as in the control. Therefore, for normal growth and AOX expression, the cell requires a YVH1 protein with a functional zinc-domain, but the phosphatase activity is not required. The phosphatase domain has been shown to dephosphorylate a template *in vitro* (PARK *et al.* 1996). However, exactly what it dephosphorylates *in vivo* in any organism, remains to be determined. It appears that this domain does not have a role in AOX production and is not required for normal growth in *N. crassa*. It is possible that the domain may carry out a different function in the cell not observed in this study.

Inactivation of the zinc-domain appears to lead to the localization of YVH1 solely to the nucleus, even after 48 hr (Figure 16B, C). This suggests that the protein requires a functional zinc-binding domain to shuttle from the nucleus to the cytosol. As a trans-acting factor in ribosome assembly in yeast, the zinc

domain may be required for recruitment to the pre-60S subunit. It has been shown that RPL12 is the protein required for the recruitment of YVH1 (LO *et al.* 2009). Therefore, it is possible that YVH1 without the zinc-binding domain is unable to interact with RPL12. This would mean that YVH1 lacking the zinc-domain is not recruited to the 60S ribosome subunit and therefore, is not exported out of the nucleus with the ribosome. Another possibility is that the YVH1 protein, without the zinc-domain, is still recruited to the 60S ribosome subunit, but cannot facilitate the transfer of Mrt4 off the 60S subunit, leading to YVH1 remaining in the nucleus and the subsequent production of altered ribosomes. The switching of Mrt4 with P0 has been shown to occur in either the nucleus or the cytoplasm, when YVH1 is restricted to either region (KEMMLER *et al.* 2009; LO *et al.* 2009). Although the zinc-domain mutant in this study is localized to the nucleus, it appears as though the protein cannot function properly without the two cysteines of the domain. To my knowledge, no other study has directly determined the localization of YVH1 with an inactive zinc-binding domain.

The significance of the zinc domain has also been observed in yeast. Rescue of sporulation and glycogen defects occurred with expression of a protein containing a functional zinc-domain but not the phosphatase domain (BEESER and COOPER 2000). Rescue of the slow growth yeast phenotype by the human copy of YVH1 was also shown to require a functional zinc-binding domain, suggesting cross species conservation (MUDA *et al.* 1999). A functional zinc-domain was required for the yeast cell to reach normal levels of mature 60S subunits (LIU and CHANG 2009). The zinc-domain was also required for the proper release of Mrt4 from the pre-60S subunit (KEMMLER *et al.* 2009; LO *et al.* 2009). Rescue of phenotypes observed in a human cell line lacking *hyvh1* also requires a functional zinc domain (KOZAROVA *et al.* 2011). Thus, all studies are in agreement in that the zinc-binding domain, and not the phosphatase domain, is required for YVH1 function.

4.4 RNA-seq

The RNA-seq experiment revealed roughly 1200 down-regulated genes and 500 up-regulated genes in *Δyvh1* grown in the presence of Cm compared to the control grown in the same conditions. Thus, roughly 17% of the 10,000 protein coding genes were significantly affected (at least 2 fold) by loss of *yvh1*. This may be a result of the *Δyvh1* strain attempting to compensate for a decrease in translation caused by defective ribosomes. However, it is currently unclear what genes are affected specifically due to growth in the inducer Cm. An RNA-seq experiment of the control and *Δyvh1* grown in the absence of Cm should allow for the distinction between genes specifically affected by growth in Cm and genes that are affected under both conditions in *Δyvh1*. This analysis is currently underway

There appears to be no pattern, with respect to gene families, observed when analyzing the top 20 down and up-regulated genes (Table 4 and 5, respectively). Cyanide hydratase, a hydrolase that breaks carbon-nitrogen bonds, is the greatest down-regulated gene in *Δyvh1* compared to the control (BASILE *et al.* 2008). Normally, the expression of this gene may be part of a general response to poor mitochondrial function. In the wild, *N. crassa* may encounter certain chemicals, like cyanide, that would induce this gene, and AOX, amongst others. Potentially the loss of *yvh1* could affect a general retrograde response of the mitochondria.

The next lowest expressed gene in *Δyvh1* compared to the control strain is the *yvh1* gene, which is expected, as the *Δyvh1* strain should not contain any transcript of the gene. The 17th down-regulated gene is the *aod-1* transcript encoding AOX, which validates the earlier results of the qPCR, showing there is a low amount of this transcript in *Δyvh1* when grown in the presence of Cm. The fact that the PCK gene is down-regulated in the *Δyvh1* strain suggests that the process of gluconeogenesis is also affected in the *Δyvh1* strain. In *P. anserina* (SELLEM *et al.* 2009) and *A. nidulans* (SUZUKI *et al.* 2012), the PCK gene is controlled by the orthologs of the *N. crassa* AOD2/5 transcription factors. This

also appears to be the case in *N. crassa* (Z. Qi, unpublished). Thus, there appears to be a general defect in the expression of genes controlled by AOD2 and AOD5 and it remains a possibility that the activating signal is not efficiently produced or recognized in *Δyvh1*.

The ability of the cell to increase the expression of one protein and not another, in the absence of the YVH1 ribosome biogenesis factor, could be explained by the ribosome filter hypothesis [reviewed in (MAURO and EDELMAN 2002; MAURO and EDELMAN 2007)]. This hypothesis states that translation is a form of regulation of the expression of proteins and can be controlled by such mechanisms as mRNA-rRNA interactions or by the heterogeneity of ribosomes, which is defined as the protein composition of the ribosomes. These interactions between mRNA and ribosomes would lead to a specific subset of mRNA's in a population to be translated effectively better than others. Heterogeneity of ribosome proteins has been demonstrated to be a form of translational control in yeast. Ribosomes lacking very acid ribosomal proteins associated with the 60S subunit have been shown to translate specific mRNAs differentially than 60S subunits with the very acid ribosomal proteins (REMACHA *et al.* 1995; SAENZ-ROBLES *et al.* 1990; SZICK-MIRANDA and BAILEY-SERRES 2001). Another study showed that depletion of 60S subunits or 60S ribosomal proteins leads to an increase in translation of Gcn4, a nutrient responsive factor, which promotes increased yeast lifespan (STEFFEN *et al.* 2008). Taken together it is possible that ribosome composition, affected by post-translation modifications of ribosomal proteins and different modifications of rRNA, could influence the specificity of the ribosome for certain mRNAs. Although this may explain why we see an increase in translation of certain mRNAs, it does not directly explain why we see an increase (and decrease) in transcription of certain genes over others, in the *Δyvh1* strain. It is conceivable that the level of translation of a given mRNA may affect its half-life (GHOSH and JACOBSON 2010) and that this is reflected in the RNA-seq data. It has been shown in yeast that loss of *yvh1* leads to a moderate increase in the half-lives of certain mRNAs. (SUGIYAMA *et al.* 2011).

Taken together the delay in AOX induction could be occurring via many different mechanisms. One possibility for the decrease in AOX expression in *Δyvh1* cells is that the Cm concentration in the cell is reduced (and as a result, the inhibition of mitochondrial protein synthesis is reduced) due to an increase in the drug efflux pump AtrF. Ineffective inhibition of mitochondrial translation would result in more efficient sETC function. This could lead to a decrease in the strength of the inducing signal (Figure 18A). Over time enough signal is generated, leading to the gradual temporal increase in AOX. Another possibility for the delay in AOX induction is that the AOD2 and AOD5 transcription factors are not efficiently translated (Figure 18B). This model is based on the observation that there is a lower constitutive amount of the *aod-1* transcript even under non-inducing conditions in the *Δyvh1* strain compared to the control. Over time under inducing conditions we see an increase in the *aod-1* transcript and the AOX protein, suggesting that the AOD2 and AOD5 proteins might accumulate over time and induce the expression of the AOX protein.

4.5 Significance and future directions

The work in this thesis has examined the role of YVH1 in the production of AOX in *N. crassa*. By tagging YVH1 with the HA epitope so that it could be followed in cellular fractionation experiments, I showed that the YVH1 protein localizes to the nuclei and PMP fractions of the cell, suggesting a role as a protein that shuttles between the two locations. I also showed that the zinc-binding domain, and not the phosphatase domain of the protein, was required for proper localization, and also for AOX induction. RNA-seq analysis revealed that 17% of the 10,000 predicted protein-coding genes in *N. crassa* are affected by loss of YVH1 when grown in the presence of Cm. To my knowledge, this is the first time YVH1 has been shown to have a role in the production of AOX in any organism.

The qPCR of AOX has already validated the results of the RNA-seq experiment for this gene. qPCR primers could be designed for additional up and down-regulated genes for further validation. It would be interesting to determine if the ABC-drug transporter transcript (*atrF* gene) in *Δyvh1* grown in the absence

of Cm is also up-regulated compared to the control, or if this increase in transcription is induced by growth in the presence of Cm. It would also be interesting to determine if the ABC-drug transporter is up-regulated in strains that cannot express the AOX protein, like the *aod-1*, *aod-2*, or *aod-5* knockouts, which are readily available in our lab. If it was found to be up-regulated in strains lacking AOX grown in the presence of Cm, it would suggest that up-regulation of this gene occurs in strains that cannot respire using the AOX protein. Potentially this would mean that the up-regulation of the ABC drug transporter is a secondary defense mechanism of *N. crassa* cells that cannot induce AOX when grown in the presence of inducers of the pathway.

It is important to determine if the *atrF* gene is responsible for the increase in resistance to Cm in *Δyvh1*. The simplest method of determining this would be to construct a double knockout mutant of *atrF* and *yvh1*. Both cytochrome content and the presence of AOX could be monitored following growth in Cm to determine the effects of not having the induced drug efflux pump.

Additionally, another RNA-seq experiment should be carried out using cells grown in the absence of the inducer Cm. This would allow for a comparison of transcript levels under both inducing and non-inducing conditions to observe which genes affected in *Δyvh1* are a general response to loss of *yvh1* and which are due specifically to growth in the presence of Cm. This will allow for a better understanding of the response of *Δyvh1* (and at the same time the control) to growth in the presence of Cm, and the induction of the AOX pathway. This experiment is underway.

To determine the significance of the altered localization in the zinc-domain mutant, a ribosome isolation procedure should be carried out using the zinc-domain mutant strain, to see if the mutation affects the association of YVH1 with ribosomes. The protein cannot transport out of the nucleus when the zinc-domain is mutated, potentially because it cannot interact with ribosomes. If this were the case, the zinc-domain mutant protein would be expected in only the supernatant fraction as a free protein, and not in the pellet fraction, associated with ribosome.

A

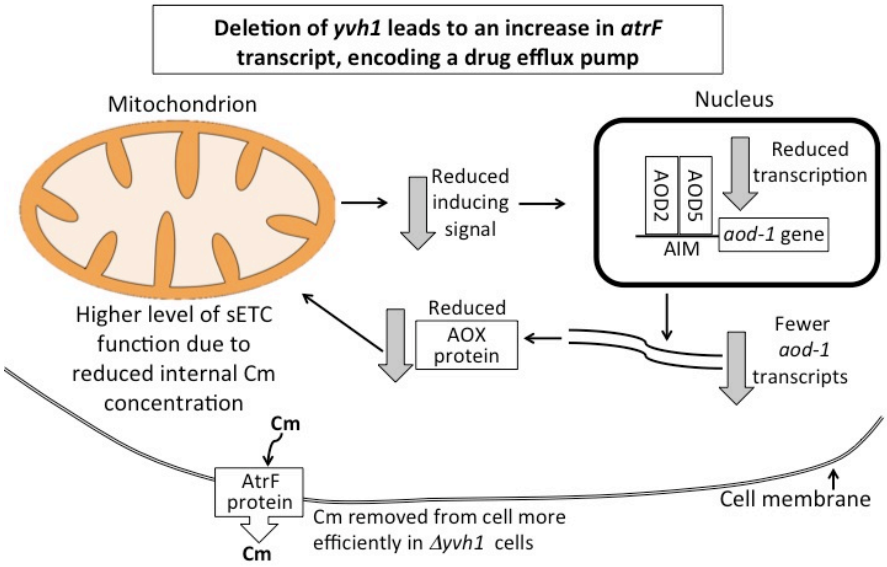

B

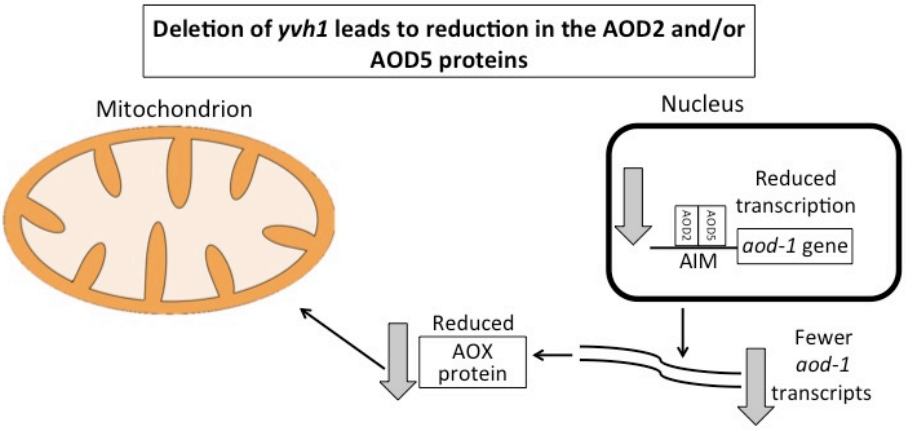

(Adapted from Chae and Nargang, 2007)

Figure 18. Two possible models for effects on AOX production caused by loss of YVH1. These models are not mutually exclusive. A) Increased expression of a drug efflux pump decreases production of the inducing signal. Growth of *Δyvh1* cells in the presence of Cm does not result in the same level of inhibition of mitochondrial protein synthesis as in control cells, possibly due to an increase in expression of a drug efflux pump (AtrF). This leads to less inhibition of the sETC, which decreases the inducing signal required for AOX induction, and decreases the level of the *aod-1* transcript and AOX protein (grey arrows). B) Translation and/or stability of AOD2 and/or AOD5 is decreased in cells lacking YVH1. Based on the observation that the constitutive levels of *aod-1* transcripts are reduced in non-induced *Δyvh1* cells. It is conceivable that the translation or stability of AOD2 and/or AOD5 may be decreased. This could lead to a lower level of *aod-1* transcripts and the AOX protein (grey arrows). The same might apply to AOD2 and/or AOD5 under inducing conditions in *Δyvh1* cells.

5 REFERENCES

ADAMS, K. L., and J. D. PALMER, 2003 Evolution of mitochondrial gene content: gene loss and transfer to the nucleus. Mol Phylogenet Evol **29:** 380-395.

ADDISON, R., 1998 A cell-free translation-translocation system reconstituted with subcellular fractions from the wall-less variant fz;sg;os-1V of Neurospora crassa. Fungal Genet Biol **24:** 345-353.

ALBURY, M. S., C. ELLIOTT and A. L. MOORE, 2009 Towards a structural elucidation of the alternative oxidase in plants. Physiol Plant **137:** 316-327.

ALLEN, J. F., 2003 The function of genomes in bioenergetic organelles. Philos Trans R Soc Lond B Biol Sci **358:** 19-37; discussion 37-18.

ANDERSSON, M. E., and P. NORDLUND, 1999 A revised model of the active site of alternative oxidase. FEBS Lett **449:** 17-22.

ANDERSSON, S. G., O. KARLBERG, B. CANBACK and C. G. KURLAND, 2003 On the origin of mitochondria: a genomics perspective. Philos Trans R Soc Lond B Biol Sci **358:** 165-177; discussion 177-169.

ANDERSSON, S. G., A. ZOMORODIPOUR, J. O. ANDERSSON, T. SICHERITZ-PONTEN, U. C. ALSMARK *et al.*, 1998 The genome sequence of Rickettsia prowazekii and the origin of mitochondria. Nature **396:** 133-140.

ANGIOY, A. M., M. C. STENSMYR, I. URRU, M. PULIAFITO, I. COLLU *et al.*, 2004 Function of the heater: the dead horse arum revisited. Proc Biol Sci **271 Suppl 3:** S13-15.

AZCON-BIETO, J., M. RIBAS-CARBO, M. A. GONZALEZ-MELER and J. PENUELAS, 1989 Sulfide-Resistant Respiration in Leaves of Elodea canadensis Michx: Comparison with Cyanide-Resistant Respiration. Plant Physiol **90:** 1249-1251.

BASILE, L. J., R. C. WILLSON, B. T. SEWELL and M. J. BENEDIK, 2008 Genome mining of cyanide-degrading nitrilases from filamentous fungi. Appl Microbiol Biotechnol **80:** 427-435.

BEESER, A. E., and T. G. COOPER, 1999 The dual-specificity protein phosphatase Yvh1p acts upstream of the protein kinase mck1p in promoting spore development in Saccharomyces cerevisiae. J Bacteriol **181:** 5219-5224.

BEESER, A. E., and T. G. COOPER, 2000 The dual-specificity protein phosphatase Yvh1p regulates sporulation, growth, and glycogen accumulation independently of catalytic activity in Saccharomyces cerevisiae via the cyclic AMP-dependent protein kinase cascade. J Bacteriol **182:** 3517-3528.

BERTHOLD, D. A., M. E. ANDERSSON and P. NORDLUND, 2000 New insight into the structure and function of the alternative oxidase. Biochim Biophys Acta **1460:** 241-254.

BERTHOLD, D. A., and P. STENMARK, 2003 Membrane-bound diiron carboxylate proteins. Annu Rev Plant Biol **54:** 497-517.

BERTRAND, H., A. ARGAN and N. A. SZAKACS, 1983 Genetic control of the biogenesis of cyanide insensitive respiration in *Neurospora crassa*, pp. 495-507 in *Mitochondria*, edited by R. J. S. K. W. F. KAUDEWITZ. Walter de Gruyter Co., Germany.

BERTRAND, H., and T. H. PITTENGER, 1969 Cytoplasmic Mutants Selected from Continuously Growing Cultures of *Neurospora crassa*. Genetics **61:** 643-659.

BIERNACKI, M. A., O. MARINA, W. ZHANG, F. LIU, I. BRUNS *et al.*, 2010 Efficacious immune therapy in chronic myelogenous leukemia (CML) recognizes antigens that are expressed on CML progenitor cells. Cancer Res **70:** 906-915.

BOEKEMA, E. J., and H. P. BRAUN, 2007 Supramolecular structure of the mitochondrial oxidative phosphorylation system. J Biol Chem **282:** 1-4.

BONHAM, C. A., and P. O. VACRATSIS, 2009 Redox regulation of the human dual specificity phosphatase YVH1 through disulfide bond formation. J Biol Chem **284:** 22853-22864.

BOTTORFF, D. A., S. PARMAKSIZOGLU, E. G. LEMIRE, J. W. COFFIN, H. BERTRAND *et al.*, 1994 Mutations in the structural gene for cytochrome c result in deficiency of both cytochromes aa3 and c in Neurospora crassa. Curr Genet **26:** 329-335.

BOZDECH, Z., M. LLINAS, B. L. PULLIAM, E. D. WONG, J. ZHU *et al.*, 2003 The transcriptome of the intraerythrocytic developmental cycle of Plasmodium falciparum. PLoS Biol **1:** E5.

BRICENO, V., H. CAMARGO, M. REMACHA, C. SANTOS and J. P. BALLESTA, 2009 Structural and functional characterization of the amino terminal domain of the yeast ribosomal stalk P1 and P2 proteins. Int J Biochem Cell Biol **41:** 1315-1322.

BUTOW, R. A., and N. G. AVADHANI, 2004 Mitochondrial signaling: the retrograde response. Mol Cell **14:** 1-15.

CAIN, E. L., S. E. BRAUN and A. BEESER, 2011 Characterization of a human cell line stably over-expressing the candidate oncogene, dual specificity phosphatase 12. PLoS One **6:** e18677.

CARDENAS, D., J. REVUELTA-CERVANTES, A. JIMENEZ-DIAZ, H. CAMARGO, M. REMACHA *et al.*, 2012 P1 and P2 protein heterodimer binding to the P0 protein of Saccharomyces cerevisiae is relatively non-specific and a source of ribosomal heterogeneity. Nucleic Acids Res **40:** 4520-4529.

CASTRO-GUERRERO, N. A., K. KRAB and R. MORENO-SANCHEZ, 2004 The alternative respiratory pathway of euglena mitochondria. J Bioenerg Biomembr **36:** 459-469.

CASTRO-GUERRERO, N. A., J. S. RODRIGUEZ-ZAVALA, A. MARIN-HERNANDEZ, S. RODRIGUEZ-ENRIQUEZ and R. MORENO-SANCHEZ, 2008 Enhanced alternative oxidase and antioxidant enzymes under Cd(2+) stress in Euglena. J Bioenerg Biomembr **40:** 227-235.

CAVALIER-SMITH, T., 1987 The simultaneous symbiotic origin of mitochondria, chloroplasts, and microbodies. Ann N Y Acad Sci **503:** 55-71.

CAVALIER-SMITH, T., 2006 Origin of mitochondria by intracellular enslavement of a photosynthetic purple bacterium. Proc Biol Sci **273:** 1943-1952.

CHACINSKA, A., C. M. KOEHLER, D. MILENKOVIC, T. LITHGOW and N. PFANNER, 2009 Importing mitochondrial proteins: machineries and mechanisms. Cell **138:** 628-644.

CHAE, M. S., C. C. LIN, K. E. KESSLER, C. E. NARGANG, L. L. TANTON *et al.*, 2007a Identification of an alternative oxidase induction motif in the promoter region of the aod-1 gene in Neurospora crassa. Genetics **175:** 1597-1606.

CHAE, M. S., C. E. NARGANG, I. A. CLEARY, C. C. LIN, A. T. TODD *et al.*, 2007b Two zinc-cluster transcription factors control induction of alternative oxidase in Neurospora crassa. Genetics **177:** 1997-2006.

CHAE, M. S., and F. E. NARGANG, 2009 Investigation of regulatory factors required for alternative oxidase production in Neurospora crassa. Physiol Plant **137:** 407-418.

CHAUDHURI, M., R. D. OTT and G. C. HILL, 2006 Trypanosome alternative oxidase: from molecule to function. Trends Parasitol **22:** 484-491.

CHAUDHURI, M., R. SHARAN and G. C. HILL, 2002 Trypanosome alternative oxidase is regulated post-transcriptionally at the level of RNA stability. J Eukaryot Microbiol **49:** 263-269.

CHIOU, J. C., X. P. LI, M. REMACHA, J. P. BALLESTA and N. E. TUMER, 2008 The ribosomal stalk is required for ribosome binding, depurination of the rRNA and cytotoxicity of ricin A chain in Saccharomyces cerevisiae. Mol Microbiol **70:** 1441-1452.

CLARK, C. G., and A. J. ROGER, 1995 Direct evidence for secondary loss of mitochondria in Entamoeba histolytica. Proc Natl Acad Sci U S A **92:** 6518-6521.

CLAROS, M. G., J. PEREA, Y. SHU, F. A. SAMATEY, J. L. POPOT *et al.*, 1995 Limitations to in vivo import of hydrophobic proteins into yeast mitochondria. The case of a cytoplasmically synthesized apocytochrome b. Eur J Biochem **228:** 762-771.

CLIFTON, R., A. H. MILLAR and J. WHELAN, 2006 Alternative oxidases in Arabidopsis: a comparative analysis of differential expression in the gene family provides new insights into function of non-phosphorylating bypasses. Biochim Biophys Acta **1757:** 730-741.

COLLINS, S. R., P. KEMMEREN, X. C. ZHAO, J. F. GREENBLATT, F. SPENCER *et al.*, 2007 Toward a comprehensive atlas of the physical interactome of Saccharomyces cerevisiae. Mol Cell Proteomics **6:** 439-450.

COLOT, H. V., G. PARK, G. E. TURNER, C. RINGELBERG, C. M. CREW *et al.*, 2006 A high-throughput gene knockout procedure for Neurospora reveals functions for multiple transcription factors. Proc Natl Acad Sci U S A **103:** 10352-10357.

CONSIDINE, M. J., R. C. HOLTZAPFFEL, D. A. DAY, J. WHELAN and A. H. MILLAR, 2002 Molecular distinction between alternative oxidase from monocots and dicots. Plant Physiol **129:** 949-953.

COPELAND, J. M., J. CHO, T. LO, JR., J. H. HUR, S. BAHADORANI *et al.*, 2009 Extension of Drosophila life span by RNAi of the mitochondrial respiratory chain. Curr Biol **19:** 1591-1598.

COSTA, J. H., D. F. DE MELO, Z. GOUVEIA, H. G. CARDOSO, A. PEIXE *et al.*, 2009 The alternative oxidase family of Vitis vinifera reveals an attractive model to study the importance of genomic design. Physiol Plant **137:** 553-565.

COSTA, J. H., Y. JOLIVET, M. P. HASENFRATZ-SAUDER, E. G. ORELLANO, M. DA GUIA SILVA LIMA *et al.*, 2007 Alternative oxidase regulation in roots of Vigna unguiculata cultivars differing in drought/salt tolerance. J Plant Physiol **164:** 718-727.

CRISTINA, D., M. CARY, A. LUNCEFORD, C. CLARKE and C. KENYON, 2009 A regulated response to impaired respiration slows behavioral rates and increases lifespan in Caenorhabditis elegans. PLoS Genet **5:** e1000450.

CVETKOVSKA, M., and G. C. VANLERBERGHE, 2013 Alternative oxidase impacts the plant response to biotic stress by influencing the mitochondrial generation of reactive oxygen species. Plant Cell and Environment **36:** 721-732.

DALEY, D. O., R. CLIFTON and J. WHELAN, 2002 Intracellular gene transfer: reduced hydrophobicity facilitates gene transfer for subunit 2 of cytochrome c oxidase. Proc Natl Acad Sci U S A **99:** 10510-10515.

DALEY, D. O., and J. WHELAN, 2005 Why genes persist in organelle genomes. Genome Biol **6:** 110.

DAS, S. K., W. S. CHU, T. C. HALE, X. WANG, R. L. CRAIG *et al.*, 2006 Polymorphisms in the glucokinase-associated, dual-specificity phosphatase 12 (DUSP12) gene under chromosome 1q21 linkage peak are associated with type 2 diabetes. Diabetes **55:** 2631-2639.

DAVIS, F. F., and F. J. DE SERRES, 1970 Genetic and microbiological research techniques for *Neurospora crassa*. Methods Enzymol **17A:** 70-143.

DAY, D. A., and J. T. WISKICH, 1995 Regulation of alternative oxidase activity in higher plants. J Bioenerg Biomembr **27:** 379-385.

DE GREY, A. D. N. J., 2005 Forces maintaining organellar genomes: is any as strong as genetic code disparity or hydrophobicity? Bioessays **27:** 436-446.

DEQUARD-CHABLAT, M., M. RIVA, C. CARLES and A. SENTENAC, 1991 RPC19, the gene for a subunit common to yeast RNA polymerases A (I) and C (III). J Biol Chem **266:** 15300-15307.

DESCHENEAU, A. T., I. A. CLEARY and F. E. NARGANG, 2005 Genetic evidence for a regulatory pathway controlling alternative oxidase production in Neurospora crassa. Genetics **169:** 123-135.

DJAJANEGARA, I., P. M. FINNEGAN, C. MATHIEU, T. MCCABE, J. WHELAN *et al.*, 2002 Regulation of alternative oxidase gene expression in soybean. Plant Mol Biol **50:** 735-742.

DUARTE, M., and A. VIDEIRA, 2009 Effects of mitochondrial complex III disruption in the respiratory chain of Neurospora crassa. Mol Microbiol **72:** 246-258.

DUKANOVIC, J., and D. RAPAPORT, 2011 Multiple pathways in the integration of proteins into the mitochondrial outer membrane. Biochim Biophys Acta **1808:** 971-980.

EDERLI, L., R. MORETTINI, A. BORGOGNI, C. WASTERNACK, O. MIERSCH *et al.*, 2006 Interaction between nitric oxide and ethylene in the induction of alternative oxidase in ozone-treated tobacco plants. Plant Physiol **142:** 595-608.

EDWARDS, D. L., J. CHALMERS, J. H., H. J. GUZIK and J. T. WARDEN, 1976 *Assembly of the cyanide-insensitive respiratory pathway in Neurospora crassa*. Elservier/North-Holland Biomedical Press, Amsterdam.

EDWARDS, D. L., E. RSENBERG and P. A. MARONEY, 1974 Induction of cyanide-insensitive respiration in Neurospora crassa. J Biol Chem **249:** 3551-3556.

EGEA, P. F., R. M. STROUD and P. WALTER, 2005 Targeting proteins to membranes: structure of the signal recognition particle. Curr Opin Struct Biol **15:** 213-220.

ELHAFEZ, D., M. W. MURCHA, R. CLIFTON, K. L. SOOLE, D. A. DAY *et al.*, 2006 Characterization of mitochondrial alternative NAD(P)H dehydrogenases in Arabidopsis: intraorganelle location and expression. Plant Cell Physiol **47:** 43-54.

EMBLEY, T. M., and W. MARTIN, 2006 Eukaryotic evolution, changes and challenges. Nature **440:** 623-630.

EMELYANOV, V. V., 2001 Rickettsiaceae, rickettsia-like endosymbionts, and the origin of mitochondria. Biosci Rep **21:** 1-17.

ENDO, T., K. YAMANO and S. KAWANO, 2011 Structural insight into the mitochondrial protein import system. Biochim Biophys Acta **1808:** 955-970.

ESTAQUIER, J., F. VALLETTE, J. L. VAYSSIERE and B. MIGNOTTE, 2012 The mitochondrial pathways of apoptosis. Adv Exp Med Biol **942:** 157-183.

EUBEL, H., J. HEINEMEYER, S. SUNDERHAUS and H. P. BRAUN, 2004 Respiratory chain supercomplexes in plant mitochondria. Plant Physiol Biochem **42:** 937-942.

FINNEGAN, P. M., A. L. UMBACH and J. A. WILCE, 2003 Prokaryotic origins for the mitochondrial alternative oxidase and plastid terminal oxidase nuclear genes. FEBS Lett **555:** 425-430.

FREIJE, W. A., S. MANDAL and U. BANERJEE, 2012 Expression Profiling of Attenuated Mitochondrial Function Identifies Retrograde Signals in Drosophila. G3-Genes Genomes Genetics **2:** 843-851.

FRIEDMAN, J. R., L. L. LACKNER, M. WEST, J. R. DIBENEDETTO, J. NUNNARI *et al.*, 2011 ER tubules mark sites of mitochondrial division. Science **334:** 358-362.

GAVIN, A. C., P. ALOY, P. GRANDI, R. KRAUSE, M. BOESCHE *et al.*, 2006 Proteome survey reveals modularity of the yeast cell machinery. Nature **440:** 631-636.

GEBERT, N., M. T. RYAN, N. PFANNER, N. WIEDEMANN and D. STOJANOVSKI, 2011 Mitochondrial protein import machineries and lipids: a functional connection. Biochim Biophys Acta **1808:** 1002-1011.

GHOSH, S., and A. JACOBSON, 2010 RNA decay modulates gene expression and controls its fidelity. Wiley Interdiscip Rev RNA **1:** 351-361.

GIRAUD, E., L. H. HO, R. CLIFTON, A. CARROLL, G. ESTAVILLO *et al.*, 2008 The absence of ALTERNATIVE OXIDASE1a in Arabidopsis results in acute sensitivity to combined light and drought stress. Plant Physiol **147:** 595-610.

GIRAUD, E., O. VAN AKEN, L. H. HO and J. WHELAN, 2009 The transcription factor ABI4 is a regulator of mitochondrial retrograde expression of ALTERNATIVE OXIDASE1a. Plant Physiol **150:** 1286-1296.

GLANCY, B., and R. S. BALABAN, 2012 Role of mitochondrial Ca2+ in the regulation of cellular energetics. Biochemistry **51:** 2959-2973.

GONZALO, P., and J. P. REBOUD, 2003 The puzzling lateral flexible stalk of the ribosome. Biol Cell **95:** 179-193.

GOOD, A. G., and W. L. CROSBY, 1989 Anaerobic induction of alanine aminotransferase in barley root tissue. Plant Physiol **90:** 1305-1309.

GRANNEMAN, S., and S. J. BASERGA, 2004 Ribosome biogenesis: of knobs and RNA processing. Exp Cell Res **296:** 43-50.

GRATIAS, S., A. SCHULER, L. K. HITPASS, H. STEPHAN, H. RIEDER *et al.*, 2005 Genomic gains on chromosome 1q in retinoblastoma: consequences on gene expression and association with clinical manifestation. Int J Cancer **116:** 555-563.

GRAY, M. W., 2012 Mitochondrial evolution. Cold Spring Harb Perspect Biol **4**.

GRAY, M. W., G. BURGER and B. F. LANG, 1999 Mitochondrial evolution. Science **283:** 1476-1481.

GRAY, M. W., G. BURGER and B. F. LANG, 2001 The origin and early evolution of mitochondria. Genome Biol **2:** REVIEWS1018.

GRAY, M. W., B. F. LANG, R. CEDERGREN, G. B. GOLDING, C. LEMIEUX *et al.*, 1998 Genome structure and gene content in protist mitochondrial DNAs. Nucleic Acids Res **26:** 865-878.

GUAN, K., D. J. HAKES, Y. WANG, H. D. PARK, T. G. COOPER *et al.*, 1992 A yeast protein phosphatase related to the vaccinia virus VH1 phosphatase is induced by nitrogen starvation. Proc Natl Acad Sci U S A **89:** 12175-12179.

GUHA, M., H. PAN, J. K. FANG and N. G. AVADHANI, 2009 Heterogeneous Nuclear Ribonucleoprotein A2 Is a Common Transcriptional Coactivator in the Nuclear Transcription Response to Mitochondrial Respiratory Stress. Mol Biol Cell **20:** 4107-4119.

HANAOKA, N., T. UMEYAMA, K. UENO, K. UEDA, T. BEPPU *et al.*, 2005 A putative dual-specific protein phosphatase encoded by YVH1 controls growth, filamentation and virulence in Candida albicans. Microbiology **151:** 2223-2232.

HARNER, M., C. KORNER, D. WALTHER, D. MOKRANJAC, J. KAESMACHER *et al.*, 2011 The mitochondrial contact site complex, a determinant of mitochondrial architecture. EMBO J **30:** 4356-4370.

HEGDE, R. S., and R. J. KEENAN, 2011 Tail-anchored membrane protein insertion into the endoplasmic reticulum. Nat Rev Mol Cell Biol **12:** 787-798.

HIGGINS, C. F., 2001 ABC transporters: physiology, structure and mechanism--an overview. Res Microbiol **152:** 205-210.

HILTUNEN, J. K., K. J. AUTIO, M. S. SCHONAUER, V. A. KURSU, C. L. DIECKMANN *et al.*, 2010 Mitochondrial fatty acid synthesis and respiration. Biochim Biophys Acta **1797:** 1195-1202.

HIRAI, M., S. YOSHIDA, H. KASHIWAGI, T. KAWAMURA, T. ISHIKAWA *et al.*, 1999 1q23 gain is associated with progressive neuroblastoma resistant to aggressive treatment. Genes Chromosomes Cancer **25:** 261-269.

HO, L. H., E. GIRAUD, R. LISTER, D. THIRKETTLE-WATTS, J. LOW *et al.*, 2007 Characterization of the regulatory and expression context of an alternative oxidase gene provides insights into cyanide-insensitive respiration during growth and development. Plant Physiol **143:** 1519-1533.

HOPPINS, S., S. R. COLLINS, A. CASSIDY-STONE, E. HUMMEL, R. M. DEVAY *et al.*, 2011 A mitochondrial-focused genetic interaction map reveals a scaffold-like complex required for inner membrane organization in mitochondria. J Cell Biol **195:** 323-340.

HOPPINS, S., L. LACKNER and J. NUNNARI, 2007a The machines that divide and fuse mitochondria. Annu Rev Biochem **76:** 751-780.

HOPPINS, S. C., N. E. GO, A. KLEIN, S. SCHMITT, W. NEUPERT *et al.*, 2007b Alternative splicing gives rise to different isoforms of the Neurospora crassa Tob55 protein that vary in their ability to insert beta-barrel proteins into the outer mitochondrial membrane. Genetics **177:** 137-149.

HUANG, X., U. VON RAD and J. DURNER, 2002 Nitric oxide induces transcriptional activation of the nitric oxide-tolerant alternative oxidase in Arabidopsis suspension cells. Planta **215:** 914-923.

HUH, W. K., and S. O. KANG, 2001 Characterization of the gene family encoding alternative oxidase from Candida albicans. Biochem J **356:** 595-604.

ITO, Y., D. SAISHO, M. NAKAZONO, N. TSUTSUMI and A. HIRAI, 1997 Transcript levels of tandem-arranged alternative oxidase genes in rice are increased by low temperature. Gene **203:** 121-129.

JARMUSZKIEWICZ, W., M. BEHRENDT, R. NAVET and F. E. SLUSE, 2002 Uncoupling protein and alternative oxidase of Dictyostelium discoideum: occurrence, properties and protein expression during vegetative life and starvation-induced early development. FEBS Lett **532:** 459-464.

JARMUSZKIEWICZ, W., M. CZARNA and F. E. SLUSE, 2005 Substrate kinetics of the Acanthamoeba castellanii alternative oxidase and the effects of GMP. Biochim Biophys Acta **1708:** 71-78.

JAZWINSKI, S. M., and A. KRIETE, 2012 The yeast retrograde response as a model of intracellular signaling of mitochondrial dysfunction. Front Physiol **3:** 139.

JUSZCZUK, I. M., and A. M. RYCHTER, 2003 Alternative oxidase in higher plants. Acta Biochim Pol **50:** 1257-1271.

KABIR, M. A., and F. SHERMAN, 2008 Overexpressed ribosomal proteins suppress defective chaperonins in Saccharomyces cerevisiae. FEMS Yeast Res **8:** 1236-1244.

KEMMLER, S., L. OCCHIPINTI, M. VEISU and V. G. PANSE, 2009 Yvh1 is required for a late maturation step in the 60S biogenesis pathway. J Cell Biol **186:** 863-880.

KIEFEL, B. R., P. R. GILSON and P. L. BEECH, 2004 Diverse eukaryotes have retained mitochondrial homologues of the bacterial division protein FtsZ. Protist **155:** 105-115.

KIRIMURA, K., S. OGAWA, T. HATTORI and K. KINO, 2006 Expression analysis of alternative oxidase gene (aox1) with enhanced green fluorescent protein as marker in citric acid-producing Aspergillus niger. J Biosci Bioeng **102:** 210-214.

KORNER, C., M. BARRERA, J. DUKANOVIC, K. EYDT, M. HARNER *et al.*, 2012 The C-terminal domain of Fcj1 is required for formation of crista junctions and interacts with the TOB/SAM complex in mitochondria. Mol Biol Cell **23:** 2143-2155.

KOZAROVA, A., J. W. HUDSON and P. O. VACRATSIS, 2011 The dual-specificity phosphatase hYVH1 (DUSP12) is a novel modulator of cellular DNA content. Cell Cycle **10:** 1669-1678.

KRESSLER, D., E. HURT and J. BASSLER, 2010 Driving ribosome assembly. Biochim Biophys Acta **1803:** 673-683.

KRESSLER, D., D. ROSER, B. PERTSCHY and E. HURT, 2008 The AAA ATPase Rix7 powers progression of ribosome biogenesis by stripping Nsa1 from pre-60S particles. J Cell Biol **181:** 935-944.

KROKOWSKI, D., A. BOGUSZEWSKA, D. ABRAMCZYK, A. LILJAS, M. TCHORZEWSKI *et al.*, 2006 Yeast ribosomal P0 protein has two separate binding sites for P1/P2 proteins. Mol Microbiol **60:** 386-400.

KUMAR, R., A. MUSIYENKO, E. CIOFFI, A. OLDENBURG, B. ADAMS *et al.*, 2004 A zinc-binding dual-specificity YVH1 phosphatase in the malaria parasite, Plasmodium falciparum, and its interaction with the nuclear protein, pescadillo. Mol Biochem Parasitol **133:** 297-310.

LAEMMLI, U. K., 1970 Cleavage of structural proteins during the assembly of the head of bacteriophage T4. Nature **227:** 680-685.

LAMBOWITZ, A. M., J. R. SABOURIN, H. BERTRAND, R. NICKELS and L. MCINTOSH, 1989 Immunological identification of the alternative oxidase of Neurospora crassa mitochondria. Mol Cell Biol **9:** 1362-1364.

LAMBOWITZ, A. M., E. W. SMITH and C. W. SLAYMAN, 1972 Oxidative phosphorylation in Neurospora mitochondria. Studies on wild type, poky, and chloramphenicol-induced wild type. J Biol Chem **247:** 4859-4865.

LANG, B. F., M. W. GRAY and G. BURGER, 1999 Mitochondrial genome evolution and the origin of eukaryotes. Annu Rev Genet **33:** 351-397.

LAPOINTE, J., and S. HEKIMI, 2008 Early mitochondrial dysfunction in long-lived Mclk1+/- mice. J Biol Chem **283:** 26217-26227.

LEA, P. J., R. J. TEMKIN, K. B. FREEMAN, G. A. MITCHELL and B. H. ROBINSON, 1994 Variations in mitochondrial ultrastructure and dynamics observed by high resolution scanning electron microscopy (HRSEM). Microsc Res Tech **27:** 269-277.

LEE, S. J., A. B. HWANG and C. KENYON, 2010 Inhibition of respiration extends C. elegans life span via reactive oxygen species that increase HIF-1 activity. Curr Biol **20:** 2131-2136.

LENAZ, G., and M. L. GENOVA, 2010 Structure and organization of mitochondrial respiratory complexes: a new understanding of an old subject. Antioxid Redox Signal **12:** 961-1008.

LENAZ, G., and M. L. GENOVA, 2012 Supramolecular organisation of the mitochondrial respiratory chain: a new challenge for the mechanism and control of oxidative phosphorylation. Adv Exp Med Biol **748:** 107-144.

LEONARD, P. J., P. K. RATHOD and J. GOLIN, 1994 Loss of function mutation in the yeast multiple drug resistance gene PDR5 causes a reduction in chloramphenicol efflux. Antimicrob Agents Chemother **38:** 2492-2494.

LI, C. R., D. D. LIANG, J. LI, Y. B. DUAN, H. LI *et al.*, 2013 Unravelling mitochondrial retrograde regulation in the abiotic stress induction of rice ALTERNATIVE OXIDASE 1 genes. Plant Cell Environ **36:** 775-788.

LI, Q., R. G. RITZEL, L. L. MCLEAN, L. MCINTOSH, T. KO *et al.*, 1996 Cloning and analysis of the alternative oxidase gene of Neurospora crassa. Genetics **142:** 129-140.

LI, X. P., P. GRELA, D. KROKOWSKI, M. TCHORZEWSKI and N. E. TUMER, 2010 Pentameric organization of the ribosomal stalk accelerates recruitment of ricin a chain to the ribosome for depurination. J Biol Chem **285:** 41463-41471.

LIAO, X., and R. A. BUTOW, 1993 RTG1 and RTG2: two yeast genes required for a novel path of communication from mitochondria to the nucleus. Cell **72:** 61-71.

LIAO, X. S., W. C. SMALL, P. A. SRERE and R. A. BUTOW, 1991 Intramitochondrial functions regulate nonmitochondrial citrate synthase (CIT2) expression in Saccharomyces cerevisiae. Mol Cell Biol **11:** 38-46.

LILL, R., B. HOFFMANN, S. MOLIK, A. J. PIERIK, N. RIETZSCHEL *et al.*, 2012 The role of mitochondria in cellular iron-sulfur protein biogenesis and iron metabolism. Biochim Biophys Acta **1823:** 1491-1508.

LIU, Y., and A. CHANG, 2009 A mutant plasma membrane protein is stabilized upon loss of Yvh1, a novel ribosome assembly factor. Genetics **181:** 907-915.

LIU, Z., and R. A. BUTOW, 2006 Mitochondrial retrograde signaling. Annu Rev Genet **40:** 159-185.

LIU, Z., T. SEKITO, M. SPIREK, J. THORNTON and R. A. BUTOW, 2003 Retrograde signaling is regulated by the dynamic interaction between Rtg2p and Mks1p. Mol Cell **12:** 401-411.

LO, K. Y., Z. LI, F. WANG, E. M. MARCOTTE and A. W. JOHNSON, 2009 Ribosome stalk assembly requires the dual-specificity phosphatase Yvh1 for the exchange of Mrt4 with P0. J Cell Biol **186:** 849-862.

LOGAN, D. C., 2006 The mitochondrial compartment. J Exp Bot **57:** 1225-1243.

MACPHERSON, S., M. LAROCHELLE and B. TURCOTTE, 2006 A fungal family of transcriptional regulators: the zinc cluster proteins. Microbiol Mol Biol Rev **70:** 583-604.

MAGNANI, T., F. M. SORIANI, P. MARTINS VDE, A. C. POLICARPO, C. A. SORGI *et al.*, 2008 Silencing of mitochondrial alternative oxidase gene of Aspergillus fumigatus enhances reactive oxygen species production and killing of the fungus by macrophages. J Bioenerg Biomembr **40:** 631-636.

MAGNANI, T., F. M. SORIANI, V. P. MARTINS, A. M. NASCIMENTO, V. G. TUDELLA *et al.*, 2007 Cloning and functional expression of the

mitochondrial alternative oxidase of Aspergillus fumigatus and its induction by oxidative stress. FEMS Microbiol Lett **271:** 230-238.

MANNELLA, C. A., 2006 The relevance of mitochondrial membrane topology to mitochondrial function. Biochim Biophys Acta **1762:** 140-147.

MANNELLA, C. A., M. MARKO, P. PENCZEK, D. BARNARD and J. FRANK, 1994 The internal compartmentation of rat-liver mitochondria: tomographic study using the high-voltage transmission electron microscope. Microsc Res Tech **27:** 278-283.

MARATHE, S., Y. G. YU, G. E. TURNER, C. PALMIER and R. L. WEISS, 1998 Multiple forms of arginase are differentially expressed from a single locus in Neurospora crassa. J Biol Chem **273:** 29776-29785.

MARQUES, I., N. A. DENCHER, A. VIDEIRA and F. KRAUSE, 2007 Supramolecular organization of the respiratory chain in Neurospora crassa mitochondria. Eukaryot Cell **6:** 2391-2405.

MARTIN, W., and M. MULLER, 1998 The hydrogen hypothesis for the first eukaryote. Nature **392:** 37-41.

MARTIN, W. F., 2011 Early evolution without a tree of life. Biol Direct **6:** 36.

MARTINEZ-GIL, L., A. SAURI, M. A. MARTI-RENOM and I. MINGARRO, 2011 Membrane protein integration into the endoplasmic reticulum. FEBS J **278:** 3846-3858.

MARTINS, V. P., T. M. DINAMARCO, F. M. SORIANI, V. G. TUDELLA, S. C. OLIVEIRA *et al.*, 2011 Involvement of an alternative oxidase in oxidative stress and mycelium-to-yeast differentiation in Paracoccidioides brasiliensis. Eukaryot Cell **10:** 237-248.

MAURO, V. P., and G. M. EDELMAN, 2002 The ribosome filter hypothesis. Proc Natl Acad Sci U S A **99:** 12031-12036.

MAURO, V. P., and G. M. EDELMAN, 2007 The ribosome filter redux. Cell Cycle **6:** 2246-2251.

MAXWELL, D. P., R. NICKELS and L. MCINTOSH, 2002 Evidence of mitochondrial involvement in the transduction of signals required for the induction of genes associated with pathogen attack and senescence. Plant Journal **29:** 269-279.

MAY, K. L., X. P. LI, F. MARTINEZ-AZORIN, J. P. BALLESTA, P. GRELA *et al.*, 2012 The P1/P2 proteins of the human ribosomal stalk are required for ribosome binding and depurination by ricin in human cells. FEBS J **279:** 3925-3936.

MCDONALD, A., and G. VANLERBERGHE, 2004 Branched mitochondrial electron transport in the Animalia: presence of alternative oxidase in several animal phyla. IUBMB Life **56:** 333-341.

MCDONALD, A. E., 2008 Alternative oxidase: an inter-kingdom perspective on the function and regulation of this broadly distributed 'cyanide-resistant' terminal oxidase. Functional Plant Biology **35:** 535-552.

MCDONALD, A. E., and G. C. VANLERBERGHE, 2006 Origins, evolutionary history, and taxonomic distribution of alternative oxidase and plastoquinol terminal oxidase. Comp Biochem Physiol Part D Genomics Proteomics **1:** 357-364.

McKee, E. E., M. Ferguson, A. T. Bentley and T. A. Marks, 2006 Inhibition of mammalian mitochondrial protein synthesis by oxazolidinones. Antimicrob Agents Chemother **50:** 2042-2049.

Metzenberg, R. L., 2003 Vogel's Medium N salts: avoiding the need for ammonium nitrate. Fungal Genet Newsl **50:** 14.

Meyers, S., W. Schauer, E. Balzi, M. Wagner, A. Goffeau *et al.*, 1992 Interaction of the yeast pleiotropic drug resistance genes PDR1 and PDR5. Curr Genet **21:** 431-436.

Miceli, M. V., J. C. Jiang, A. Tiwari, J. F. Rodriguez-Quinones and S. M. Jazwinski, 2011 Loss of mitochondrial membrane potential triggers the retrograde response extending yeast replicative lifespan. Front Genet **2:** 102.

Millar, A. H., J. T. Wiskich, J. Whelan and D. A. Day, 1993 Organic acid activation of the alternative oxidase of plant mitochondria. FEBS Lett **329:** 259-262.

Mochizuki, M., M. Kitamyo, T. Miyoshi, K. Ito and T. Uchiumi, 2012 Analysis of chimeric ribosomal stalk complexes from eukaryotic and bacterial sources: structural features responsible for specificity of translation factors. Genes to Cells **17:** 273-284.

Moore, A. L., J. E. Carre, C. Affourtit, M. S. Albury, P. G. Crichton *et al.*, 2008 Compelling EPR evidence that the alternative oxidase is a diiron carboxylate protein. Biochim Biophys Acta **1777:** 327-330.

Moore, A. L., A. L. Umbach and J. N. Siedow, 1995 Structure-function relationships of the alternative oxidase of plant mitochondria: a model of the active site. J Bioenerg Biomembr **27:** 367-377.

Mossmann, D., C. Meisinger and F. N. Vogtle, 2012 Processing of mitochondrial presequences. Biochim Biophys Acta **1819:** 1098-1106.

Muda, M., E. R. Manning, K. Orth and J. E. Dixon, 1999 Identification of the human YVH1 protein-tyrosine phosphatase orthologue reveals a novel zinc binding domain essential for in vivo function. J Biol Chem **274:** 23991-23995.

Nakamura, K., K. Sakamoto, Y. Kido, Y. Fujimoto, T. Suzuki *et al.*, 2005 Mutational analysis of the Trypanosoma vivax alternative oxidase: the E(X)6Y motif is conserved in both mitochondrial alternative oxidase and plastid terminal oxidase and is indispensable for enzyme activity. Biochem Biophys Res Commun **334:** 593-600.

Nargang, F. E., K. Adames, C. Rub, S. Cheung, N. Easton *et al.*, 2012 Identification of Genes Required for Alternative Oxidase Production in the Neurospora crassa Gene Knockout Library. G3 (Bethesda) **2:** 1345-1356.

Nargang, F. E., and D. Rapaport, 2007 Neurospora crassa as a model organism for mitochondrial biogenesis. Methods Mol Biol **372:** 107-123.

Nicholls, C., H. Li and J. P. Liu, 2012 GAPDH: a common enzyme with uncommon functions. Clin Exp Pharmacol Physiol **39:** 674-679.

Ninomiya, Y., K. Suzuki, C. Ishii and H. Inoue, 2004 Highly efficient gene replacements in Neurospora strains deficient for nonhomologous end-joining. Proc Natl Acad Sci U S A **101:** 12248-12253.

NISSAN, T. A., J. BASSLER, E. PETFALSKI, D. TOLLERVEY and E. HURT, 2002 60S pre-ribosome formation viewed from assembly in the nucleolus until export to the cytoplasm. EMBO J **21:** 5539-5547.

NUNNARI, J., and A. SUOMALAINEN, 2012 Mitochondria: in sickness and in health. Cell **148:** 1145-1159.

O'MALLEY, M. A., 2010 The first eukaryote cell: an unfinished history of contestation. Stud Hist Philos Biol Biomed Sci **41:** 212-224.

OEFFINGER, M., A. LEUNG, A. LAMOND and D. TOLLERVEY, 2002 Yeast Pescadillo is required for multiple activities during 60S ribosomal subunit synthesis. RNA **8:** 626-636.

OKAMOTO, K., and J. M. SHAW, 2005 Mitochondrial morphology and dynamics in yeast and multicellular eukaryotes. Annu Rev Genet **39:** 503-536.

PAIETTA, J. V., and G. A. MARZLUF, 1985 Gene disruption by transformation in Neurospora crassa. Mol Cell Biol **5:** 1554-1559.

PALADE, G. E., 1952 The fine structure of mitochondria. Anat Rec **114:** 427-451.

PALL, M. L., and J. P. BRUNELLI, 1993 A series of six compact fungal transformation vectors containing polylinkers with multiple unique restriction sites. Fungal Genet Newsl **40:** 59-63.

PALMER, C. S., L. D. OSELLAME, D. STOJANOVSKI and M. T. RYAN, 2011 The regulation of mitochondrial morphology: intricate mechanisms and dynamic machinery. Cell Signal **23:** 1534-1545.

PARK, H. D., A. E. BEESER, M. J. CLANCY and T. G. COOPER, 1996 The S. cerevisiae nitrogen starvation-induced Yvh1p and Ptp2p phosphatases play a role in control of sporulation. Yeast **12:** 1135-1151.

PASTORE, D., D. TRONO, M. N. LAUS, N. DI FONZO and S. PASSARELLA, 2001 Alternative oxidase in durum wheat mitochondria. Activation by pyruvate, hydroxypyruvate and glyoxylate and physiological role. Plant Cell Physiol **42:** 1373-1382.

PATTERSON, K. I., T. BRUMMER, P. M. O'BRIEN and R. J. DALY, 2009 Dual-specificity phosphatases: critical regulators with diverse cellular targets. Biochem J **418:** 475-489.

POLIDOROS, A. N., P. V. MYLONA and B. ARNHOLDT-SCHMITT, 2009 Aox gene structure, transcript variation and expression in plants. Physiol Plant **137:** 342-353.

POLIDOROS, A. N., P. V. MYLONA, K. PASENTSIS, J. G. SCANDALIOS and A. S. TSAFTARIS, 2005 The maize alternative oxidase 1a (Aox1a) gene is regulated by signals related to oxidative stress. Redox Rep **10:** 71-78.

POPOT, J. L., and C. DE VITRY, 1990 On the microassembly of integral membrane proteins. Annu Rev Biophys Biophys Chem **19:** 369-403.

PRASAD, R., P. DE WERGIFOSSE, A. GOFFEAU and E. BALZI, 1995 Molecular cloning and characterization of a novel gene of Candida albicans, CDR1, conferring multiple resistance to drugs and antifungals. Curr Genet **27:** 320-329.

PUTHIYAVEETIL, S., I. M. IBRAHIM, B. JELICIC, A. TOMASIC, H. FULGOSI *et al.*, 2010 Transcriptional control of photosynthesis genes: the evolutionarily

conserved regulatory mechanism in plastid genome function. Genome Biol Evol **2:** 888-896.

REICHERT, A. S., and W. NEUPERT, 2002 Contact sites between the outer and inner membrane of mitochondria-role in protein transport. Biochim Biophys Acta **1592:** 41-49.

REMACHA, M., A. JIMENEZ-DIAZ, B. BERMEJO, M. A. RODRIGUEZ-GABRIEL, E. GUARINOS *et al.*, 1995 Ribosomal acidic phosphoproteins P1 and P2 are not required for cell viability but regulate the pattern of protein expression in Saccharomyces cerevisiae. Mol Cell Biol **15:** 4754-4762.

RHOADS, D. M., and L. MCINTOSH, 1993 The salicylic acid-inducible alternative oxidase gene aox1 and genes encoding pathogenesis-related proteins share regions of sequence similarity in their promoters. Plant Mol Biol **21:** 615-624.

RHOADS, D. M., and C. C. SUBBAIAH, 2007 Mitochondrial retrograde regulation in plants. Mitochondrion **7:** 177-194.

RHOADS, D. M., A. L. UMBACH, C. R. SWEET, A. M. LENNON, G. S. RAUCH *et al.*, 1998 Regulation of the cyanide-resistant alternative oxidase of plant mitochondria. Identification of the cysteine residue involved in alpha-keto acid stimulation and intersubunit disulfide bond formation. J Biol Chem **273:** 30750-30756.

RODRIGUEZ-GABRIEL, M. A., M. REMACHA and J. P. G. BALLESTA, 2000 The RNA interacting domain but not the protein interacting domain is highly conserved in ribosomal protein P0. Journal of Biological Chemistry **275:** 2130-2136.

RODRIGUEZ-MATEOS, M., J. J. GARCIA-GOMEZ, R. FRANCISCO-VELILLA, M. REMACHA, J. DE LA CRUZ *et al.*, 2009 Role and dynamics of the ribosomal protein P0 and its related trans-acting factor Mrt4 during ribosome assembly in Saccharomyces cerevisiae. Nucleic Acids Res **37:** 7519-7532.

RUTLEDGE, R. M., L. ESSER, J. MA and D. XIA, 2011 Toward understanding the mechanism of action of the yeast multidrug resistance transporter Pdr5p: a molecular modeling study. J Struct Biol **173:** 333-344.

SAENZ-ROBLES, M. T., M. REMACHA, M. D. VILELLA, S. ZINKER and J. P. BALLESTA, 1990 The acidic ribosomal proteins as regulators of the eukaryotic ribosomal activity. Biochim Biophys Acta **1050:** 51-55.

SAGAN, L., 1967 On the origin of mitosing cells. J Theor Biol **14:** 255-274.

SAISHO, D., E. NAMBARA, S. NAITO, N. TSUTSUMI, A. HIRAI *et al.*, 1997 Characterization of the gene family for alternative oxidase from Arabidopsis thaliana. Plant Mol Biol **35:** 585-596.

SAKUMOTO, N., H. YAMASHITA, Y. MUKAI, Y. KANEKO and S. HARASHIMA, 2001 Dual-specificity protein phosphatase Yvh1p, which is required for vegetative growth and sporulation, interacts with yeast pescadillo homolog in Saccharomyces cerevisiae. Biochem Biophys Res Commun **289:** 608-615.

SAMBROOK, J., and D. W. RUSSELL, 2001 *Molecular cloning. A laboratory manual.* Cold Spring Harbor Laboratory Press, Cold Spring Harbor, New York.

SCHAGGER, H., and K. PFEIFFER, 2000 Supercomplexes in the respiratory chains of yeast and mammalian mitochondria. EMBO J **19:** 1777-1783.

SCHLITT, S. C., and P. J. RUSSELL, 1974 Neurospora crassa cytoplasmic ribosomes: isolation and characterization of a cold-sensitive mutant defective in ribosome biosynthesis. J Bacteriol **120:** 666-671.

SCHMIDT, O., N. PFANNER and C. MEISINGER, 2010 Mitochondrial protein import: from proteomics to functional mechanisms. Nat Rev Mol Cell Biol **11:** 655-667.

SCHNEIDER, A., 2011 Mitochondrial tRNA import and its consequences for mitochondrial translation. Annu Rev Biochem **80:** 1033-1053.

SCHONBAUM, G. R., W. D. BONNER, JR., B. T. STOREY and J. T. BAHR, 1971 Specific inhibition of the cyanide-insensitive respiratory pathway in plant mitochondria by hydroxamic acids. Plant Physiol **47:** 124-128.

SCHWARZLANDER, M., and I. FINKEMEIER, 2013 Mitochondrial Energy and Redox Signaling in Plants. Antioxid Redox Signal.

SCHWARZLANDER, M., M. D. FRICKER and L. J. SWEETLOVE, 2009 Monitoring the in vivo redox state of plant mitochondria: Effect of respiratory inhibitors, abiotic stress and assessment of recovery from oxidative challenge. Biochimica Et Biophysica Acta-Bioenergetics **1787:** 468-475.

SEKITO, T., J. THORNTON and R. A. BUTOW, 2000 Mitochondria-to-nuclear signaling is regulated by the subcellular localization of the transcription factors Rtg1p and Rtg3p. Mol Biol Cell **11:** 2103-2115.

SELLEM, C. H., E. BOVIER, S. LORIN and A. SAINSARD-CHANET, 2009 Mutations in two zinc-cluster proteins activate alternative respiratory and gluconeogenic pathways and restore senescence in long-lived respiratory mutants of Podospora anserina. Genetics **182:** 69-78.

SHARDA, P. R., C. A. BONHAM, E. J. MUCAKI, Z. BUTT and P. O. VACRATSIS, 2009 The dual-specificity phosphatase hYVH1 interacts with Hsp70 and prevents heat-shock-induced cell death. Biochem J **418:** 391-401.

SHIBA, T., Y. KIDO, K. SAKAMOTO, D. K. INAOKA, C. TSUGE *et al.*, 2013 Structure of the trypanosome cyanide-insensitive alternative oxidase. Proc Natl Acad Sci U S A **110:** 4580-4585.

SHUTT, T. E., and H. M. MCBRIDE, 2013 Staying cool in difficult times: mitochondrial dynamics, quality control and the stress response. Biochim Biophys Acta **1833:** 417-424.

SIEDOW, J. N., A. L. UMBACH and A. L. MOORE, 1995 The active site of the cyanide-resistant oxidase from plant mitochondria contains a binuclear iron center. FEBS Lett **362:** 10-14.

SRINIVASAN, V., A. KRIETE, A. SACAN and S. M. JAZWINSKI, 2010 Comparing the yeast retrograde response and NF-kappaB stress responses: implications for aging. Aging Cell **9:** 933-941.

STEFAN DIMMER, K., and D. RAPAPORT, 2010 The enigmatic role of Mim1 in mitochondrial biogenesis. Eur J Cell Biol **89:** 212-215.

STEFFEN, K. K., V. L. MACKAY, E. O. KERR, M. TSUCHIYA, D. HU *et al.*, 2008 Yeast life span extension by depletion of 60s ribosomal subunits is mediated by Gcn4. Cell **133:** 292-302.

STROH, A., O. ANDERKA, K. PFEIFFER, T. YAGI, M. FINEL *et al.*, 2004 Assembly of respiratory complexes I, III, and IV into NADH oxidase supercomplex stabilizes complex I in Paracoccus denitrificans. J Biol Chem **279:** 5000-5007.

SUGIYAMA, M., S. NUGROHO, N. IIDA, T. SAKAI, Y. KANEKO *et al.*, 2011 Genetic interactions of ribosome maturation factors Yvh1 and Mrt4 influence mRNA decay, glycogen accumulation, and the expression of early meiotic genes in Saccharomyces cerevisiae. J Biochem **150:** 103-111.

SUZUKI, Y., S. L. MURRAY, K. H. WONG, M. A. DAVIS and M. J. HYNES, 2012 Reprogramming of carbon metabolism by the transcriptional activators AcuK and AcuM in Aspergillus nidulans. Mol Microbiol **84:** 942-964.

SZICK-MIRANDA, K., and J. BAILEY-SERRES, 2001 Regulated heterogeneity in 12-kDa P-protein phosphorylation and composition of ribosomes in maize (Zea mays L.). J Biol Chem **276:** 10921-10928.

TALBOT, K. J., and P. J. RUSSELL, 1982 Nuclear buoyant density determination and the purification and characterization of wild-type neurospora nuclei using percoll density gradients. Plant Physiol **70:** 704-708.

TANTON, L. L., C. E. NARGANG, K. E. KESSLER, Q. LI and F. E. NARGANG, 2003 Alternative oxidase expression in Neurospora crassa. Fungal Genet Biol **39:** 176-190.

TANUDJI, M., S. SJOLING, E. GLASER and J. WHELAN, 1999 Signals required for the import and processing of the alternative oxidase into mitochondria. J Biol Chem **274:** 1286-1293.

THIRKETTLE-WATTS, D., T. C. MCCABE, R. CLIFTON, C. MOORE, P. M. FINNEGAN *et al.*, 2003 Analysis of the alternative oxidase promoters from soybean. Plant Physiol **133:** 1158-1169.

THOMAZELLA, D. P., P. J. TEIXEIRA, H. C. OLIVEIRA, E. E. SAVIANI, J. RINCONES *et al.*, 2012 The hemibiotrophic cacao pathogen Moniliophthora perniciosa depends on a mitochondrial alternative oxidase for biotrophic development. New Phytol **194:** 1025-1034.

TIMMIS, J. N., M. A. AYLIFFE, C. Y. HUANG and W. MARTIN, 2004 Endosymbiotic gene transfer: organelle genomes forge eukaryotic chromosomes. Nat Rev Genet **5:** 123-135.

TSCHOCHNER, H., and E. HURT, 2003 Pre-ribosomes on the road from the nucleolus to the cytoplasm. Trends Cell Biol **13:** 255-263.

TURNER, G. E., and R. L. WEISS, 2006 Developmental expression of two forms of arginase in Neurospora crassa. Biochim Biophys Acta **1760:** 848-857.

UMBACH, A. L., V. S. NG and J. N. SIEDOW, 2006 Regulation of plant alternative oxidase activity: a tale of two cysteines. Biochim Biophys Acta **1757:** 135-142.

UMBACH, A. L., and J. N. SIEDOW, 1993 Covalent and Noncovalent Dimers of the Cyanide-Resistant Alternative Oxidase Protein in Higher Plant Mitochondria and Their Relationship to Enzyme Activity. Plant Physiol **103:** 845-854.

UMBACH, A. L., and J. N. SIEDOW, 1996 The reaction of the soybean cotyledon mitochondrial cyanide-resistant oxidase with sulfhydryl reagents suggests

that alpha-keto acid activation involves the formation of a thiohemiacetal. J Biol Chem **271:** 25019-25026.

UMBACH, A. L., and J. N. SIEDOW, 2000 The cyanide-resistant alternative oxidases from the fungi Pichia stipitis and Neurospora crassa are monomeric and lack regulatory features of the plant enzyme. Arch Biochem Biophys **378:** 234-245.

VAN DER GIEZEN, M., 2009 Hydrogenosomes and mitosomes: conservation and evolution of functions. J Eukaryot Microbiol **56:** 221-231.

VAN DER GIEZEN, M., J. TOVAR and C. G. CLARK, 2005 Mitochondrion-derived organelles in protists and fungi. Int Rev Cytol **244:** 175-225.

VAN DER LAAN, M., M. BOHNERT, N. WIEDEMANN and N. PFANNER, 2012 Role of MINOS in mitochondrial membrane architecture and biogenesis. Trends Cell Biol **22:** 185-192.

VANLERBERGHE, G. C., 2013 Alternative Oxidase: A Mitochondrial Respiratory Pathway to Maintain Metabolic and Signaling Homeostasis during Abiotic and Biotic Stress in Plants. Int J Mol Sci **14:** 6805-6847.

VANLERBERGHE, G. C., and L. MCINTOSH, 1996 Signals regulating the expression of the nuclear gene encoding alternative oxidase of plant mitochondria. Plant Physiol **111:** 589-595.

VANLERBERGHE, G. C., L. MCINTOSH and J. Y. YIP, 1998 Molecular localization of a redox-modulated process regulating plant mitochondrial electron transport. Plant Cell **10:** 1551-1560.

VEIGA, A., J. D. ARRABACA and M. C. LOUREIRO-DIAS, 2003 Cyanide-resistant respiration, a very frequent metabolic pathway in yeasts. FEMS Yeast Res **3:** 239-245.

VESTEG, M., and J. KRAJCOVIC, 2011 The falsifiability of the models for the origin of eukaryotes. Curr Genet **57:** 367-390.

VOGEL, F., C. BORNHOVD, W. NEUPERT and A. S. REICHERT, 2006 Dynamic subcompartmentalization of the mitochondrial inner membrane. J Cell Biol **175:** 237-247.

VON DER MALSBURG, K., J. M. MULLER, M. BOHNERT, S. OELJEKLAUS, P. KWIATKOWSKA *et al.*, 2011 Dual role of mitofilin in mitochondrial membrane organization and protein biogenesis. Dev Cell **21:** 694-707.

WADE, C., K. A. SHEA, R. V. JENSEN and M. A. MCALEAR, 2001 EBP2 is a member of the yeast RRB regulon, a transcriptionally coregulated set of genes that are required for ribosome and rRNA biosynthesis. Mol Cell Biol **21:** 8638-8650.

WANG, J., N. RAJAKULENDRAN, S. AMIRSADEGHI and G. C. VANLERBERGHE, 2011 Impact of mitochondrial alternative oxidase expression on the response of Nicotiana tabacum to cold temperature. Physiol Plant **142:** 339-351.

WATLING, J. R., S. A. ROBINSON and R. S. SEYMOUR, 2006 Contribution of the alternative pathway to respiration during thermogenesis in flowers of the sacred lotus. Plant Physiol **140:** 1367-1373.

WESTERMANN, B., 2008 Molecular machinery of mitochondrial fusion and fission. J Biol Chem **283:** 13501-13505.

WESTERMANN, B., 2010 Mitochondrial dynamics in model organisms: what yeasts, worms and flies have taught us about fusion and fission of mitochondria. Semin Cell Dev Biol **21:** 542-549.

WILSON, D. N., and J. H. DOUDNA CATE, 2012 The structure and function of the eukaryotic ribosome. Cold Spring Harb Perspect Biol **4**.

WOODSON, J. D., and J. CHORY, 2008 Coordination of gene expression between organellar and nuclear genomes. Nat Rev Genet **9:** 383-395.

XU, T., F. YAO, W. S. LIANG, Y. H. LI, D. R. LI *et al.*, 2012 Involvement of alternative oxidase in the regulation of growth, development, and resistance to oxidative stress of Sclerotinia sclerotiorum. J Microbiol **50:** 594-602.

YANG, D., Y. OYAIZU, H. OYAIZU, G. J. OLSEN and C. R. WOESE, 1985 Mitochondrial origins. Proc Natl Acad Sci U S A **82:** 4443-4447.

YUKIOKA, H., S. INAGAKI, R. TANAKA, K. KATOH, N. MIKI *et al.*, 1998 Transcriptional activation of the alternative oxidase gene of the fungus Magnaporthe grisea by a respiratory-inhibiting fungicide and hydrogen peroxide. Biochim Biophys Acta **1442:** 161-169.

ZEMP, I., and U. KUTAY, 2007 Nuclear export and cytoplasmic maturation of ribosomal subunits. FEBS Lett **581:** 2783-2793.

ZUK, D., J. P. BELK and A. JACOBSON, 1999 Temperature-sensitive mutations in the Saccharomyces cerevisiae MRT4, GRC5, SLA2 and THS1 genes result in defects in mRNA turnover. Genetics **153:** 35-47.